Durham University

Durham E-Theses

Measurements of energy loss of cosmic ray - mesons and protons

A. K. Abdelhady

How to cite:

Abdelhady, A. K. (1974) Measurements of energy loss of cosmic ray - mesons and protons. Masters thesis, Durham University.

Use policy

The full-text may be used and/or reproduced, and given to third parties in any format or medium, without prior permission or charge, for personal research or study, educational, or not-for-profit purposes provided that:

- a full bibliographic reference is made to the original source
- a https://etheses.durham.ac.uk/id/eprint/8938/ is made to the metadata record in Durham E-Theses
- the full-text is not changed in any way

The full-text must not be sold in any format or medium without the formal permission of the copyright holders.

Please consult the full Durham E-Theses policy for further details.

Academic Support Office, The Palatine Centre, Durham University, Stockton Road, Durham, DH1 3LE
e-mail: e-theses.admin@durham.ac.uk Tel: +44 0191 334 6107
https://etheses.durham.ac.uk

Measurements of Energy Loss of Cosmic Ray μ - mesons and Protons.

By

A.K. Abdelhady

A thesis submitted to the University of Durham in accordance with the Regulation for the Degree of Master of Science.

Department of Physics,
University of Durham

August, 1974.

The Magnet House Nuclear Active Particle Spectrograph in The University of Durham; Department of Physics.

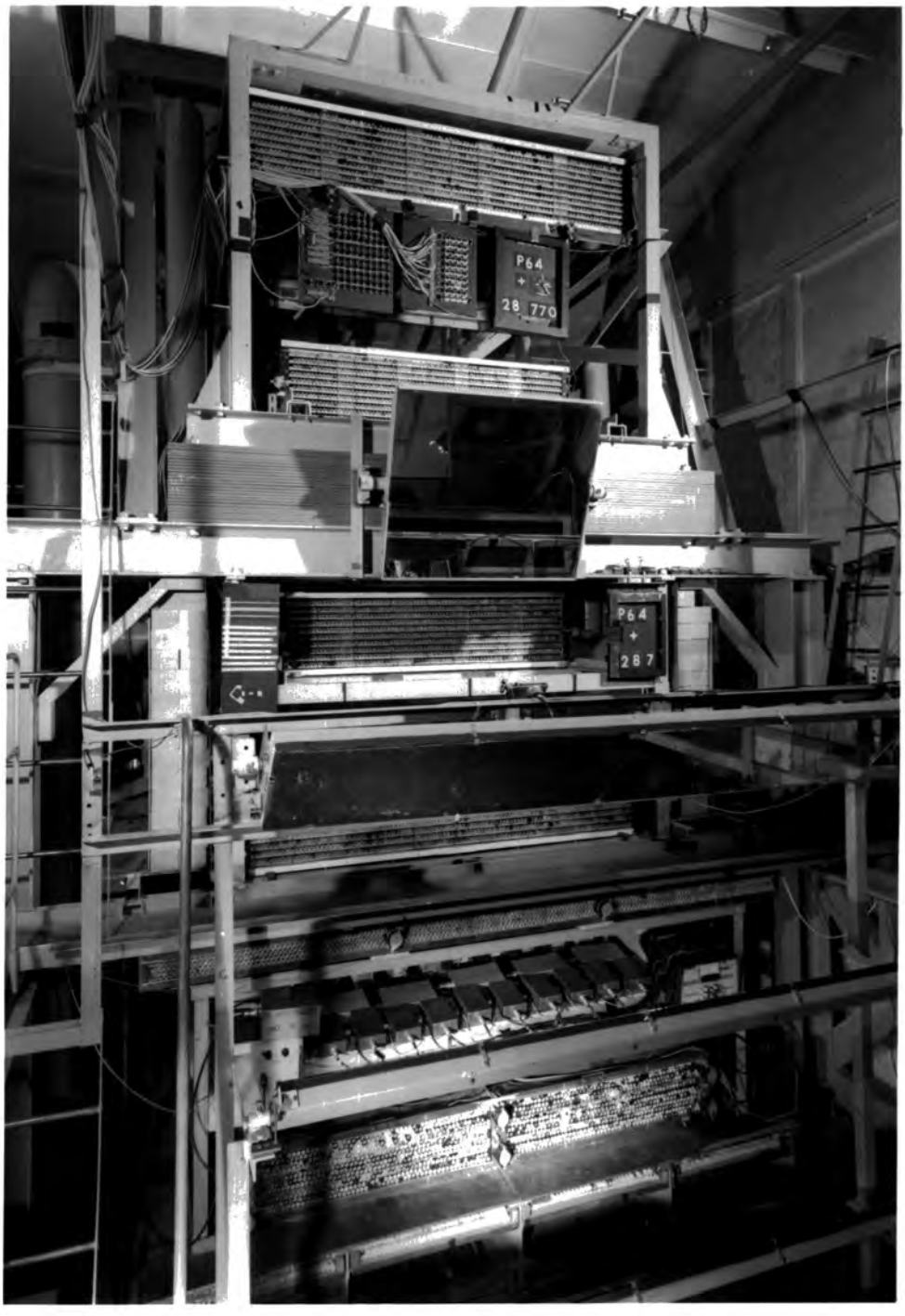
P64
28 770
P64
287

The two arms of the spectrograph, (The Momentum Trays.)

The first arm:

Tray A1 and A3.

The second arm:

Tray B3 and B1.

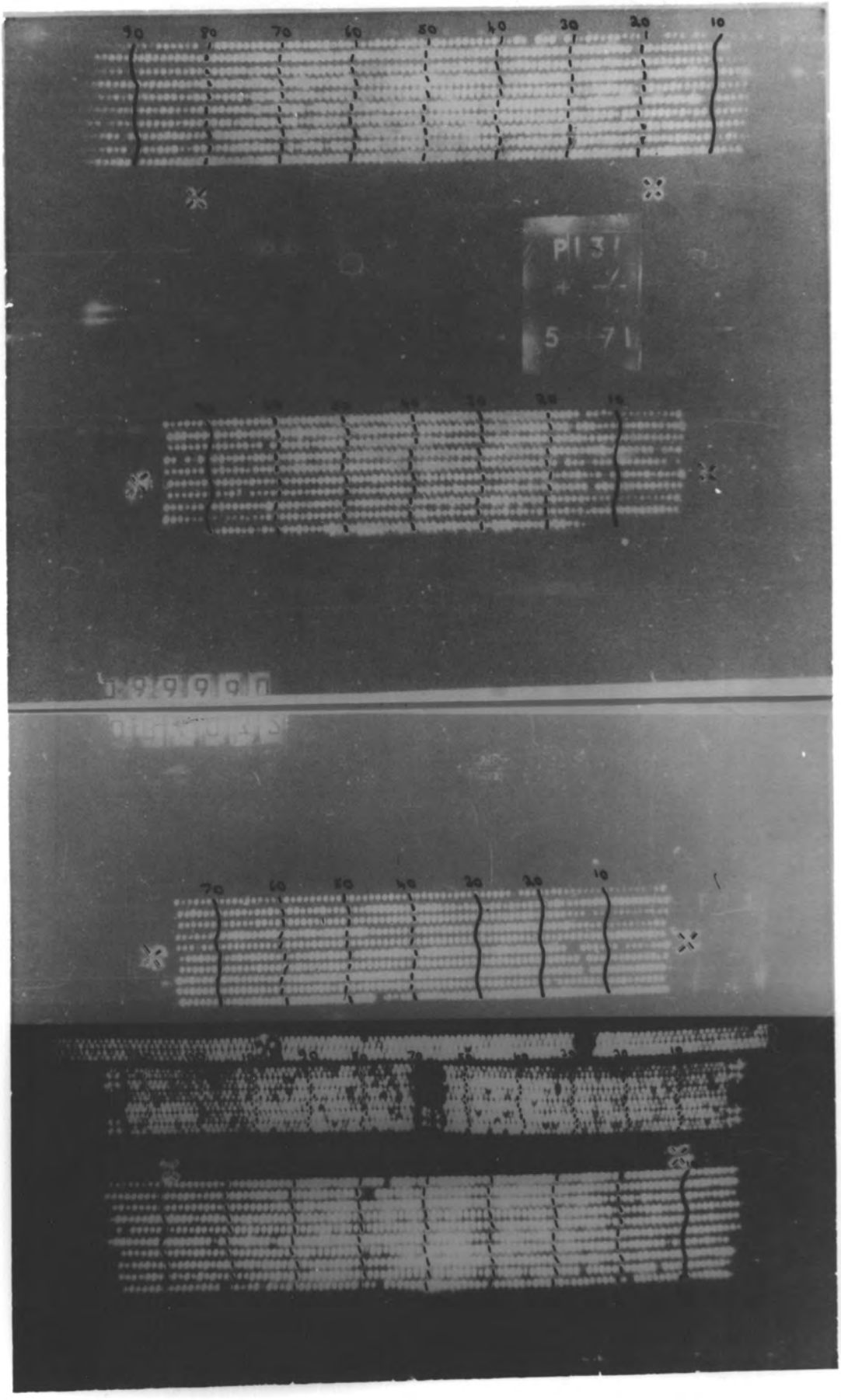
90 80 70 60 50 40 30 20 10
P 13
5 71
70 60 50 40 30 20 10

CONTENTS

ABSTRACT

The aim of the work concerns the use of Conversi Counters (Neon Flash Tubes), in conjunction with a nuclear active particle spectrograph, to measure the energy loss of mesons and protons of known momentum, in the range 0.1 - 10 GeV/c. The experimental results are related to theoretical work in this field, with special reference to that of Sternheimer (1956), and Lloyd (1960).

The results show that neon flash tubes are satisfactory indicators of energy loss for mesons, and their performance is in substantial agreement with expectation on the basis of the model for flash tube behaviour suggested by Lloyd (1960). The situation concerning the energy loss for protons is that the data are not sufficiently precise to allow a satisfactory comparison to be made.

Some additional results have been taken from the plastic scintillator detector in the apparatus. The mean pulse amplitude from the plastic scintillator has been taken as a measure of energy loss, for mesons and protons of various momenta. Good agreement with theory has been shown for mesons.

Some comparison has been outlined between the results, and the work of other authors using the same and other techniques.

Results were also obtained from a water Čerenkov detector, which operated in the apparatus, to study the characteristics of Čerenkov pulse amplitude versus momentum for mesons.

PREFACE

The results presented in this thesis were obtained using the data from the Magnet House Nuclear Active Particle Spectrograph which is situated in the University of Durham. The construction of the instrument was carried out previously by Hook (1973). The operation of the instrument was carried out by I.S. Diggory, the author's colleague. The author assisted with the experimental work in 1973. The data analysis was the responsibility of the author using the procedure derived by I.S. Diggory.

The main aim of the present work is the study of the theoretical aspect of energy loss of cosmic ray particles and its relation to the experimental results. The present work was to test the response of neon flash tubes, in conjunction with the Spectrograph, to mesons and protons of known momentum in the range 0.1 - 10 GeV/c.

This work was carried out at the University of Durham, Department of Physics, by the author during the years 1972/73 and 1973/74, under the formal supervision of Professor A.W. Wolfendale. The actual research was performed in Dr. K.E. Turver's research group.

CHAPTER ONE

INTRODUCTION

1.1 General and Scope of the Present Work

A steady rain of charged particles moving at nearly the speed of light falls upon the earth from all directions. These particles, known as cosmic rays, were discovered sixty years ago, but still their study is important in Physics and Astrophysics.

The primary radiation, which comes from outer space (primary energy less than 1 GeV up to a maximum of 10^{10} - 10^{11} GeV), on entering the earth's atmosphere interacts strongly with air nuclei to give a flux of secondary particles. The primary particles lose a large fraction of their initial energy in generating the secondary products (the atmosphere represents about 12 to 13 interaction mean free paths).

All the particles, both primary and secondary, lose energy also through ionization loss in the atmosphere. For example a cosmic ray μ - meson loses about 2 Gev by ionization in travelling from its origin near the top of the atmosphere to sea-level. The ionization loss is usually taken to include excitation loss, in which the energy transferred to the electron is too low to detach it from its atom.

The problem of energy loss of rapidly moving electrically charged particles in matter, the subject of this thesis, has been treated by many workers. Bohr (1913) was the first physicist to develop the theory of energy loss by ionization using semiclassical procedures. In the early 1930's Bethe and Bloch improved the

DURHAM UNIVERSITY
20 MAY 1975

treatment by using quantum mechanical methods. Some workers have treated the problem of energy loss theoretically and others experimentally. For example Fermi (1939, 1940) has treated the problem by taking into account the polarization properties of the medium traversed. Fermi characterised the medium traversed by a dielectric constant produced by electrons bound with a single frequency and damped in their motion. He obtained the important result that in condensed media the loss depends not only on the physical parameters which enter into the Bethe formula but also on the dielectric properties of the medium. Similar work has been done by Halpern and Hall, who showed that the reduction in ionization loss depends strongly on the description of the dielectric properties of the medium.

Many experimentalists and theorists have discussed the problem, among them, Heitler (1936), Rossi (1939), Williams (1929), Landau (1958), Jones et al (1963), Crispin et al. (1970), Ashton et al (1971) and Diggory et al (1971). It has been considered necessary to re-examine the region of the minimum ionization and Fermi plateau and this is the purpose of the thesis.

This thesis summarizes briefly the theoretical work in field of energy loss by charged particles in matter and relates it to the experimental results, with special reference to the energy loss of cosmic ray mesons and protons of known momentum in the range 0.1 - 10 Gev/c.

A brief description is given in this chapter of the processes which occur when a high energy primary particle enters the earth's atmosphere. The theoretical aspects of the problems of ionization

losses are discussed in chapter two, this chapter also contains the theory of flash tube operation suggested by Lloyd (1960).

The description of the equipment (the magnet spectrograph and its detectors), its design and construction and data recording are given in chapter three. Chapter four describes the analysis of the data. The previous work using different techniques to measure the energy loss of charged particles are outlined in chapter five. The experimental results on the energy loss for mesons and protons using the flash tube data are estimated in chapter six, this chapter also concerns some experimental results obtained from plastic scintillator detectors and a threshold water Čerenkov detector. The aim of the latter point is to examine the characteristics of Čerenkov pulse amplitude versus particles momentum.

In order to estimate the precision of the present work comparison has been made with the results of Diggory et al (1971), because the experiments were very similar. The comparison also included the work of Ashton et al (1971).

Good agreement with Sternheimer (1956) and Lloyd's theory of flash tube operation has been shown in chapter six, in the case of mesons, but for protons a lack of agreement with theory still exists due largely to the small sample size analysed.

In the following a brief description will be given about the characteristics of the primary cosmic radiation.

1.2 The characteristics of the primary cosmic radiation:

Waddington (1960) has estimated that the primary composition consists of proton: 85.9%, α - particles: 12.7% and a small mixture of

about 1.4% of heavy nuclei up to Z=29. Some of the primary particles will have been present at the site of their original acceleration (the so called "primordial" particles) and other will arise as a result of interactions in the intervening interstellar matter.

Extremely heavy nuclei have been detected by Fowler et al (1967, 1970) and Fleischer et al(1967) and a summary by Blandford et al (1971) gives for their total flux at the top of the atmosphere the following formula:

$$J\ (Z > 96) = (2 \pm 1)\ 10^{-7}\ m^{-2}\ s^{-1}\ sr^{-1}$$

Shapiro and his associates (Shapiro and Silberberg 1970, Shapiro et al, 1971) have made further analysis as successive improvements in the data have been made and their current conclusions on the primordial composition from measurements below 10^9 eV/nucleon are given in table 1.1.

Measurements on the various component indicate that the primaries must have traversed an amount of material from their origin until they reached the earth's atmosphere of about 4 $g \cdot cm^{-2}$. The integral primary spectrum for the primaries varies with energy as shown in figure 1.1. From this graph it is clear that the exponent of the integral primary spectrum is - 1.6 up to 10^{15} eV increasing to about - 2.2 at higher energies. One interpretation of the steepening is that it is due to the inability of the galactic magnetic field to contain protons inside the galaxy above this energy.

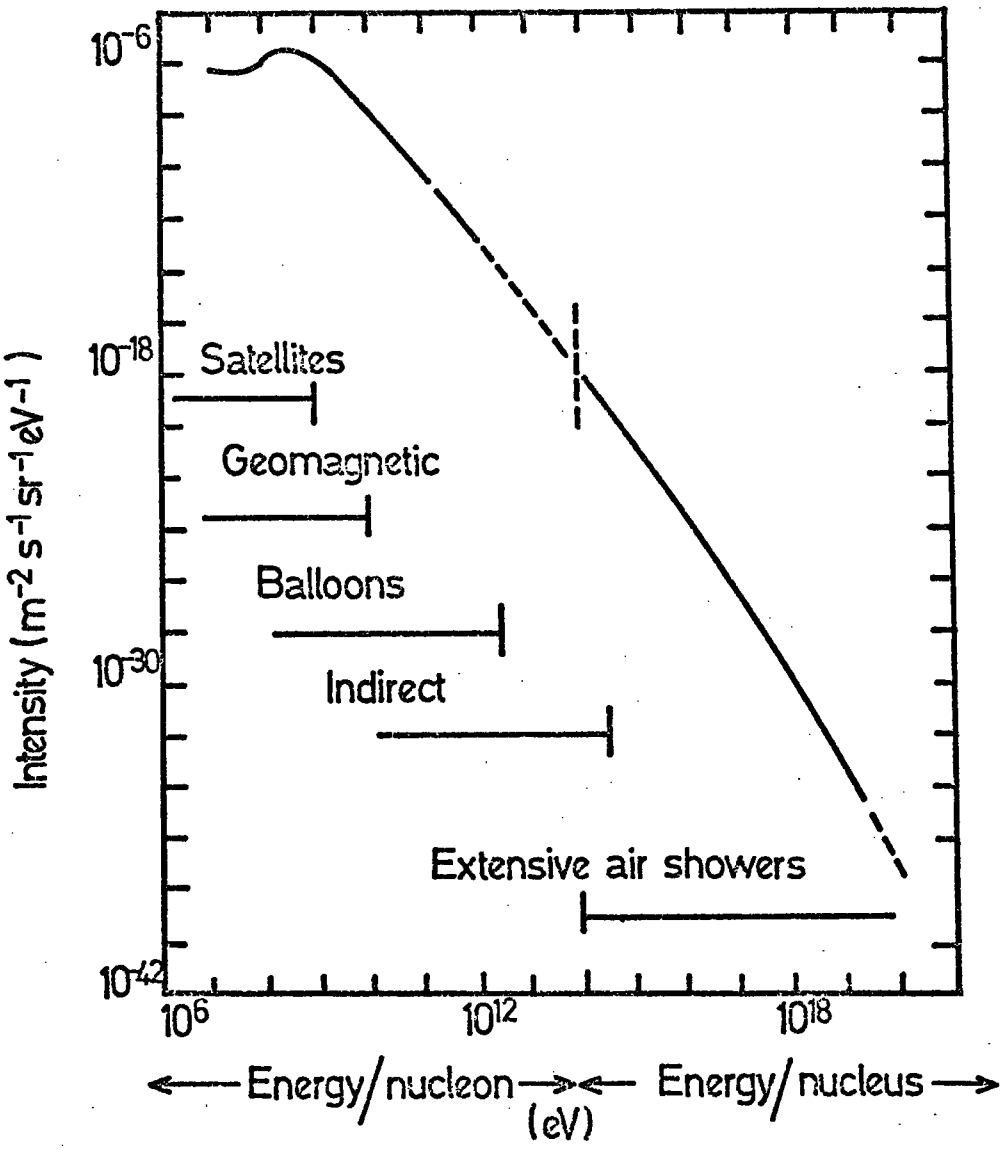

Figure 11. The primary spectrum of protons in the cosmic radiation.

(After A.W. Wolfendale, 1973.).

1.3 Interaction of the primary cosmic rays in the atmosphere

As soon as the primaries enter the earth's atmosphere (assume the primary energy $\gtrsim 10^{11}$ eV) multiple collisions readily take place with atmospheric atoms, and the result of these high energy interactions is a large number of secondary particles, mainly π - mesons (pions). The primary particle on average loses just under half of its energy (45%) in generation of the secondary particles, and the total multiplicity of secondaries increases with primary energy E_p, the approximate relationship being $N_s = 2.7\ E_p^{1/4}$ where E_p in GeV.

The primary protons make a number of collisions before reaching sea-level and pions are generated in these collisions; if the energy is high enough more pions are generated by the interactions of the secondary pions themselves.

The charged pions are unstable with a mean lifetime of about 2.6×10^{-8}s (at rest) and then decay by the scheme $\pi \rightarrow$ muon + neutrino. The neutral pion has a much shorter mean life (7.6×10^{-17}s at rest) for which the decay scheme is $\pi^o \rightarrow \gamma + \gamma$.

The γ-rays produce electron pairs and electrons interact with air nuclei by way of bremsstrahlung to produce more γ-rays so that a complex electron - photon cascade is built up.

The μ - meson (muon) is also unstable:

$$\mu^+ \rightarrow e^+ + \nu_e + \bar{\nu}_\mu \quad \text{and} \quad \mu^- \rightarrow e^- + \bar{\nu}_e + \nu_\mu$$

and the muon has a mean lifetime at rest of 2.2×10^{-6}s. Thus, some of the less energetic muons decay before reaching sea-level.

Figure 1.2 summarises the situation.

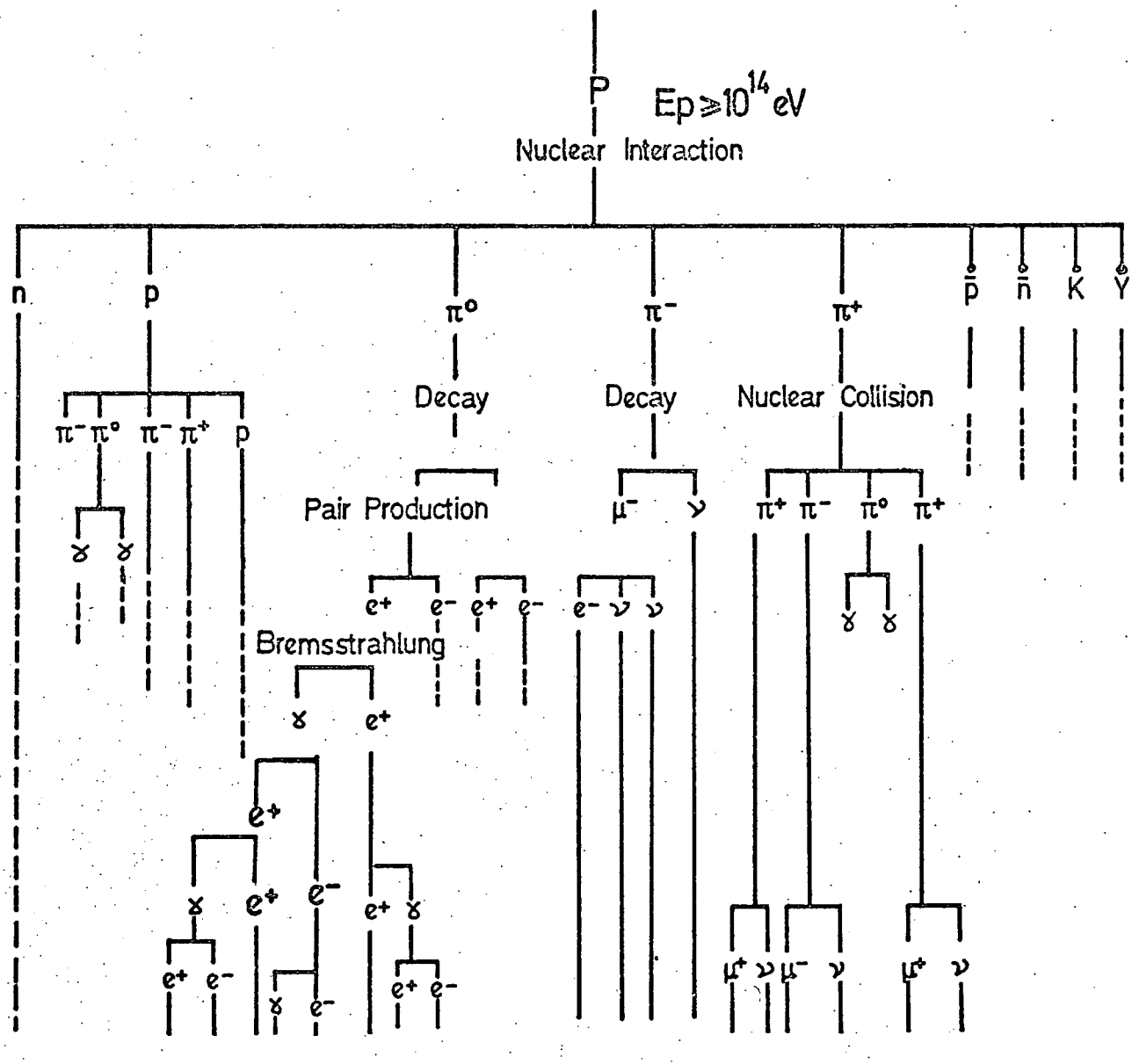

FIG.1.2

The interactions between a high energy primary proton and the air nuclei of the atmosphere together with the secondary and later interactions.

1.4 The secondary Cosmic Radiation at Sea level as a source of the charged particles which penetrate the magnet spectrograph:

The secondary cosmic radiation which arrives at sea level can be considered as a potential source of particles which can penetrate the magnetic spectrograph. The electron photon component will be mainly absorbed by the lead layer on the top of the instrument, but the μ-meson component and nuclear active component (nucleons and pions) should be able to penetrate the materials in the instrument. These are the particles which can be studied using the equipment and it is their rate of energy loss which is the subject of this thesis.

Table 1.1.

The primordial composition of the more abundant cosmic rays, normalised to carbon. The data which refer to energies below 1 GeV per nucleon are taken from the work of Shapiro et al (1971).

Nucleus	Relative number
H	5×10^{4}*
He	$(2.7 \pm 0.5) \times 10^{3}$
C	100
N	12 ± 3
O	102 ± 6
Ne	20 ± 3
Mg	27 ± 4
Si	23 ± 4
Fe	23 ± 5

Z Groupings	Intensity $m^{-2} s^{-1} sr.^{-1}$
$29 \leqslant Z \leqslant 43$	$\simeq 10^{-2}$
$44 \leqslant Z \leqslant 59$	$\simeq 3 \times 10^{-4}$
$68 \leqslant Z \leqslant 83$	$\simeq 3 \times 10^{-4}$
$90 \leqslant Z \leqslant 96$	$\simeq 2 \times 10^{-4}$

* This value applies to source spectra that follow a power law in energy per nucleon.

CHAPTER TWO

The Energy Loss of Charged Particles in Matter

2.1 Introduction:

A charged particle moving fast enough in any medium leaves around its path a trail of ions, electrons and excited atoms. It is clear that collisions between charged particles and atoms of gases result partly in excitation and partly in ionization of the atoms. Most of the electrons ejected in the ionization process have energies very small compared with the energy of the primary particle, yet larger than the ionization energy of the atoms. They are able therefore to produce several ion pairs before coming to rest.

A charged particle loses energy as a consequence of collisions with atomic electrons and nuclei in one or more of the following processes:

1. Ionization and excitation
2. Bremmstrahlung
3. Direct pair production
4. Nuclear Interaction
5. Čerenkov radiation.

It may be remarked here that the dominant mechanisms by which a low energy charged particle loses its energy are ionization and excitation. The radiation losses are of importance at higher energies (i.e. outside the range of energy 0.1 - 10 Gev in our measurements).

To calculate the ionization loss it is usual to divide the collisions into two classes. In the first we have close collisions where the impact parameters are small and the electrons taking

part in the collisions can be regarded as free. In the second class, we have distant collisions (much larger impact parameters) and for these the binding of the electrons to the atoms must be taken into account (smaller energy transfer). Thus the larger the impact parameter, the smaller the energy transfer involved in the collision.

If the distance of closest approach is small the electron is ejected from the atom with considerable energy. This phenomenon is often referred to as the 'knock-on' process. When the energy acquired by secondary electrons is large compared with the binding energy, the phenomenon can be treated as an interaction between the passing particle and a free electron. (Radiation phenomena can still be neglected). In the following it is appropriate to give some details of the dynamics of this collision and its probability of occurence.

2.2 The Dynamics of Collisions

Here we discuss the dynamics of the collision between the fast charged particle with mass m and an atomic electron. Consider a particle with mass m which collides with an electron of mass m_e as shown in figure 2.1; let us further assume that the momentum of the incident particle is p, the momentum of the electron after collision is p' and the momentum of the incident particle after the collision is p". The angle between the initial trajectory of the primary particle and the direction of motion of the electron after the collision is θ. The principle of the conservation of energy gives:

$$\sqrt{p^2c^2 + m^2c^4} + m_e c^2 = \sqrt{p''^2c^2 + m^2c^4} + E' + m_e c^2 \quad (1)$$

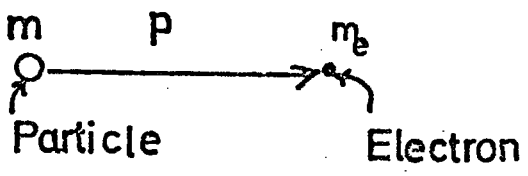

(A) Before

(B) After

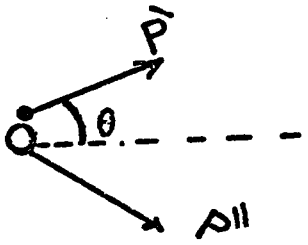

Figure 2-1. The dynamics of the collisions between a charged particle and an electron. (A) Before and (B) After collision.

where E' represents the energy of recoil of the electron and is given by:

$$E' = \sqrt{c^2 p'^2 + m_e^2 c^4} - m_e c^2 \qquad \ldots(1a)$$

The conservation of momentum requires that:

$$p''^2 = p'^2 + p^2 - 2pp' \cos\theta \qquad \ldots(2)$$

By elimination of p'' and p' between equation (1), (1a) and (2) the energy of recoil of the electron, E', which is ejected at angle θ to the direction of the incident particle is given by:

$$E' = 2m_e c^2 \frac{p^2 c^2 \cos^2\theta}{\left[m_e c^2 + (p^2 c^2 + m^2 c^4)^{\frac{1}{2}}\right]^2 - p^2 c^2 \cos^2\theta} \qquad \ldots(3)$$

From the above equation it is clear that the kinetic energy E' of the recoil electron increases with decreasing θ so it is true that knock-on electrons at a small angle have high energy. The maximum transferable energy corresponds to a head-on collision and is given by the following formula:

$$E'_m = 2m_e c^2 \frac{p^2 c^2}{m_e^2 c^4 + m^2 c^4 + 2m_e c^2 (p^2 c^2 + m^2 c^4)^{\frac{1}{2}}} \qquad \ldots(4)$$

The term $m_e^2 c^4$ can be neglected for mesons and protons having $m \gg m_e$ for very large momenta ($P \gg m^2 c/m_e$).

Equation (4) can then be written:-

$$E'_m \approx Pc \approx E \qquad \ldots(5)$$

Thus a very high energy meson or proton can be practically "stopped" by a head-on collision with an electron.

If $m \gg m_e$ and $P \ll m^2c/m_e$, equation (4) takes the following form:

$$E'_m \approx 2\, m_e c^2 \left(\frac{P}{mc}\right)^2 = 2\, m_e c^2 \quad \frac{\beta^2}{1-\beta^2} \qquad \ldots(6)$$

It is clear from the last equation that for heavy particles of sufficiently small momenta, the most important parameter for the maximum transferable energy is the velocity.

2.3 The Probability of Collision

When a fast charged particle with kinetic energy E passes through a medium it will pass the atoms at a wide variety of impact parameters for each of which there is an energy transfer E'. The probability of collision will increase with the thickness of the medium traversed and if we assume that E' is sufficiently large the atomic electrons may be regarded as free. It is convenient in calculations of this type to measure the thickness of the medium traversed in units g cm^{-2}. Thus if the charged particle moves a distance t cm in a medium of density ρ g cm^{-3}, the thickness traversed is $t\rho$ g cm^{-2}.

Rutherford derived an approximate relation for the probability of a collision for a charged particle with kinetic energy E, velocity βc and charge Z traversing a thickness dx g cm^{-2}, and resulting in an energy transfer between E' and E' + dE' to an atomic electron:-

$$\oint (E')\, dE'\, dx = \frac{2\, Cm_e c^2 Z^2}{\beta^2} \quad \frac{dE'}{(E')^2} \quad dx \qquad \ldots(7)$$

The constant C is given by:

$$C = \pi N \frac{Z}{A} r_e^2 = 0.150 \frac{Z}{A} g^{-1} cm^2$$

Where Z, A are the atomic number and atomic weight of the medium respectively, N is Avogadros number and $r_e = e^2/m_e c^2$ is the classical radius of the electron.

The Rutherford formula is accurate for energies well below the maximum transferable energy E'_m, but breaks down when the energy of the knock-on electron is high. The correction terms necessary were derived by Bhabha (1938) and the full expression is:

$$\oint(E,E')dE'dx = \frac{2Cm_e c^2 Z^2}{\beta^2} \frac{dE'}{(E')^2} dx \left[1-\beta^2 \frac{E'}{E'_m} + \frac{1}{2} \left(\frac{E'}{E + mc^2}\right)^2\right] \quad ...(9)$$

The total rate of energy loss by collision for both close and distant collisions is given by the following:

$$-\frac{dE}{dx} = \frac{2Cm_e c^2 Z^2}{\beta^2} \left[\ln\left(\frac{4m_e^2 c^4 \beta^4}{(1-\beta^2)^2 I^2(Z)}\right) - 2\beta^2\right] \quad ...(10)$$

Where I(Z) is the average ionization potential and is a measure of the smallest amount of energy which can be transferred, on the average, to a bound electron. The value I(Z) can be deduced from experimental results or can be calculated theoretically. In 1933 Bloch suggested that $I(Z) = L_H Z$ where $I_H = 13.5$. The average ionization potential has been calculated by Wick (1943), and Halpern (1948) for different materials.

From the previous equation it seems that the parameters which are fundamental importance in the energy loss by a particle are its velocity and charge.

2.4 The Average Energy Loss

From the theoretical curve for energy loss shown in figure 2.2, it is clear that the reduction in energy loss in region (1) is due to the shorter and shorter time spent by the charged particle in the vicinity of each electron and when $\beta \rightarrow 1.0$ no further reduction can occur and the region (2) of minimum ionization is reached.

The region (3) of logarithmic rise corresponds to a relativistic effect and is due to the relativistic extension of the Coulomb field and increases the maximum transferable energy E'_m.

The Fermi plateau (region (4)) of the so called density effect refers to the effect of the medium through which the particle was passing which limits the relativistic extension of the electric field because of the polarizability of the atoms in the medium, as suggested by Swann (1938).

It is more helpful to have an expression for ionization loss by treating the energy which will be transferred to the atom as a whole causing the excitation. Bohr (1915) derived a simple classical theory of ionization loss in which he assumed that the electrons are in a free state; he derived an expression for the average rate of energy loss for a particle having a charge Z_e and velocity V traversing a medium as:

$$-\frac{dE}{dx} = 4\frac{Z^2 e^4 n}{mv^2} \ln \frac{b_{max}}{b_{min}} \qquad \ldots(11)$$

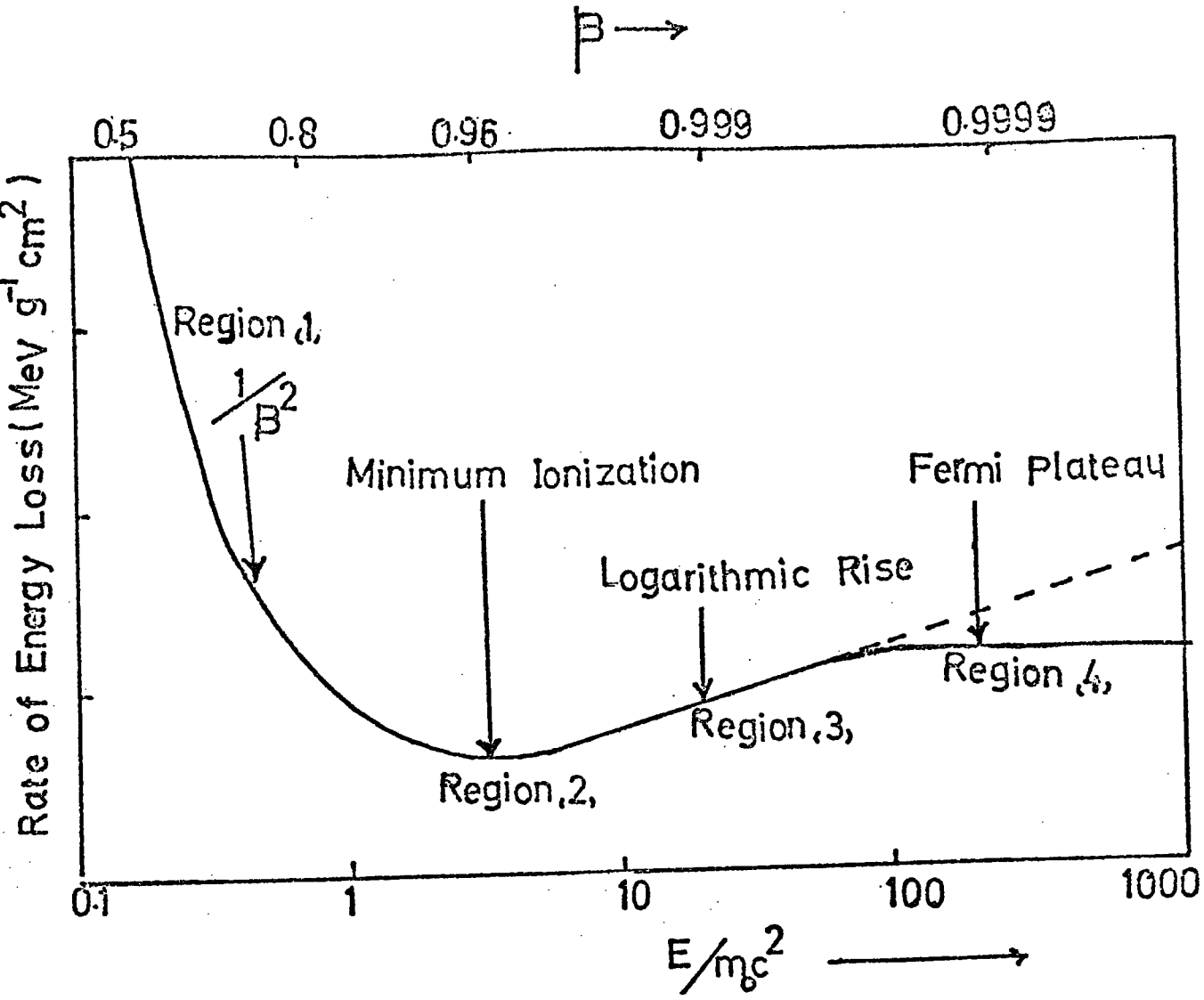

Figure 2-2. A schematic representation of the average energy loss of a charged particle in matter.

Here n represents the number of electrons per g cm^{-2}, m represents the electron mass, and b_{max} and b_{min} represent the maximum and minimum impact parameters respectively. Some workers have used a more direct approach to the problem of the impact parameters. Among them Bethe (1932 - 1933), considered that the energy loss is due to the distant collisions, and he derived the energy loss for a singly charged particle by using Born's approximation :-

$$-\frac{dE}{dx} = \frac{2\pi e^4}{mV^2} N\frac{Z}{A}\left[\ln\left\{\frac{2mc^2\beta^2\eta}{(1-\beta^2)I^2(Z)}\right\} - \beta^2\right] \quad ...(12)$$

η represents the maximum transferable energy and I(Z), the average ionization potential. For both close and distant collisions, the total energy loss is given by the following formula :

$$-\frac{dE}{dx} = \frac{2\pi e^4}{mV^2} N\frac{Z}{A}\left[\ln\left\{\frac{2mc^2\beta^2 E_{max}}{(1-\beta^2)\ I^2(Z)}\right\} - 2\beta^2\right] \quad ...(13)$$

Where E_{max} is the maximum energy transfer (the energy loss from the incident particle) and can be determined from the following formula:

$$E_{max} = \frac{E_o^2 - M^2c^4}{Mc^2\ (M/2m + m/2M + E_o/Mc^2)} \quad ...(14)$$

M is the rest mass of the incident particle and E its total energy. If $M >> m$ or $\frac{M}{m} >> E_o / Mc^2$, then

$E'_{max} \simeq \frac{2mc^2\beta^2}{1-\beta^2}$ is a valid approximation

Therefore

$$-\frac{dE}{dx} = \frac{4\pi e^4}{mV^2} N\frac{Z}{A}\left[\ln\left\{\frac{2mc^2\beta^2}{(1-\beta^2)I^2(Z)}\right\} - 2\beta^2\right] \quad ...(15)$$

Another important quantity is the most probable energy loss. The form derived by Landau is shown in figure 2.3.

It may be mentioned that most experiments measure not the average but the most probable ionization loss which is determined almost entirely by the distant collisions. Another important point is that $-\left(\frac{dE}{dx}\right)_{av}$ (and the most probable loss) is proportional to Z^2, and the average loss does not depend separately on the momentum and on the mass of the incident particle, but only on the ratio of these two quantities (i.e. for all particles of unit charge, the graph of $-\left(\frac{dE}{dx}\right)_{av}$ versus β will be a universal curve).

2.5 The Primary and Secondary Ionization

The ionization produced directly by the primary particle is called the primary ionization. This type of ionization has been discussed by Bethe (1933). If the electrons are removed completely from the atom during the primary ionization process, and have high energy, they can produce further ionization. The latter process of ionization is called secondary ionization.

2.6 The Energy Loss per Ion Pair

The value of the energy loss per ion pair produced is $\approx$ 30 eV for all gases, and is often assumed to be constant for a given material. To determine the value of the energy loss per ion pair there are three important parameters to be discussed:

(A) The type of the gas

(B) The type of the particle used to ionize the gas, and

(C) The energy of the primary ionizing particle.

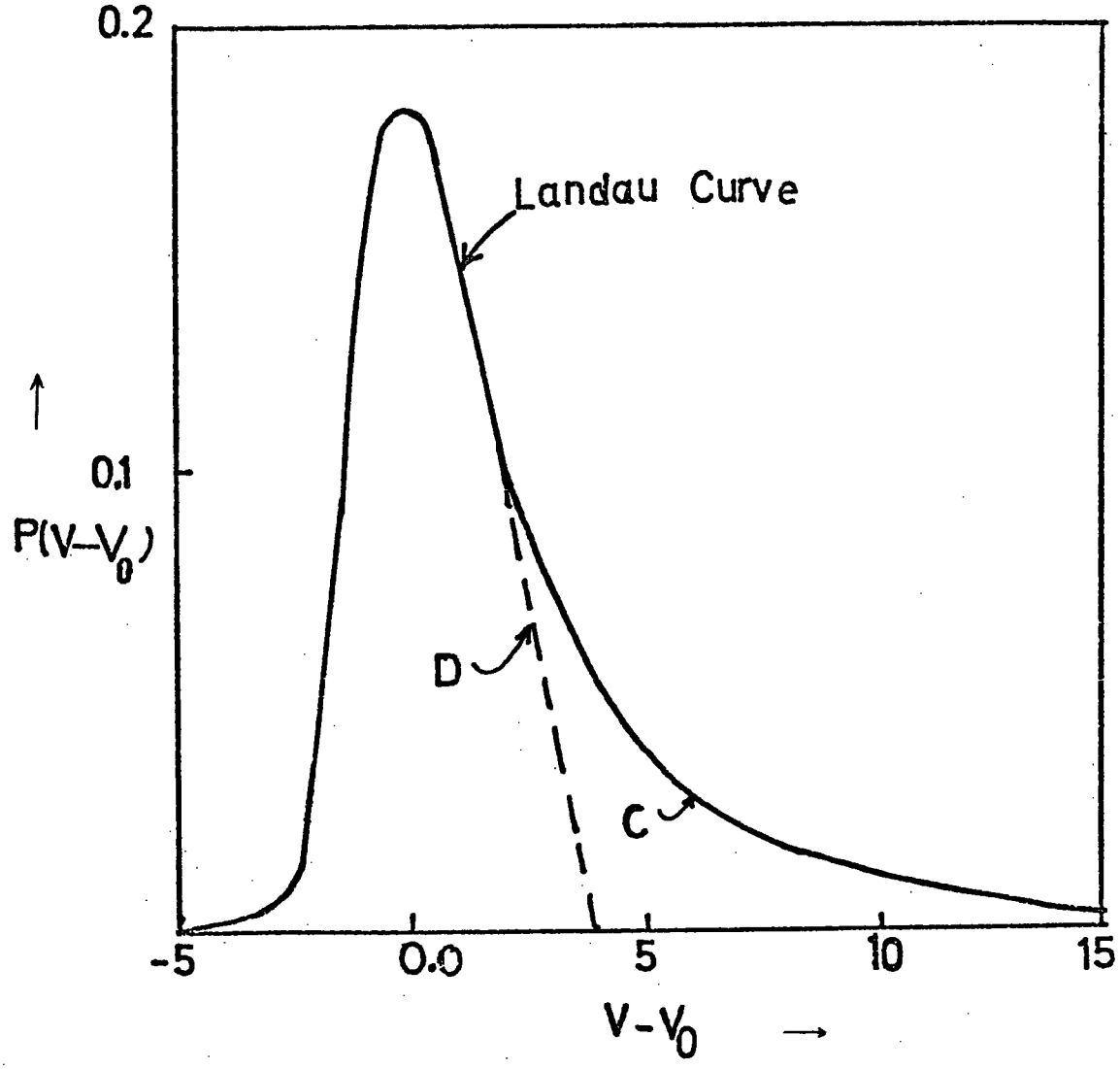

Figure 2-3. The expected frequency distribution of energy loss for distant, D, and close, C, collisions. V_0 is the most probable energy loss. and V the actual loss.
(after Landau (1944)).

Many workers have tabulated the values of energy loss per ion pair including Jesse and Sadauskis (1955), Weiss and Bernstein (1956) and Jesse (1961). A summary of their results is given in table 2.1.

2.7 The Mean Excitation Potential

Few accurate experimental measurements of the mean excitation potential have been made. A rough empirical rule has been found that $I(Z) = 13\ Z$ eV. Kepler (1958) has pointed out that the numerical constant for argon is about 14.6 eV and 24.7 eV for helium.

Turner (1964) and Sternheimer (1966) have obtained a good result from the following relationship:

$$I/Z = 9.76 + 58.8\ Z^{-1.19}\ \text{eV}. \qquad \ldots(16)$$

2.8 Fluctuations in the Energy Loss by Collision

Bohr (1913, 1915), Williams (1929), and Landau (1944) have pointed out that since the energy lost by a charged particle passing through matter is the result of a large number of independent events, the process is a statistical phenomenon, i.e. no unique value for the energy loss is obtained. Thus energy losses may vary; we therefore have a statistical phenomenon. From the point of view of the above authors we can conclude that a large amount of energy can be transferred to the target electron in a single collision. From the results of many experiments, we can observe that in a thin absorber presence of such events can result in relatively large random statistical variations in the total energy loss magnitude.

It is important here to remark that the main difference between the mean and the most probable energy loss is related to close collisions where the impact parameter is small. In fact, the high energy transfers (close-collisions) are also generally difficult to record satisfactorily.

Table 2.1 The energy loss per ion pair (in eV) for various gases

Gas	Weiss and Bernstein (1956)	Jesse and Sadauskis (1955)	Jesse (1961)
Air	33.9	34.1	33.8
H_2	36.3 ± 0.7	36.3	-
He	40.3 ± 0.8	42.3	-
Ne	35.3 ± 0.7	36.7	-
A	25.8 ± 0.5	26.4	-
Kr	24.7 ± 0.5	24.2	-
Xe	22.0 ± 0.4	22.2	-
O_2	31.2 ± 0.6	30.9	-
N	34.6 ± 0.7	34.7	35.0
C_2H_4	26.4 ± 0.5	26.3	26.2

2.9 The Theory of Neon Flash Tube operation:-

2.9.1 Introduction:

Coxell and Wolfendale (1960) measured the characteristics of neon flash tubes and showed that they have a high efficiency for flashing after traversal by ionizing particles, a short sensitive time, a low rate of spurious flashing, high spatial resolution, good stability of operation and long lifetime. The experimental results of Coxell and Wolfendale (1960), and Ashton (1971) are shown in figures 2.4, 2.5, 2.6. The process of electron diffusion, fundamental to the operation of the devices, has been studied by the above authors and a detailed theory has been evolved by Lloyd (1960).

Lloyd gives universal curves for the expected variation of efficiency with time delay in terms of the parameter $a.f_1.Q$ where a is the tube radius, f_1 is the average probability that a single electron is capable of producing a flash when the high voltage pulse is applied and Q is average number of initial electrons produced per unit length in the neon gas. Lloyd predicted that the efficiency is a function of the time that elapses between the passage of the primary particle and the application of the electric field. This prediction is based upon the postulate that each free electron has a chance f, of starting a discharge, and that f depends on the tube operation conditions in an unspecified way, but not on time.

The aim of the author here is to review ideas about the flash tube discharge mechanism, in particular Lloyd's theory for flash tube operation.

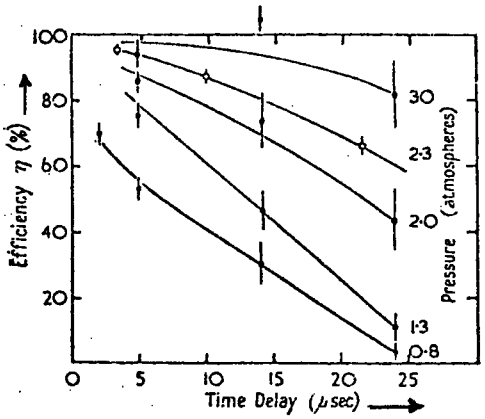

Figure 2.4

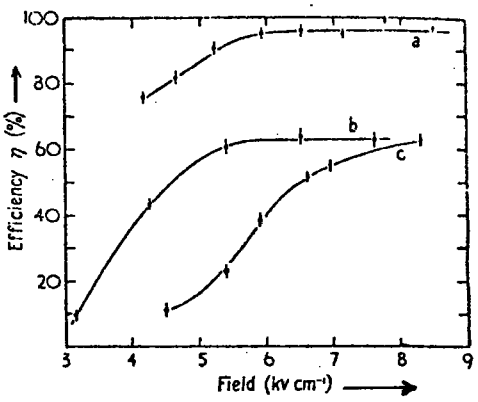

Figure 2.5

Figure 2.4 The efficiency, time delay characteristics of flash tubes with gas pressure as parameter. $E_{max} = 6{\cdot}3$ kv cm^{-1}, $T_R = 0{\cdot}5$ μsec and $\tau = 3{\cdot}0$ μsec.

Figure 2.5 The dependence of efficiency on field for tubes filled at 2·3 atmospheres

a, $T_R = 0{\cdot}5$ μsec, $\tau = 3{\cdot}5$ μsec, $T_D = 3{\cdot}4$ μsec;
b, $T_R = 0{\cdot}5$ μsec, $\tau = 3{\cdot}5$ μsec, $T_D = 26$ μsec;
c, $T_R = 2{\cdot}0$ μsec, $\tau = 3{\cdot}5$ μsec, $T_D = 4{\cdot}0$ μsec.

(After Coxell and Wolfendale (1960)).

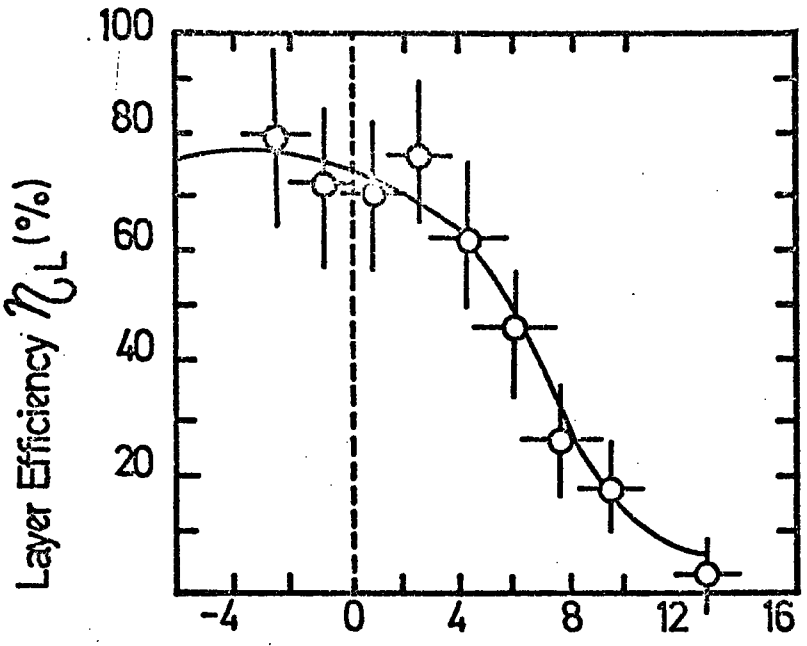

FIG. 2.6. The variation of mean layer efficiency with distance from the electrode edge when tubes of length greater than the electrode length are used. The flashes beyond 4cm. are presumed to be due in the main to photons generated in weak discharges, which then produce photo-electrons between the electrodes.
(After Ashton et al (1971))

2.9.2. The Flash Tube Discharge Mechanisms

When an ionizing particle passes through neon gas in the glass tube it leaves a trail of positive ions, electrons and excited atoms, and, these, with photons, must include the agents which initiate the discharge when the electric field is applied. Gardener et al (1957) have pointed out that the positive ions can play no part, because of their low mobility, the fact that recombination is negligible and they are too few to distort the applied field significantly.

When an ionizing particle passes through the tube electrons must be liberated from the neon atoms; in the presence of an electric field the electrons will be accelerated towards the positive electrode and the electrons undergo elastic and inelastic collisions with the gas atoms. Therefore further ionization takes place. The electric field on the other hand, will also accelerate the newly produced electrons; these latter electrons contribute to the ionization process. Thus an electron avalanche is formed which leaves behind a cloud of positive ions drifting slowly under the action of the field. The transition from an electron avalanche to streamer is characterised by a rapid increase in the ion density. In 1953 Meek and Craggs proposed that this increase was produced by a subsidiary avalanche close to the stem of the main avalanche being diverted into the main avalanche. This diversion was caused by the action of the space charge field of the main avalanche which itself also provides the photons to initiate the subsidiary avalanches. Thus a highly developed avalanche would rapidly cross the anode - cathode gap and a streamer would result. In the flash-tube photons propagate the discharge along the tube and many streamers merge to form a continuous glow.

2.9.3 The Probability of Flashing and Free Electrons in the tube

It seems reasonable to suppose that free electrons present in the gas at the start of the pulse, or produced during the pulse, are solely responsible for the initiation of the discharge. The probability that the tube will flash must then depend upon the number of electrons which have remained in the gas.

2.9.4 Electron Diffusion:

In 1952 Massey and Burhop showed that electrons which reach a glass wall will usually become attached on colliding with it or once in the vicinity of the wall will repeatedly collide with it until they stick.

Electrons which have stuck to the wall probably skate over the surface when the field is applied without re-entering the neon gas again. (In 1947 Carslaw and Jaeger pointed out, that the electron wanders from its starting point).

It seems to us, from the work of Coxell and Wolfendale (1960), that the reduction in efficiency of the flash tube with increasing time delay must be due to some process which removes the free electrons, liberated by the ionizing particle, during the delay time. Four possible mechanisms are capable of producing this effect:

(1) The recombination of the electrons with the positive ions,

(2) The thermal diffusion of these electrons to the walls of the tube and subsequent attachment,

(3) The capture of the electrons by impurity atoms or molecules to form negative ions, and

(4) The sweeping out of these electrons by some residual field, caused by the application of previous pulses. This could take the form of an accumulation of charge on the tube walls or the polarization of the glass.

2.9.5 The Electron Liberation:

In 1973 Conversi pointed out that the gas of a neon flash tube does not normally contain free charges, except for a short time after the passage through it of an ionizing particle. When a single relativistic particle traverses a tube some 30 ion pairs are produced along its track and, in the time interval τ_D before the high voltage pulse is applied, the electrons drift under the influence of any clearing field that may be present and furthermore are subject to diffusion. The electrons liberated by an ionizing particle will thus be slowly removed from the gas and therefore the efficiency of the flash tube will decrease with increasing time delay.

As has been mentioned already the theory of flash tube operation was given by Lloyd (1960). He considered that electrons can be produced not only by the initial particle but also by the decay of metastable atoms and their subsequent diffusion. Lloyd estimated that the electrons are reduced to thermal energy after a short period (say one μs).

2.9.6 Knock-on electrons from the walls:

All primary particles will pass through the glass of the tube and occasionally electrons are produced due to the collision (central collisions), between the primary particle and the glass atoms. The electrons created from these collisions are the so-called knock-on electrons. These electrons will traverse the neon gas of the tubes and will also contribute to the ionization.

2.10 Brief account of the Properties of Flash Tubes and Comparison with Lloyd's Theory:

From the experimental aspects of many workers with neon flash tubes, the neon flash tube is considered to be the first of a new family of particle detectors which have played an important role in the development of cosmic ray and elementary particle physics during the last 15 years or so. The application of neon flash tubes has been mainly in the location of cosmic ray particle tracks and a vast number of experiments using the technique have been carried out, for example:

(A) Arrays of tubes have been used in magnetic spectrographs (Brooke et al. (1962)).

(B) Arrays have also been used to study the structure of extensive air showers (Earnshaw et al (1967)),and

(C) Neutrino interactions have been studied at great depths underground (Achar et al (1965)).

Conversi (1973) has pointed out that there are however, other features which make the flash tubes interesting for application as particle detectors, once their sensitive and recovery time are reduced. Electrodeless flash tubes, in fact, can operate over long periods of time without replacement of the filling gas, they can be adjusted to any given experimental geometry, in particular to give a 4π - geometry; high repetition rates can be reached in principle with current high-voltage power supplies, since the energy required to flash the tubes is small. Flash tubes also have other appealing possibilities:

(i) High efficiency detection of multitrack events with a large range of angular inclination of the tracks.

(ii) Statistical determination of the ionization of single charged particles traversing many layers of flash tubes.

(iii) Digitization of the information by means of light sensors and

(iv) Possibility of re-arranging the same tubes in several different experiments.

It has been pointed out that the neon flash tube may flash even if a particle passes through the glass wall of the tube and avoids the gas. This phenomenon is mainly due to

(A) energetic electrons knocked out of the glass by the particle and

(B) some photon, which accompanies the particle, causing photo-electric emission or Compton scattering in the gas.

The converse is also true, that is a tube might not flash if a particle does pass through the gas. This may occur when the trajectory is near the wall of the tube and the path length through the gas is much less than the spark formation distance (Breare 1973).

It is convenient to recall briefly the requirements for a satisfactory flash-tube performance and the main parameters on which it depends. The requirements for most applications are a high detection efficiency (i.e. high probability for flashing after traversal by an ionizing particle), a low rate of spurious flashes (i.e. flashes not related to any particle traversal), a good overall spacetime resolution (i.e. tubes of small diameter with sensitive times as short as allowed by the triggering requirement), a short recovery time, stability and reproducibility of operation, and a long life time.

All items or parameters listed above have been measured by the Durham University groups. I shall confine myself here to outline Lloyd's ideas relative to the flash tube operation. The main point in the following discussion is that the probability that a tube will flash must depend upon the number of free electrons which have remained in the gas; the efficiency is then a function of the time that elapses between the passage of the primary particle and the application of the electric field. On Lloyd's theory it was assumed that it at least one electron is present in the gas when the pulse is applied, the tube will flash. Coxell and Wolfendale (1960) have determined the value f in Lloyd's postulation (i.e. the probability of one electron initiating a discharge); their results give an empirical relationship between efficiency and delay as shown in figure 2.7. Some workers have found different values of f, among them Ashton et al (1971). The explanation of the differences is probably that the rise times of the pulses used were different.

In order to test Lloyd's theoretical considerations, Diggory et al (1971) demonstrated the ability of flash tubes to detect differences in ionization rates by particles of different momenta and type. They measured the flash-tube efficiency for cosmic ray protons and mesons in the momentum range 0.1 - 10 GeV/c. Time delays before pulsing of 50 μ secs and 80 μ secs were used, variations in efficiency from 58% to 38% were observed and found to be in good agreement with theoretical estimates based on Lloyd's theory.

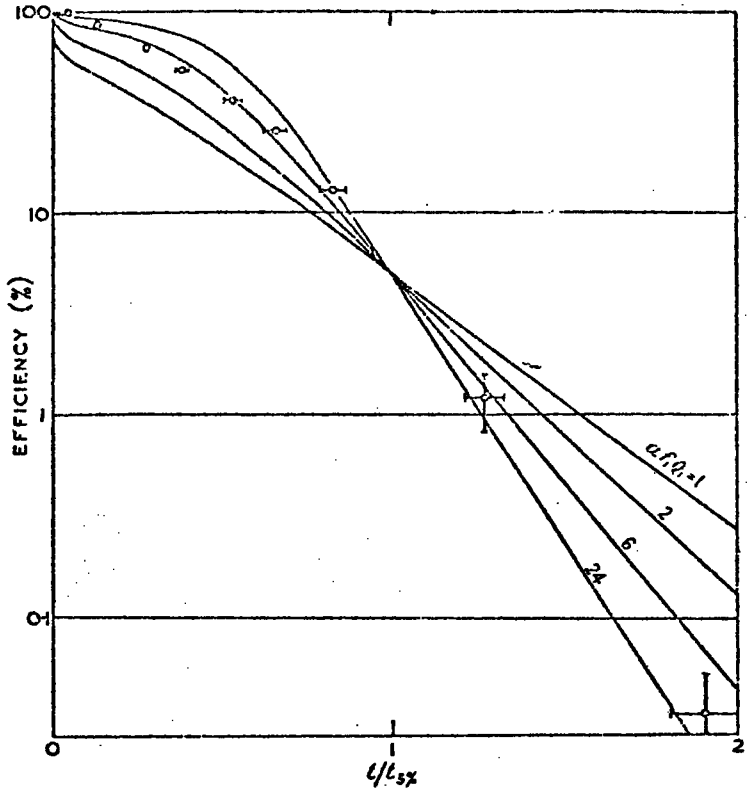

Figure 2-7. Comparison of the theoretical curves of Lloyd with results of Coxell and Wolfendale (1960).

Coxell and Wolfendale (1960).

Theory of Lloyd (1960).

a is the tube radius.

f is the average probability that a single electron is capable of producing a flash when the high voltage pulse is applied.

Q is the average number of initial electrons produced per unit length in the neon gas.

CHAPTER THREE

The Experimental Equipment

3.1 Introduction

There are two main uses for cosmic ray spectrographs. Firstly, they may be used to measure the signs and momenta of charged cosmic ray particles so enabling measurements of fundamental aspects of cosmic rays to be made and secondly they will select a beam of particles of known signs and momenta. The first measurement can give information about the interactions in which the secondary cosmic rays are formed, while the second type of use can extend our knowledge of the nature of the interactions of the particles found at a particular depth of observation in the atmosphere.

Most spectrographs are near sea-level and therefore the principal particle which can be studied is the muon, and the principal interactions are those of electro-magnetic origin. It is clear that if the acceptance area of the spectrograph is sufficiently large, the less frequent protons and pions can also be investigated.

The original spectrographs in the main used Geiger Müller counters as triggering elements, and also for measuring the particle in the magnetic fields. (Hyams et al, 1950; Brooke and Wolfendale, 1962). Some workers used additional detectors to extend the range of particle momentum which could be measured; for example Holmes et al. (1961) added three cloud chambers to the Manchester spectrograph so increasing the maximum detectable momentum (MDM) of the instrument from 21 GeV/c to 240 GeV/c. Table 3.1 summarizes spectrographs which have been operated

since 1950, and includes both air gap and solid iron types. The solid iron spectrographs generally have a higher MDM than those of the air gap type, but suffer from enhanced scattering problems.

3.2 The Instrument

The spectrograph employed in the present work is situated at Durham (200 ft. above sea-level, geographical coordinates: Latitude 54.5°N, Longitude 1.3°W). The measurements of this experiment were made during February - September, 1973. Single particles, predominantly muons in the cosmic ray beam, incident within 15° of the vertical were selected using Geiger-Müller counter trays at a rate of about 2×10^{4} day^{-1}. Those particles which are nuclear active were identified by the evaporation neutrons they produced in a modified IGY neutron monitor. The instrument is similar in principle to that used by Brooke and Wolfendale (1964) and comprises a large air gap magnet spectrograph and a neutron monitor. The equipment of the present experiment is considerably larger, provides more detailed information on the particles but does not have as high a momentum resolution as the earlier device. A full description of the instrument is given by Diggory et al (1974).

3.3 Design and Construction

The instrument used for this experiment is shown in figure 3.1. It comprises the magnetic spectrograph and modified neutron monitor system, described by Diggory et al (1974), supplemented by 20 layers of neon flash tubes (tray Y), two plastic scintillator detectors, and a water Cerenkov threshold detector.

Table 3.1 Solid iron and air gap spectrographs which have been operated since 1950, and spectrographs at present under construction

Authors	Location	MDM (GeV/c)	Acceptance (cm² sr)	Zenith angle	$\int B\,dl$ (gauss cm)	Detectors
A. *Air gap spectrographs* (post 1950)						
Hyams *et al* (1950)	Manchester, UK	21	0·93	0°	$6{\cdot}5\times10^{5}$	GM
Holmes *et al* (1961)		240	0·93	0°	$5{\cdot}97\times10^{6}$	GM and CC
Caro *et al* (1951)	Melbourne, Australia	50	0·69	0°	$6{\cdot}6\times10^{5}$†	GM
Moroney and Parry (1954)		50	0·69	0°, 30°, 60°	$6{\cdot}6\times10^{5}$†	GM
Pine *et al* (1959)	Cornell, USA	176	6·9	0°	$1{\cdot}5\times10^{6}$†	GM and CC
Pak *et al* (1961)		120		0°, 68°	$1{\cdot}5\times10^{6}$†	GM and FT
Brooke *et al* (1962)	Durham, UK	18	8·0	0°	$6{\cdot}4\times10^{5}$	GM
Hayman and Wolfendale (1962a)		443	8·0	0°	$6{\cdot}03\times10^{5}$	GM and FT
Coates and Nash (1962)	Nottingham, UK	29	0·73	0°, 30°, 45°	$1{\cdot}07\times10^{5}$	GM and FT
Judge and Nash (1965a, b)		28	0·73	30°, 45°, 60° 83°–90°	$1{\cdot}05\times10^{5}$	GM and FT
Kasha *et al* (1968)	Brookhaven, USA	950	100	75°	$1{\cdot}64\times10^{6}$	S and OSC
Asbury *et al* (1970)	Argonne, USA	830	500	75°, 80°, 85°	$3{\cdot}4\times10^{6}$	S and OSC
Flatte *et al* (1971)	Stanford, USA	2000	570	60°–87°	$3{\cdot}0\times10^{6}$	S and OSC
B. *Solid iron spectrographs*						
Kamiya *et al* (1962)	Nagoya, Japan	100		75°–90°	$4{\cdot}0\times10^{6}$†	S and FT
Ashton and Wolfendale (1963)	Durham, UK	40		80°	$9{\cdot}8\times10^{5}$	GM
Ashton *et al* (1966)		198	30	77·5°–90°	$9{\cdot}82\times10^{5}$	GM and FT
Baber *et al* (1968a, b)	Nottingham, UK	360	18·6	0°	$2{\cdot}6\times10^{6}$	GM and FT
MacKeown *et al* (1966b)	Durham, UK	1045		82·5°–90°	$1{\cdot}95\times10^{6}$	GM and FT
Aurela and Wolfendale (1967)		270	13	0°	$8{\cdot}2\times10^{5}$	GM and FT

Table 3.1-*Contd.*

Authors	Location	MDM (GeV/*c*)	Acceptance (cm^2 sr)	Zenith angle	$\int B\,dl$ (gauss cm)	Detectors
Alchudjian *et al* (1968)	Mount Aragatz, USSR	3000	105	83°–90°	$3{\cdot}65\times10^6$	GM and WSC
Palmer and Nash (1969)	Nottingham, UK	420		80°	$1{\cdot}90\times10^6$	GM and FT
Flint and Nash (1970)		428		80°	$1{\cdot}87\times10^6$	S and FT
Nandi and Sinha (1970)	Durgapur, India	520	11·7	0°	$3{\cdot}24\times10^6$	GM and FT
Fujii *et al* (1969)	Nagoya, Japan	1280	85	79°–90°	$3{\cdot}5\times10^6$	S and FT
Allkofer *et al* (1970d)	Kiel, W Germany	1000	16	Variable	$3{\cdot}2\times10^6$	S and OSC
C. *Spectrographs in course of construction or design*						
R K Adair *et al* (private communication)	Brookhaven, USA	2000	150	Variable	$4{\cdot}48\times10^6$	S and OSC
G È Masek *et al* (private communication)	San Diego, USA	4500	3000	Variable	3×10^6	S and WSC
J Cousins *et al* (1970)	Nottingham, UK	3000	120	0°	$2{\cdot}7\times10^6$	GM and FT (Vidicon camera)
F Reines *et al* (private communication)	Irvine, USA	15 000	2500	90°	$1{\cdot}8\times10^6$	S and WSC
Allkofer *et al* (1971d)	Tel Aviv	7000	1466	85°	$4{\cdot}8\times10^6$	S and WSC
Ayre *et al* (1972a, b)	Durham UK	6000	818	0°	$8{\cdot}09\times10^6$	S and FT

Key:

† Estimated value
FT = Flash-tubes
GM = Geiger counters
OSC = Optical spark chambers
S = Scintillation counters
WSC = Wire spark chambers
CC = Cloud chambers

(After Thompson (1973)).

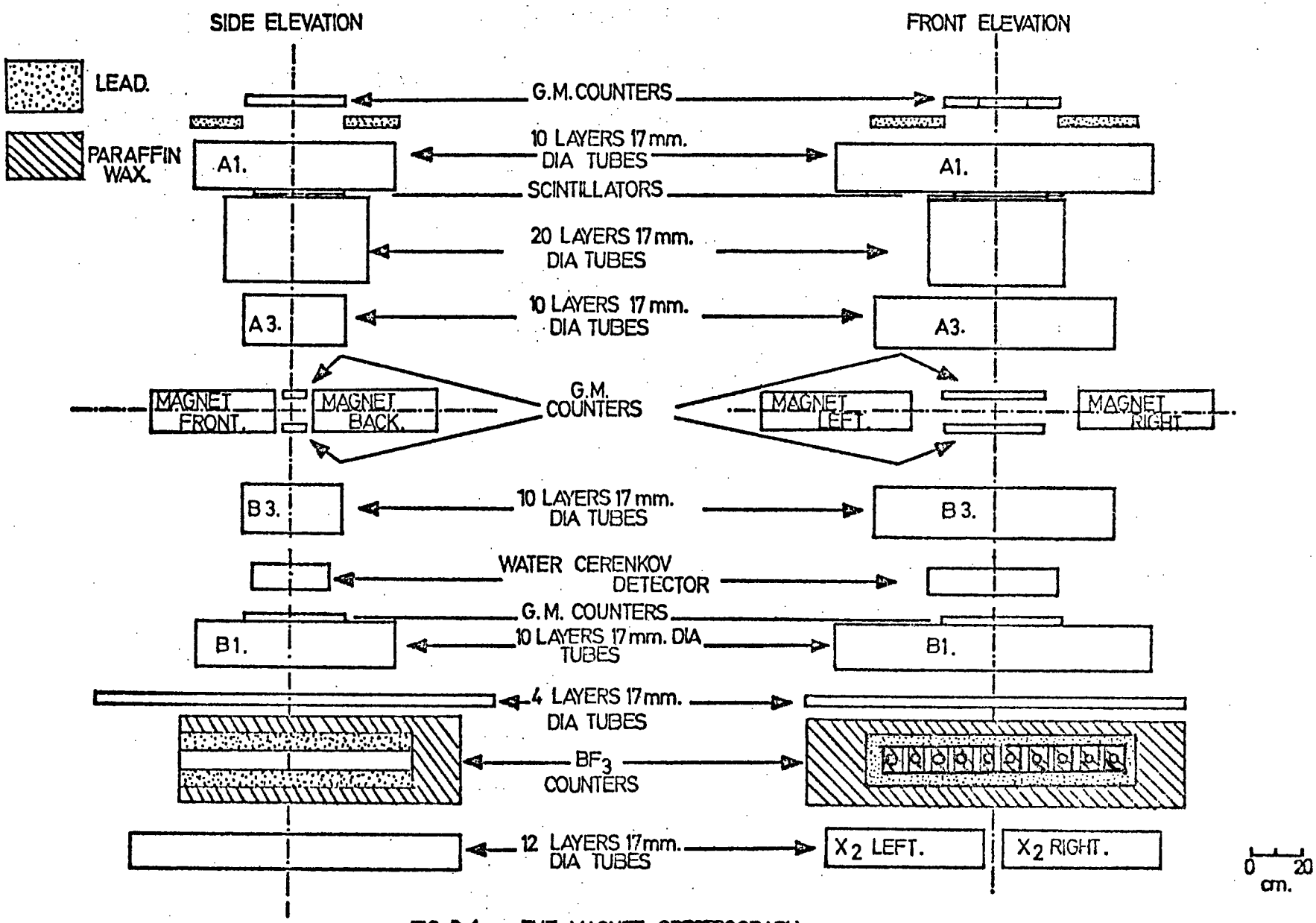

FIG. 3-1. THE MAGNET SPECTROGRAPH.

The main body of the magnet consists of twenty four pairs of iron plates situated side by side and separated as shown in figure 3.2. The total thickness of these plates is approximately 30 cm. The magnet was operated at a normal current of 20 A during the experimental run, this current giving a field of about 12,000 gauss in the pole gap. From figure 3.1, it can be seen that there are five trays of neon flash tubes (A1, Y, A3, B3 and B1). The trays A1, A3, B3, and B1 represent the momentum trays.

Tray Y has been added to the equipment to increase the number of flash tubes traversed by the ionizing particle for the present energy loss study. The characteristics and specification of each tray are tabulated in table 3.2.

The neutron monitor comprises a producing layer of lead of average thickness 285 cm^{-2} (i.e. 1.32 interaction lengths), and 10 BF_3 counters, for the detection of evaporation neutrons produced by the nuclear active particles (π - mesons and protons). The multiplicity of neutrons detected by each counter is recorded separately. A full description is given by Jenkins (1974).

3.4 Neon Flash Tubes as Visual Detectors

Many workers have used neon flash tubes as visual detectors for ionizing charged particles. These devices, invented by Conversi's group at Pisa (Conversi et al, 1955), were developed rapidly for use in cosmic ray spectrographs by the Durham group (e.g. Gardner et al, 1957; Coxell and Wolfendale, 1960).

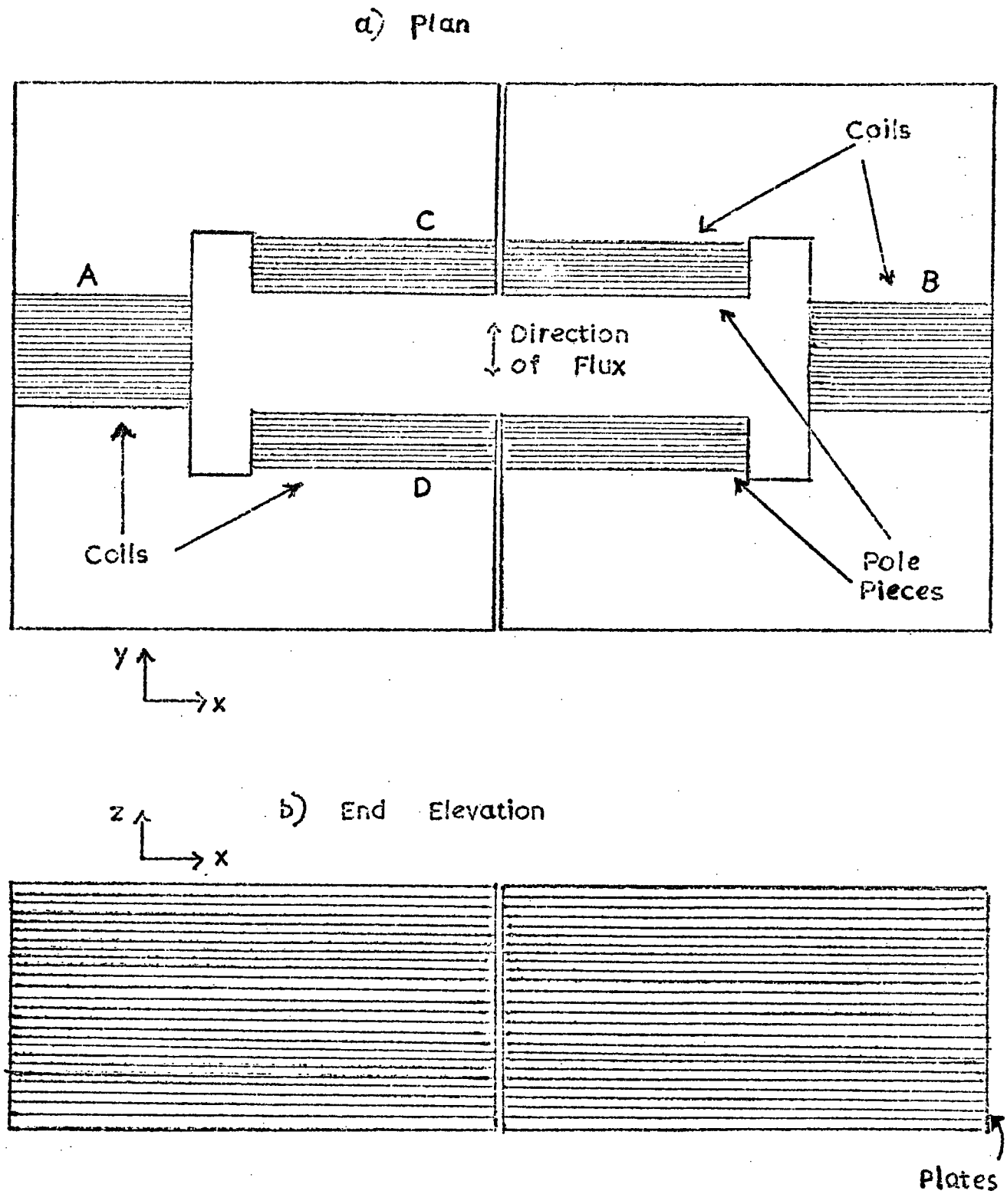

Figure 3-2. The Construction of the Air-Gap Magnet.

Table 3.2 The Flash Tube Trays

Tray	A1	A3	B3	B1	X1	X2
The Flash Tubes	Internal and External diameter = 1.6 and 1.8cm respectively. Neon gas pressure = 60 cm Hg.					
Number of Tubes	990	760	760	990	400	1284
Number of Layers	10	10	10	10	4	12
Pitch of Layers (cm)	3.2	3.2	3.2	3.2	1.8	1.8
Pitch of Tubes (cm)	1.907	1.907	1.907	1.907	1.8	1.8
Length of Tubes (cm)	120	120	60	60	250	200
Tube support	Supported at each end in accurately machined slots in rectangular duralumin tubing				Close-packed self supporting	
Arrangement of Electrodes	Between each layer				Between every two layers	

The main aim of experimentalists who used neon flash tubes in cosmic ray spectrographs addition to G.M counters was to increase the maximum detectable momentum of the spectrographs, Holmes et al (1961), MacKeown et al (1966) and Aurela and Wolfendale (1967).

As a practical technique, neon flash tubes are similar to spark chambers. The tubes consist of soda glass filled with neon which can be made to flash by applying a high voltage pulse of few kilovolts per cm Peak, within a few microseconds of the passage of the ionizing particle. One of the ends of the tubes is flat and used as a window for observing the discharge. Each tube is painted black to avoid light spreading to adjacent tubes. In the present work five stacks of neon flash tubes are used to study the energy loss of mesons and protons with known momentum in neon gas.

3.5 Recording of data

The data from the spectrograph are recorded on two films, type 35 mm, Ilford HP4, using two Shackman automatic recording cameras. The data from the two films were first analysed using the following criteria :-

(1) Film A: Each frame on this film indicated trays A1, Y and A3 and also showed digitised Čerenkov detector and scintillator pulse heights, number of flash tubes and the multiplicity of neutrons detected in each BF_3 counter.

(2) Film B: Each frame of this film showed trays B3, B1, X1 and X2. From this information, we can observe the passage of the particle in X2 beneath the neutron monitor; this information is important and leads us to identify the particle passing through the neutron monitor. (More details are shown in figure 3.3).

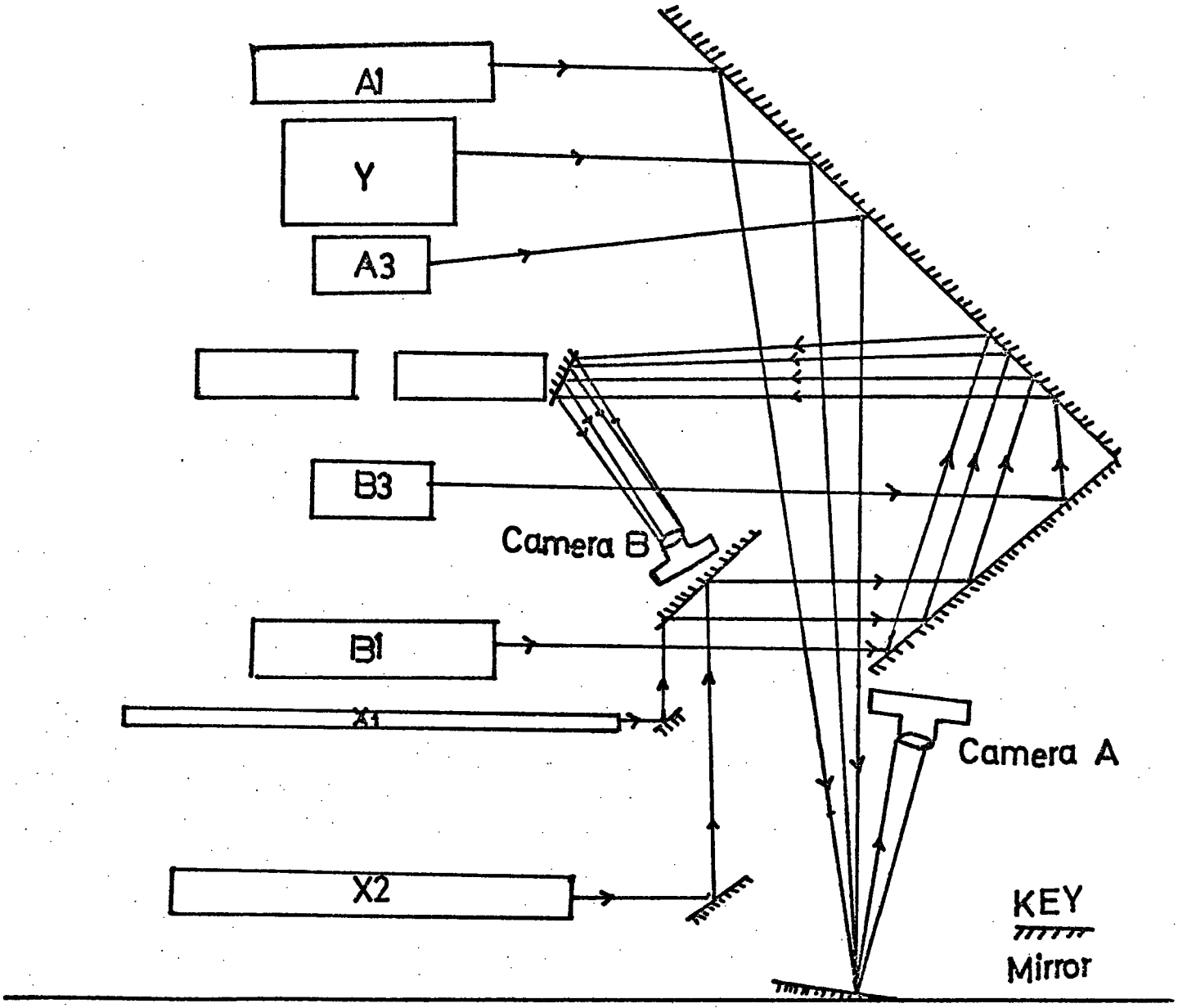

Figure 3-3 Arrangement of mirror system for array photography in The Durham University nuclear active particle spectrograph (After Hook et al 1973.).

Each film has the same frame for each event recorded. The data so recorded were summarized on special sheets and included: film number, event number, number of flash tubes flashed, the response of neutron monitor, Water Čerenkov and Scintillator signals. The momentum of the particles was assessed using the computer track fitting procedure derived by Hook (1973) (See Chapter 4 for more details).

3.6 Magnetic Deflection of the charged Particles and Estimation of the momentum:

When a charged particle penetrates the magnetic field of the spectrograph, the charged particle is deflected due to the magnetic field. In this situation Geiger counters are used to select the particles which pass through the prescribed region of field (see figure 3.4).

If the trajectory of the charged particle which penetrated the magnetic spectrograph has a radius of curvature ρ the magnetic field has strength H, and if we consider that the particle has a mass m_o, velocity V, and charge Ze, then ρ is given by the well known relation:

$$HZeV = \frac{m_o V^2}{\rho} \qquad \text{i.e.} \quad \rho = \frac{m_o V}{HZe}$$

If $d\Phi$ represents the angular deflection of the particle in moving a distance dl, then

$$\rho d\Phi = dl, \quad \text{i.e.} \quad \rho = \frac{dl}{d\Phi}$$

$$\text{thus } \frac{dl}{d\Phi} = \frac{m_o V}{HZe} \quad \text{and } Pd\Phi = ZeHdl$$

P represents the momentum of the particle,

Integrating yields $P\Phi = Ze \int dl$

$$\therefore \quad P = 300 \int \frac{Hdl}{\Phi}$$

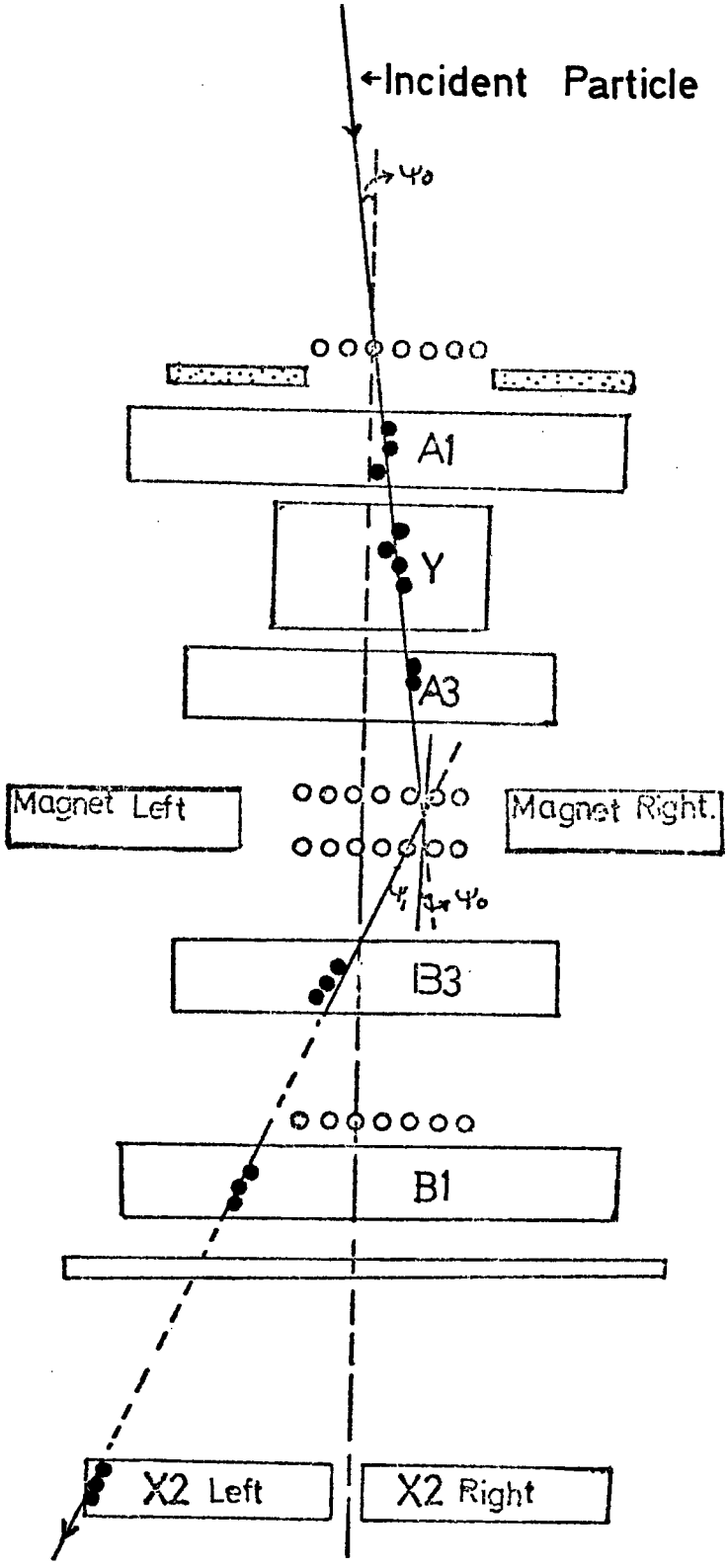

Figure 3-4 Schematic diagram of arrangement of G.M. counters and the deflection of the incident particle in the magnetic field.

Where P measured in eV/c, $\int$ Hdl in gauss.cm and Φ in radians.

The value $\int$ Hdl is constant for a given value of magnet current, and thus

$$P = \frac{\text{Constant}}{\Phi}$$

From a knowledge of Φ (from the flash tube data) and the constant of the instrument the momentum of the charged particle can be easily calculated, and from the polarity of the magnetic field the charge also can be estimated.

CHAPTER FOUR

Analysis of Data

4.1 The available information

The following data were available for each event recorded by the spectrograph:

(1) The film number and the event number.

(2) Solar time.

(3) The direction of the particle track.

(4) The value and the polarity of the magnetic field.

(5) The number of neutrons detected by each counter in the neutron monitor and the total number of recorded neutrons.

(6) The presence, or otherwise, of secondary particles beneath the neutron monitor and a measure of their scatter in the producing layer of the neutron monitor.

The information derived from the above data leads us to identify the types of events (muons or NAP). This information is the following:

(1) The momentum and charge of the particle.

(2) The track impact in the N.M.

(3) The perpendicular scattering (the distance between the actual track emerging from the neutron monitor as shown in figure 4.1).

4.2 Data Analysis

We have outlined the available information which is required to identify the type of particle triggering the instrument and now the method by which the data are obtained will be discussed.

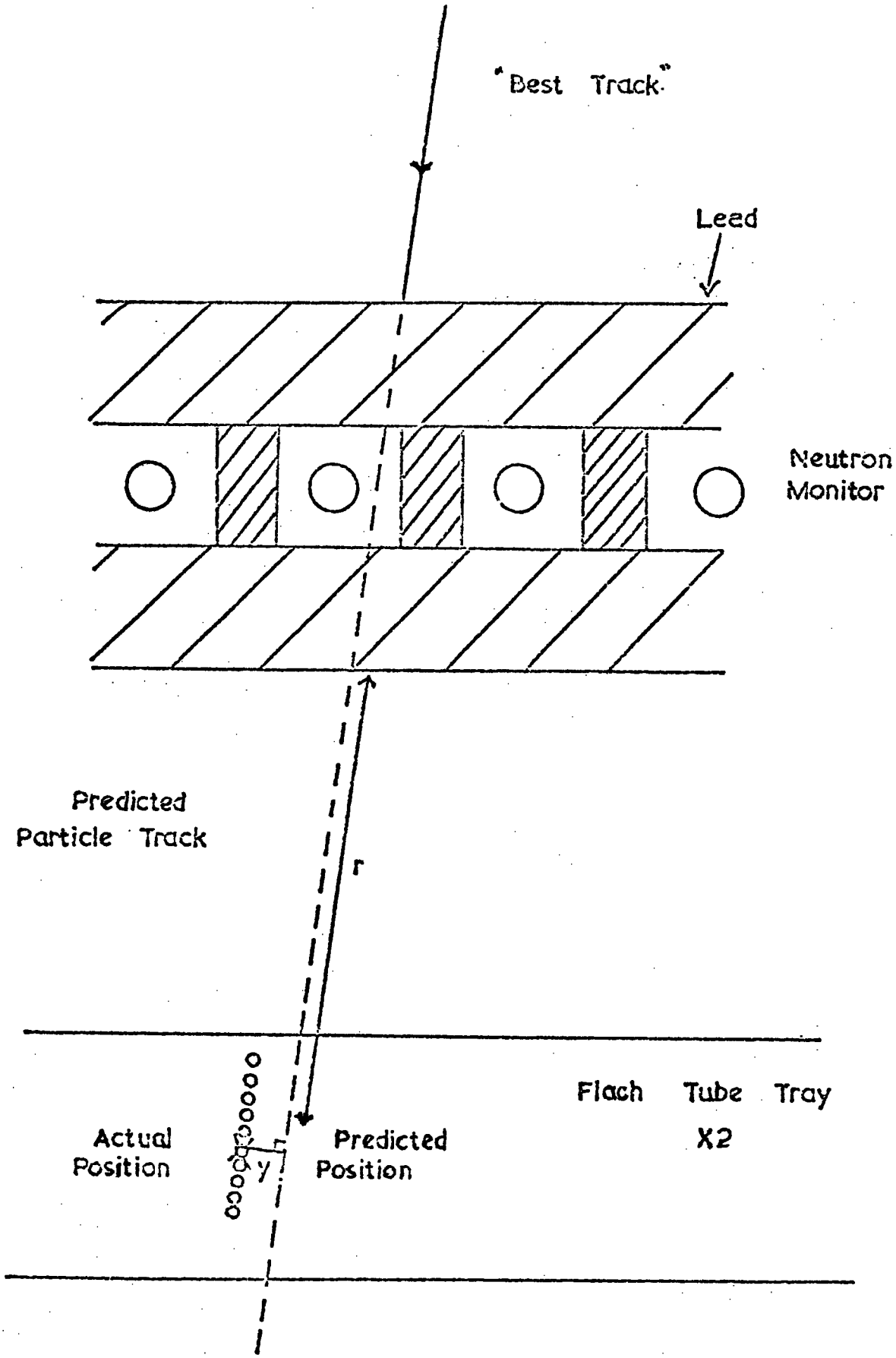

Figure 4-1. The Scattering of Particles in the Neutron Monitor.

4.2.1 Initial Scanning of Films

There are some types of events which were rejected during the analysis; these events involved either interactions in a flash tube tray or more than one particle track in a momentum measurement flash tube tray. The events analysed in the data are characterised by the following:

1. Events having one complete track in the spectrograph.
2. Events having two tracks, one of them a complete track with sufficient information to allow correct analysis.
3. Events having more than one complete track. These types of events have been studied carefully so that the best track might be estimated, i.e. the track which fits best the triggering requirements.

4.2.2 Track Count

The particle tracks were constructed using the information indicated in 4.1 and 4.2.1. In order to gain further information about the track, a check has been made about which of the flash tubes have flashed to delineate the particle track by taking two methods for enumeration, as follows:

A. Direct Enumeration:

This method involves the projection by photographic enlarger onto an underlay on which the positions of the flash tubes together with their numbers were marked. The track was counted by placing the underlay onto fixed marks and then the flash tube number was encoded on punched cards ready for analysis by computer programme derived by Hook (1973).

B. Count from Prints:

This method was used for the complex events. A photographic print was made in order to select the best track. These events were counted, using a transparent overlay on which were marked the fixed positions of the tubes in the trays.

4.3 The Computer Track Fitting Programme:

The large amount of the data to be analysed requires the computer assistance track fitting programme. The computer technique has been derived previously by Bull et al (1962). The following method developed by Hook (1973), has therefore been employed and summarized as the following procedure:

1. We consider that a tube will flash when a particle traverses it up to some distance Z from the centre.
2. A suitable trajectory was built and the probability of the observed arrangement of flashed tubes was calculated.
3. We adopted the trajectory which had the highest probability as the best estimate of the actual trajectory of the particle.

A comparison has been made of the computer method with the well - proved hand analysis method. The latter method allows the maximum track length in the non - flashed tubes.

Finally, it is important to remark that the computer track fitting programme provides us with the following information:

1. The acceptability of the best track.
2. The number of flash tubes which are not in the same direction as the computer - fitted track.
3. The efficiency of the track as a whole.

4. The momentum of the charged particle, due to the deflection in the magnetic field, and also the incident and deflection angle in each momentum tray, and in the X2 tray.
5. The approximate impact point of the best track on the N.M.
6. The amount of material traversed by the charged particle due to the interaction with the lead absorber.
7. The perpendicular scattering (the distance between the actual track and the predicted track).
8. The scattering angle of the particle due to the interactions between the charged particle and the lead - nuclei in the neutron monitor.

We note that point 7 and 8 are very important to us leading to the best identification of particles having X2 tracks.

4.4 Identification of the particles:

In the following identification it is assumed that there are no antiprotons in the cosmic radiation at sea - level. So the expected particles to be recorded in the present work can be identified in the following categories:

1. Positive and negative pions and protons, (NAP), these types of particle are characterised with a strong nuclear interaction with a nucleus in the neutron monitor.
2. Accidental cosmic ray muons, interacting muon, or NAP's with the neutron recorded by the neutron monitor.
3. A slow, stopping, negative muon which stops in the neutron monitor and is captured by a Pb - nucleus to produce a response.

4. An accidental coincidence between the single particle (GM) trigger (from the experimental facts, this type of single particle is produced by a muon that passes through the monitor without interacting) and the monitor which counts neutrons produced by low energy cosmic ray neutrons by a strong interaction with a nucleus in the monitor.

It is clear that the four processes indicated above can give rise to a single particle event with a response from the neutron monitor, this information indeed assists us to identify the types of single event.

All families of single events which were included in the basic data are shown in table 4.1. In the following discussion a brief illustration is given of the way in which muons and NAP's are separated.

4.4.1 Events with no track in F.T. tray X2

In these events there is no track observed in the flash tubes beneath the neutron monitor (see Fig. 4.1), and those particles which are nuclear are identified by the evaporation neutrons they produced in the neutron monitor.

In our measurements here there are two types of events dealing with the above heading of the section. The first type is class $B^{\pm}$ which includes positive and negative pions and protons (assuming there are no antiprotons in the cosmic ray beam at sea-level). These particles are also characterised with good impact, i.e. the majority of evaporation neutrons are detected close to their point of production.

The second type is $D^{\pm}$ which mainly represents slow positive and negative mesons associated with random neutrons. These events are characterised by bad impacts. Table 4.1 described the basic characteristics of both of these two clases.

4.4.2 Events with track in F.T. tray X2 (scattering of particle in the neutron monitor)

The charged particles emerging from the neutron monitor were observed using the X2 flash tube tray. (More details about this tray are given in table 3.2 Chapter 3). The tray X2 was used to measure the lateral position of a particle emerging from the neutron monitor, which when compared with the expected position, due allowance being made for the scattering of muon in the material of the neutron monitor, enabled the particles to be identified (Hook and Turver, 1974).

In our categories the types of particles of the above section involved class $A^{\pm}$ and $C^{\pm}$. The properties of each class can be seen in table 4.1. It is important to remark that class $A^{\pm}$ comprises a mixture of NAP's and muons. In this situation class $A^{\pm}$ consists of accidental muons, interacting muons or NAP's, so, it is clear here that for those events which have more than one track beneath the neutron monitor, the perpendicular scattering can be used to distinguish between muons and NAP's(the lateral position for a muon of momentum 3 GeV/c would be scattered in the material of the monitor by about 10 mm (Hook and Turver, 1974).

4.4.3 Identification of NAP's and muons

As remarked already, the particles which constitute muons and NAP's together in our measurements are class $A^{\pm}$ (the characteristics of this class are indicated in table 4.1), muons and NAP's were separated using the scattering in the neutron monitor. The method of scattering can be summarised as follows. Consider figure 4.1, which shows the scattering of particles in the neutron monitor. Both muons and NAP's will have undergone coulomb scattering in the material of the monitor. NAP's will also make nuclear interactions with Pb - nuclei of the monitor.

Following Hook and Turver 1971, we assume that if the emergent track is within 2 δy (where δy represent the r.m.s. value of coulomb scattering, due to collision with Pb - nuclei) then the particle is a muon . On the other hand events with values of scatter $\geq 8\delta y$ are identified as NAP's.

4.5 Summary of Information available for energy loss experiment

Including the information for the identification of the particles discussed above, the following data were available for energy loss measurement in the present work:

(1) The film number.

(2) The event number.

(3) The momentum of the particle.

(4) The number of flash tubes flashed for each single event which traversed the arrays in the spectrograph (muons and NAP's).

(5) The mean pulse amplitude for the two plastic scintillation detectors situated above the Y tray, measured in mV, in order to determine the energy loss.

Further information comprised the Čerenkov pulse amplitude from the threshold water Čerenkov detector above the B1 tray.

Table 4.1 Particle Characteristics

Class	Characteristics	Type of events
$A^{\pm}$	Good impact, with X2 track.	Mixture of NAP's and muons (interacting muons and accidental muons). The method of separation has been discussed in section 4.4.3
$B^{\pm}$	Good impact, no X2 track.	Particles characterised by a strong interaction with a nucleus in the N.M. and consists of positive and negative pions and protons (assuming there are virtually no anti-protons in the cosmic ray beam at sea level). Distinction between pions and protons made as follows. Protons have momentum usually around 1 GeV/c high flash tube number, high scintillator pulse amplitude, and zero Čerenkov pulse amplitude.
$C^{\pm}$	Bad impact, with X2 track.	Accidental muons because their scattering in the lead of the N.M. in the range $o < S_c < 7$ as shown in figures 4.2 and 4.3.
$D^{\pm}$	Bad impact, no X2 track.	Slow muons and random neutrons.

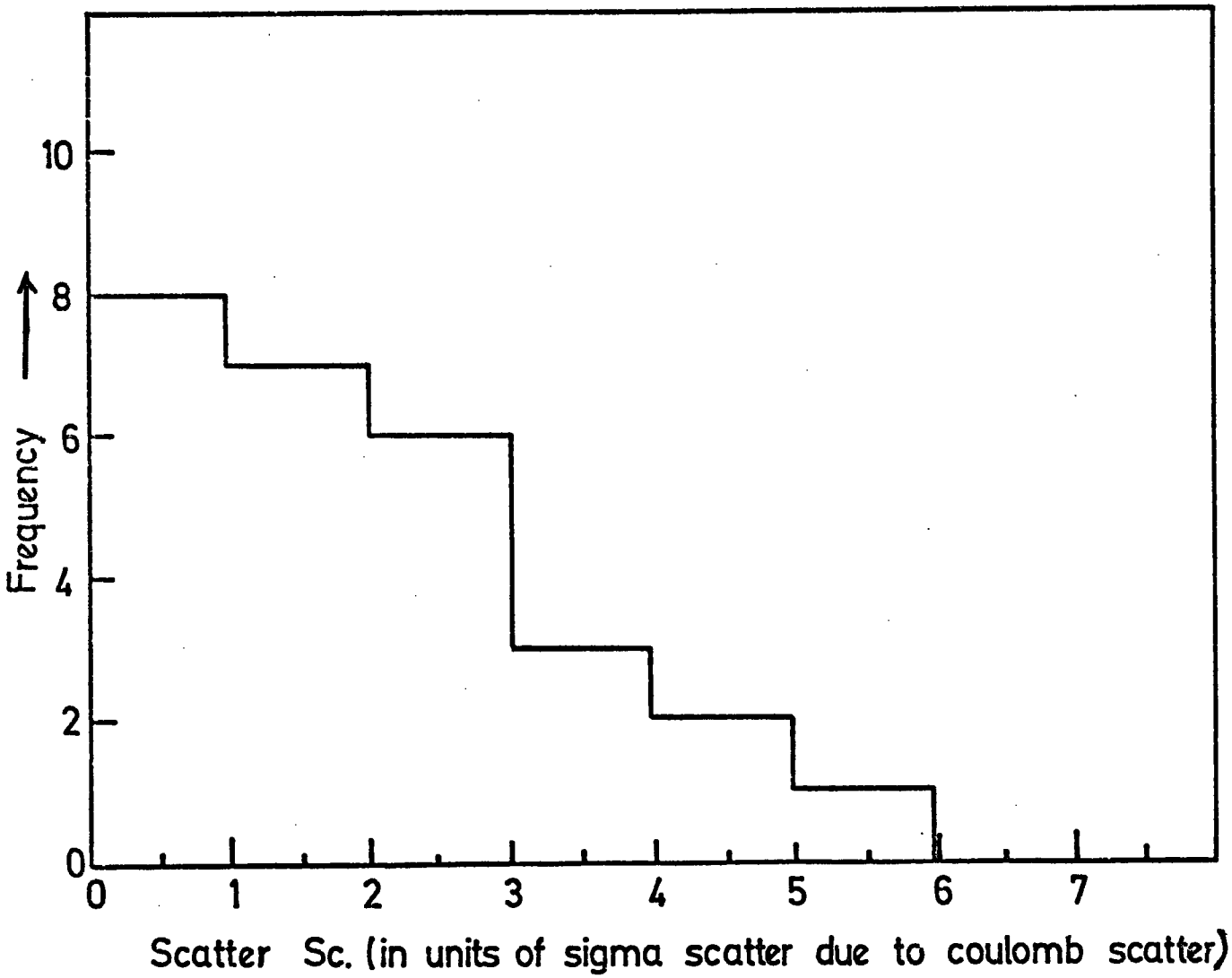

Figure 4-2.

The distribution of scattering in the lead of the N.M. for class $C^{\pm}$ events (Bad impact with X2 track.).

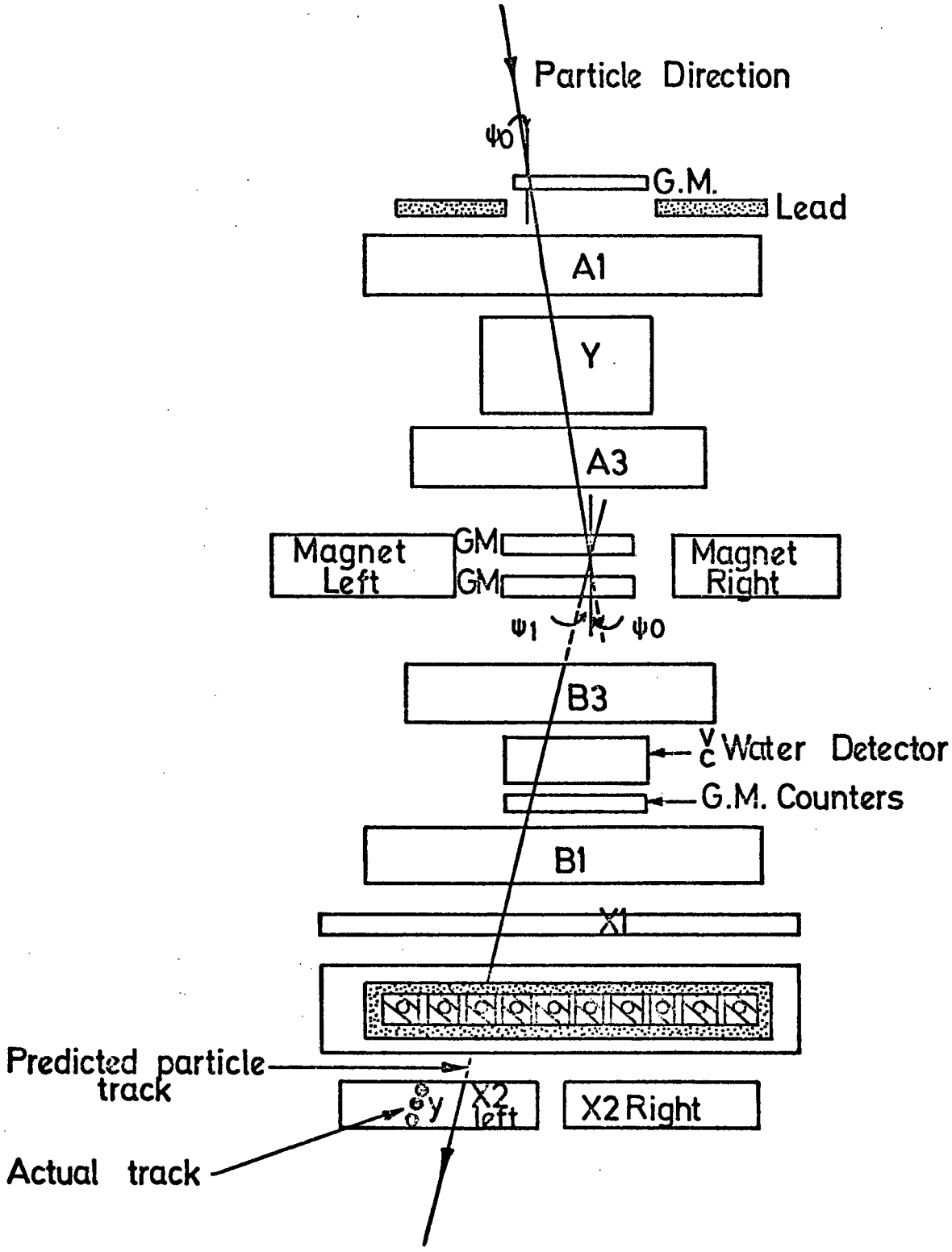

Figure 4-3. Schematic diagram showing a muon passing through the whole instrument.

CHAPTER FIVE

Previous Work on Energy Loss by Ionization

5.1 Introduction:

The energy loss by ionization of fast charged particles passing through matter has been studied by many workers, both theoretically and experimentally. It is obvious, from the experimental results in this field, that the main objective in all experiments has been the study of the logarithmic increase and the density effect.

Many different techniques have been used to measure the ionization loss of the charged particles and these can be summarized briefly as follows: (a) gaseous detectors (proportional counters, cloud chambers and ionization chambers) and (b) dense medium detectors such as scintillation counters (organic and inorganic) and nuclear emulsions. A brief account of each measurement will now be given.

5.2 Measurement with Gaseous Detectors:-

5.2.1 Proportional Counters:

Many workers have used proportional counters with different gas fillings and pressures to estimate the most probable ionization loss. Among them Eyeions (1955), Bradley(1955) and Parry et al (1953). Parry (1955) has investigated the ionization by high energy particles in neon gas, as shown in figure 5.1. These results indicated the existence of the plateau region as shown in the graph.

In 1963, Jones et al. studied the rate of energy loss of cosmic ray muons as a function of momentum by using proportional counters filled with a neon - methane mixture, over the range $3 \leqslant \beta\gamma \leqslant 300$; the

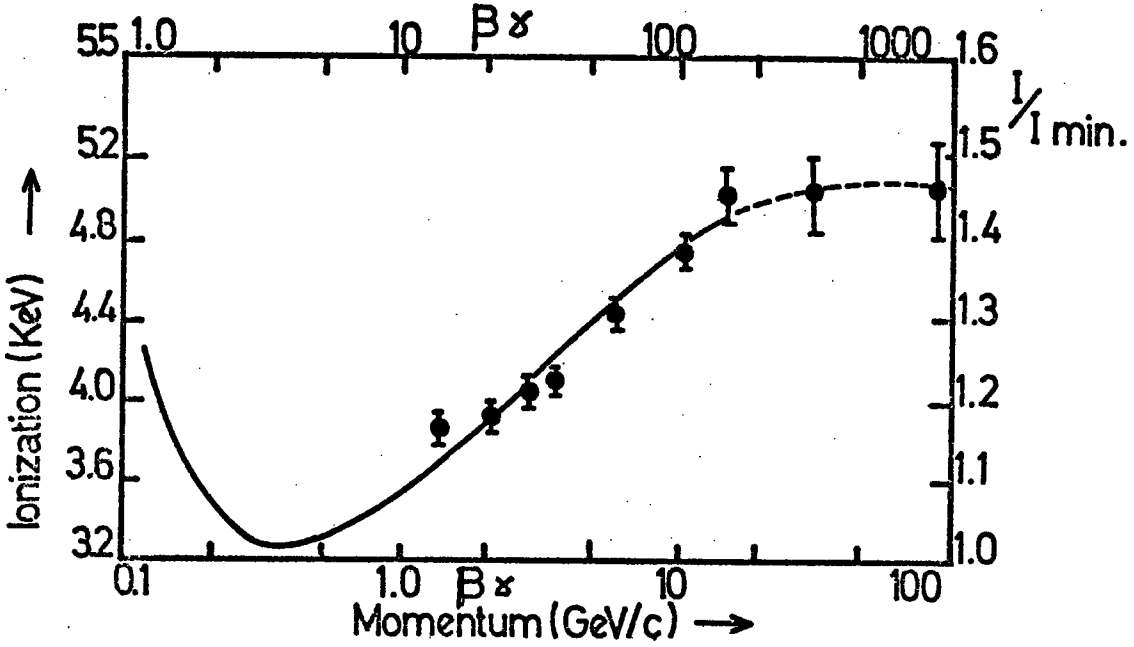

FIG.5.1 The Most Probable Ionization in Neon

(After Eyeions et al (1955))

plateau region was not reached. Their results agreed with theory over the limited momentum range investigated as indicated in their results which are shown in figure 5.2. A similar technique to that of Jones et al has been used by Smith and Steward (1966) using an argon - methane mixture to examine the ionization loss for electrons in the range $50 \leqslant \beta\gamma \leqslant 300$. Their results indicate the onset of the density effect, but unfortunately the momentum range examined was not extensive enough to allow a quantitative measurement.

In 1959, Landou and Kraybill employed four helium counters to examine the existence of the density effect in the range $31 \leqslant \beta\gamma \leqslant 1300$; the gas pressure of their detectors was 2.7 atmospheres. Their results indicate the onset of the density effect at lower particle energies, and in general their results give good agreement with the Landau treatment of collision loss corrected by Sternheimer for the density effect.

5.2.2 Cloud Chambers:

Since 1940 this technique has been used by many workers (e.g. Hazen (1944) and Sengupta (1940)) to study the loss for electrons. Their results for electrons give excellent agreement with theory but for muons does not conform with theory. In 1952, Ghosh, Jones and Wilson used Cloud Chambers with a high resolution magnetic spectrometer in order to study the relativistic rise in the momentum range 0.5 - 30 GeV/c. Their results were in excellent agreement with theory, in particular the relativistic rise region. The results obtained by Ghosh et al, have been compared by Fowler and Hall with Sternheimer theory curve; their results are in figure 5.3.

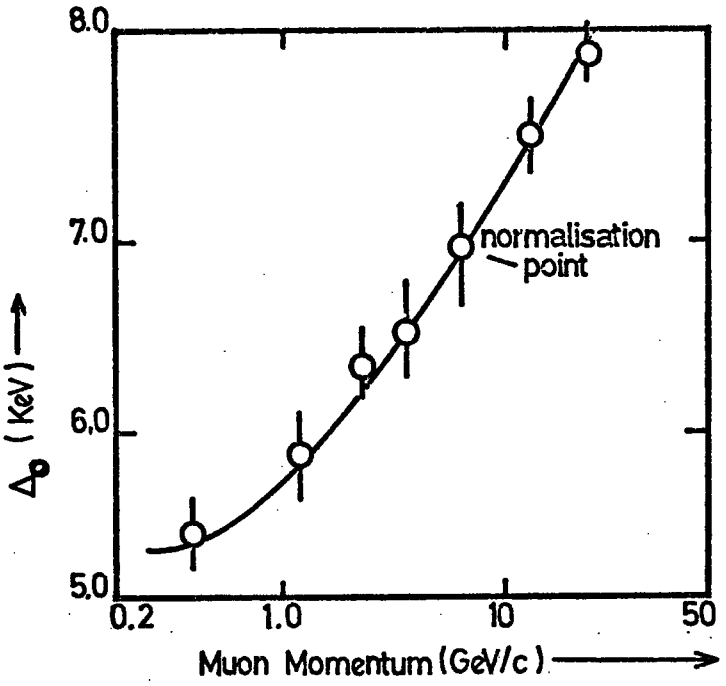

Figure 5-2: The variation with momentum of the most probable energy loss (Δ_0) of muons in a neon-methane mixture.
(After Jones et al. (1963)).

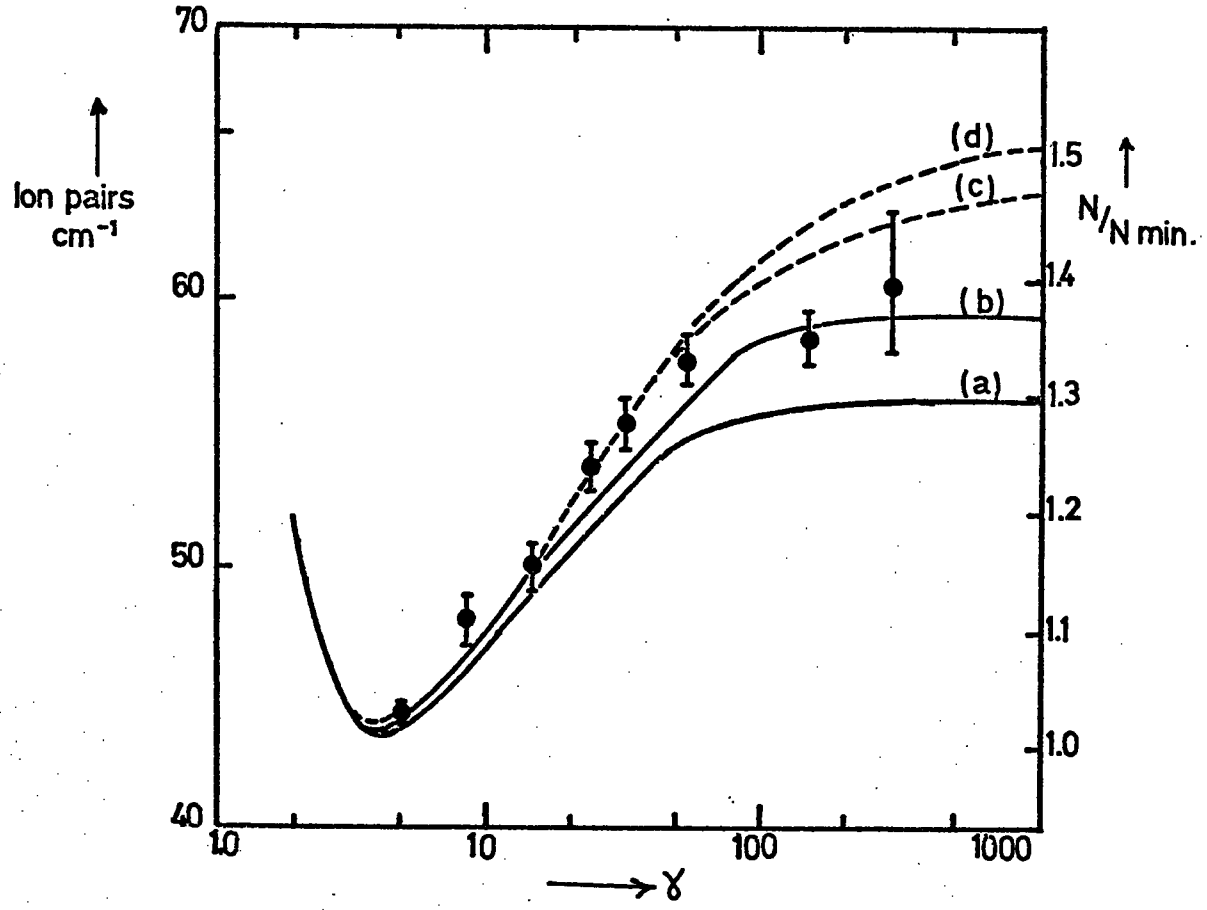

FIG. 5.3 IONIZATION OF MUONS IN OXYGEN.

a) Theoretical prediction of Budini (1963)

b) Fowler et al (1970)

c) Theoretical prediction for Sternheimer (1952, 1953) corrected for $\overset{v}{c}$ loss.

d) Theoretical prediction of Sternheimer including $\overset{v}{c}$ loss.

Experimental points are those of Ghosh et al (1952).

In 1958, Kepler et al used a cloud chamber with helium, argon and Xenon to measure the ionization loss for muons and electrons in the range $3 < \beta\gamma < 300$. The measurements of Kepler et al indicated that the rate of drop growth is limited mainly by two factors: First, by diffusion, because as the drop grows it depletes the vapour in the immediate vicinity and can grow only as vapour diffuses to it. Second, by thermal conductivity, since as the vapour condenses heat is liberated and the faster this heat escapes the faster the drop will grow; hence the worse the thermal conductivity of gas, the larger the delay required between expansion and illumination. For example a typical value in practice would be about 140 to 250 m sec, for helium and argon respectively.

In the work of Kepler et al good agreement with theory was obtained, but in argon and xenon the relativistic rise was somewhat less than predicted theoretically, as shown in figure 5.4. From the experimental facts the logarithmic rise in gaseous detectors was found to be 40 - 50%.

5.2.3 Ionization Chambers:

Barber (1955, 1956), Hall (1959), and Aggson and Fretter (1962), used the ionization chamber technique for the energy loss of charged particles. Barber measured the specified ionization in helium and hydrogen at 1 and 10 atmospheres pressure. No density effect was detected at the lower pressure, as expected, but at the higher value the familiar plateau feature was observed, as shown in figure 5.5. Some workers designed their experiments to extend Barber's measurement to higher energies and also to verify the reduction in ionization reported from cloud chambers experiments, among these workers Aggson and Fretter, and their results obtained for hydrogen were found to be in good agreement with the predictions of Budini (1953) (See Fig. 5.6).

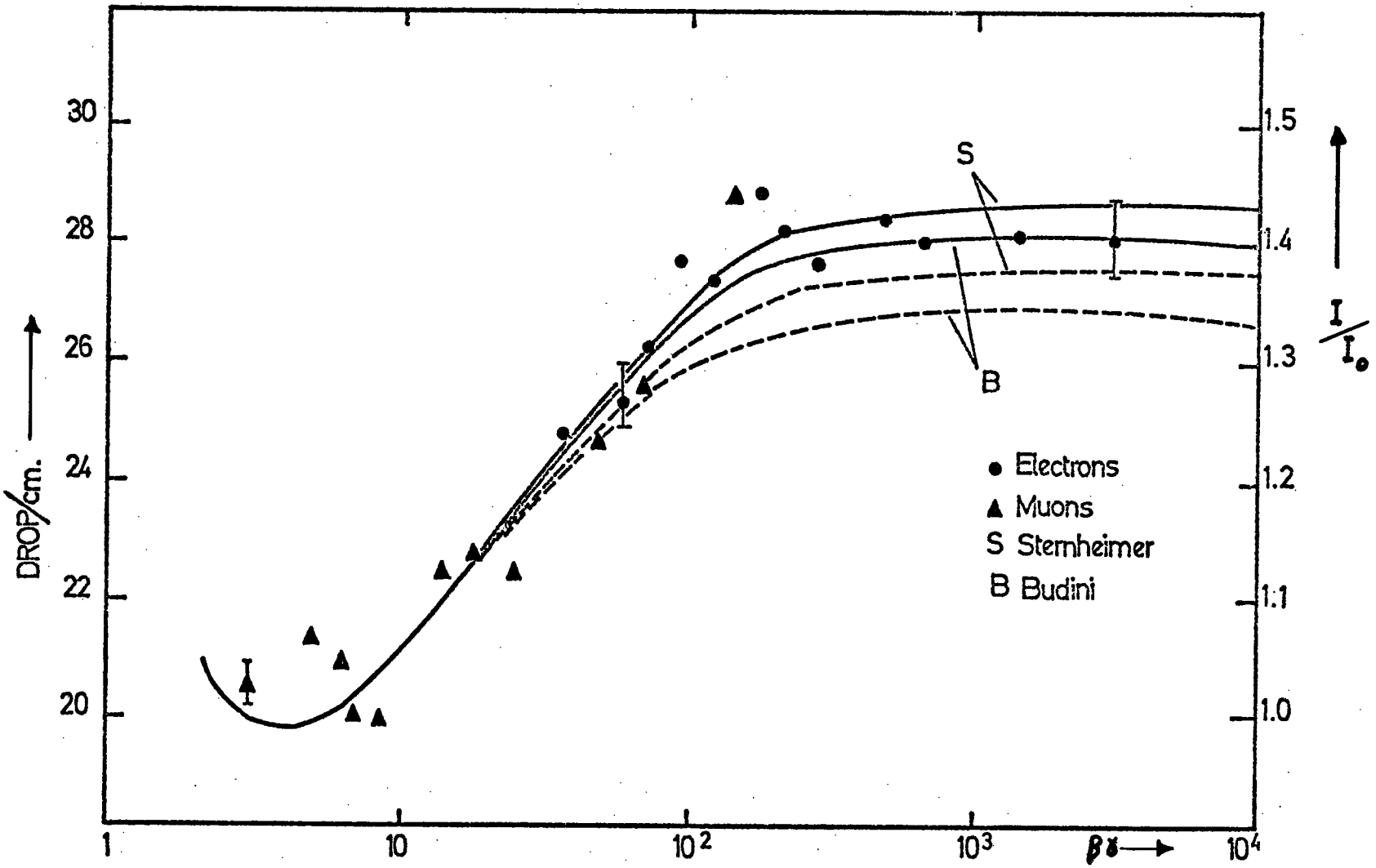

FIG. 5.4. IONIZATION LOSS IN HELIUM, AFTER KEPLER et al (1958).

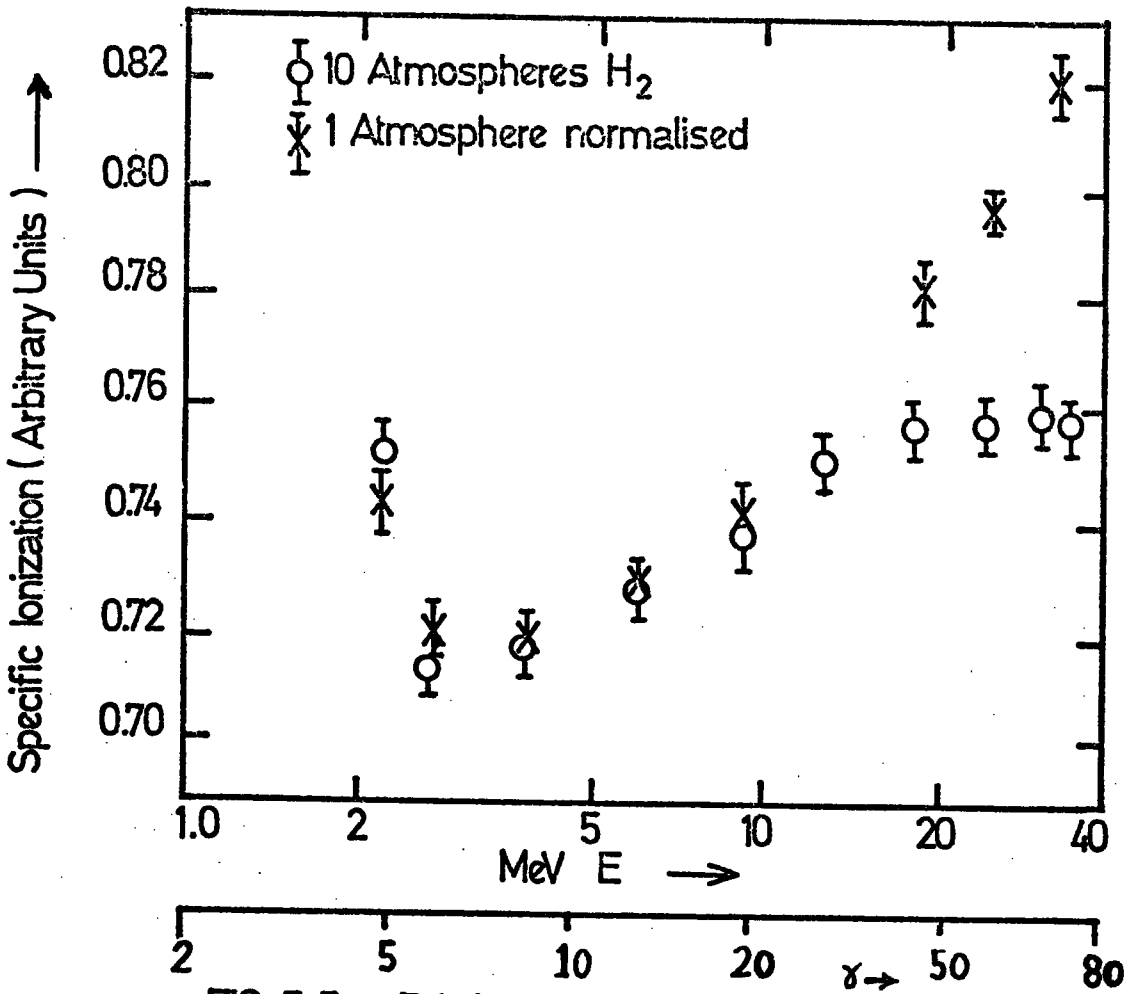

FIG. 5.5. Relative Specific Ionization in Hydrogen as Measured with a Thick-Window Ion Chamber. (After Barber (1956))

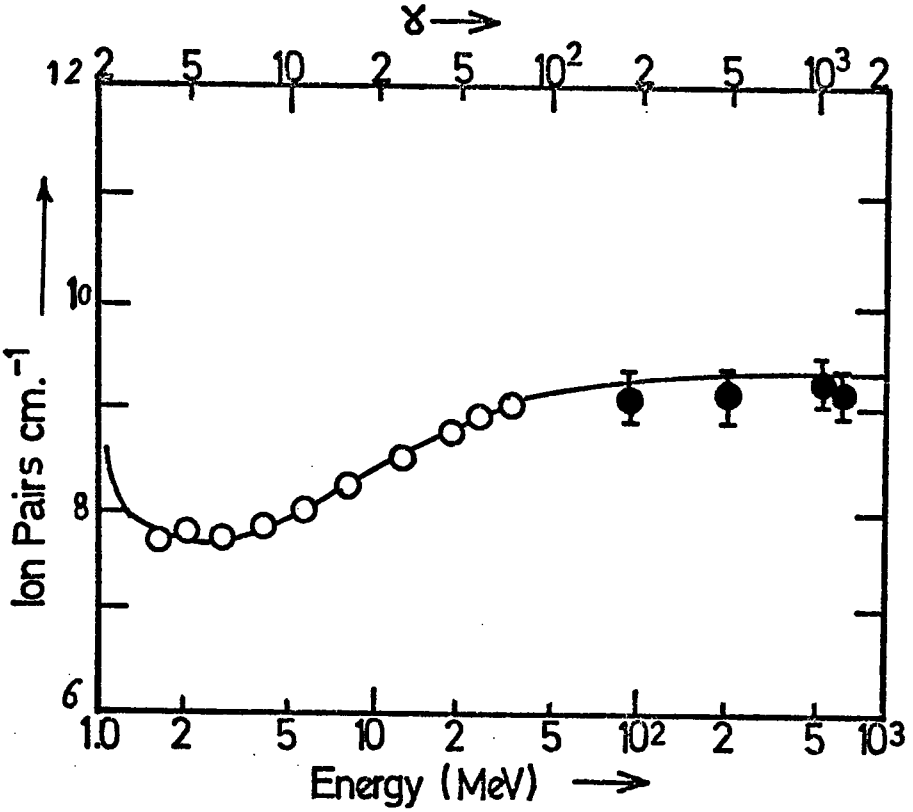

FIG.5.6. Specific Ionization in Hydrogen at NTP by Electrons.

The curve plotted was calculated from Budini's model I (1953) using W max. 38 eV/ ion pair , I (Z) = 15.5 eV (after Aggson and Fretter (1962))

5.3 Techniques using dense media:

5.3.1 Scintillator Counters

Scintillator detectors may be divided into two groups (A) Organic and (B) inorganic counter devices. The experimental results of many workers indicated that the main differences between the two should be that the density effect in the case of organic scintillators should be greater than that for inorganic scintillators; therefore the relativistic rise should be practically eliminated. In practice a commonly used type of plastic phosphor is NE 102 A with atomic number $\bar{Z} = 3.65$, atomic weight number $\bar{A} = 6.23$ and ionization potential $I(Z) = 62.6$ units. This has been used in the present experiment.

In 1952, Chou used pions and protons from the Chicago cyclotron to study the character of scintillator detectors, his results was found to be that up to three or four times the minimum value of ionization the response versus particle momentum was still constant. Similar work has been done by Baskin and Winckler (1953) to test the Chou results using organic liquid counters. They found that the ionization rise at low muon energies was much less rapid than Chou's results. Another test has been made by Barnaby (1961) and Crispin and Hayman (1964) and their results showed that there is no observable effect at low muon energies.

Bowen (1954) used Sodium Iodide scintillators and found that the relativistic increase was $10.9 \pm 1.0\%$ for energies up to 5 GeV. Smith and Stewart (1966) used Caesium Iodide crystals at high energy in the range $50 < \beta\gamma < 300$. The results of the latter workers showed a relativistic rise, and if combined with the result of Bowen (assuming here that the results are consistent) give a total rise of about $(11.3 \pm 1)\%$ from the minimum, as shown in figure 5.7.

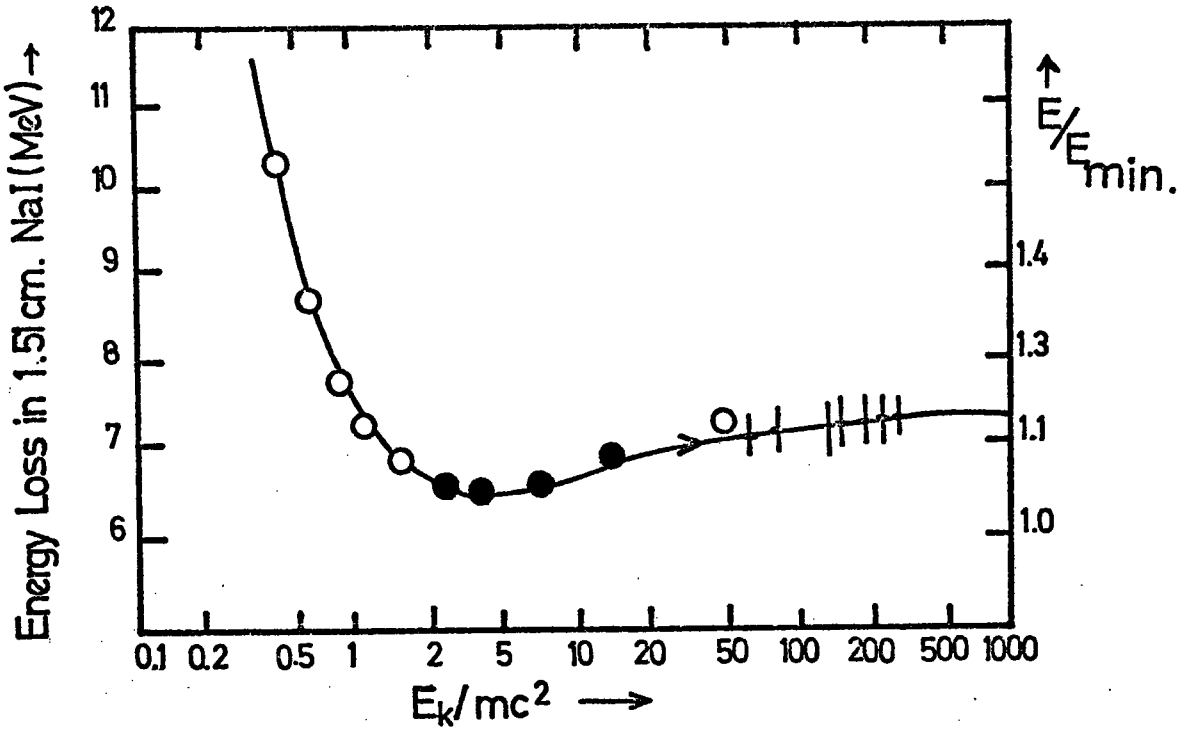

FIG.5.7. The most probable ionization loss in organic crystals, plotted as a function of kinetic energy (E_K) in units of rest mass. (After Bowen, Smith and Stewart (1966))

Since 1955 experiments with plastic phosphors have been performed by Barnaby (1961), Crispin and Hayman (1964), Smith and Stewart (1966) and more recently by Jones et al (1968). Investigations with large organic liquid counters have been performed by Miller et al (1958), and Ashton and Simpson (1963). The results obtained agree quite well with calculations (see Fig. 5.8) based on the Sternheimer theory for the most probable energy loss.

It is pointed out that Jones et al improved the precision of their experimental results by combining their data with those of Crispin and Hayman who covered the same momentum range. Millar et al used a liquid counter to study the effect of cosmic ray protons and muons from 0.3 to 2.2 GeV/c momentum, their results give good agreement with density - corrected energy loss theory.

5.3.2 Nuclear Emulsions:

There are some difficulties involved in the use of this technique which should be appreciated before an assessment of any results can be made, as has been pointed out by Hertz (1964). The main source of error is the variation of blob density with depth in the emulsion, and fluctuations from place to place. The precision achieved in ionization measurement is not yet very high.

The existence of a plateau value for the ionization loss up to the highest momenta measured has been confirmed by many experiments. Stiller et al (1963) and Stiller and Shapiro (1953) obtained a good result fc the relativistic rise of the rate of energy loss by ionization in emulsion, as shown in figure 5.9., by exposing their plates to the cosmic radiation. They made blob counts on long tracks of electrons, muons and protons. The value obtained for the logarithmic rise was (14 $\pm$ 3)%,

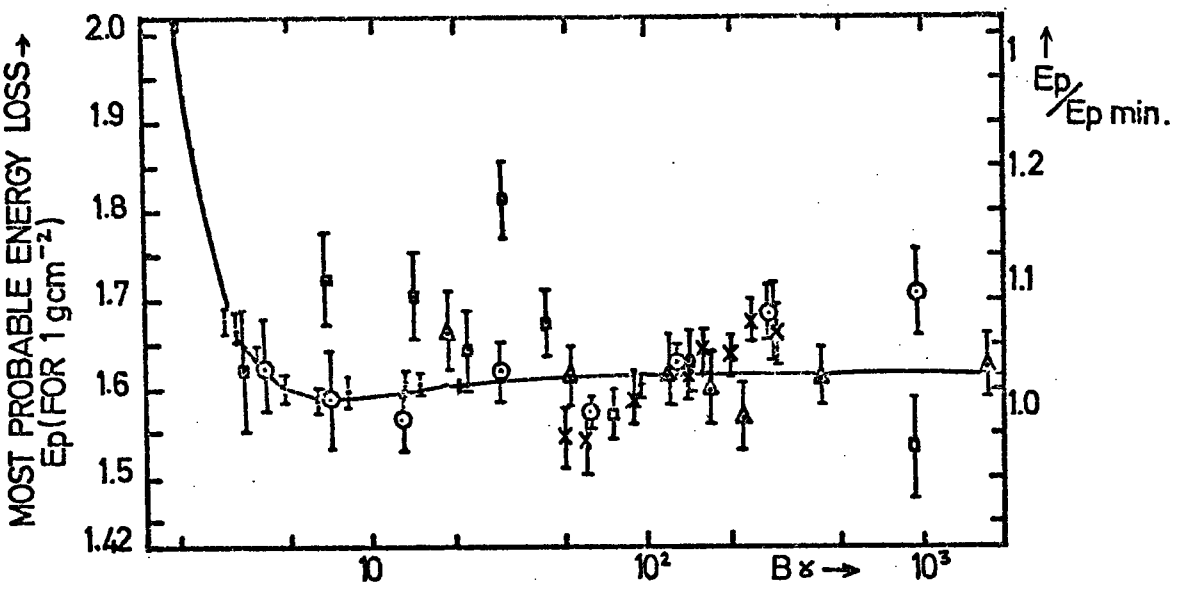

FIG.5.8 VARIATION OF Ep IN ORGANIC SCINTILLATOR AS A FUNCTION OF $\beta\gamma \rightarrow$

KEY.

- Theoretical curve (Sternheimer)
- Barnaby (1961)
- Smith and Stewart (1966)
- Ashton and Simpson (1965)
- Crispin and Hayman (1964)
- Jones et al (1968)
- Millar et al (1958)

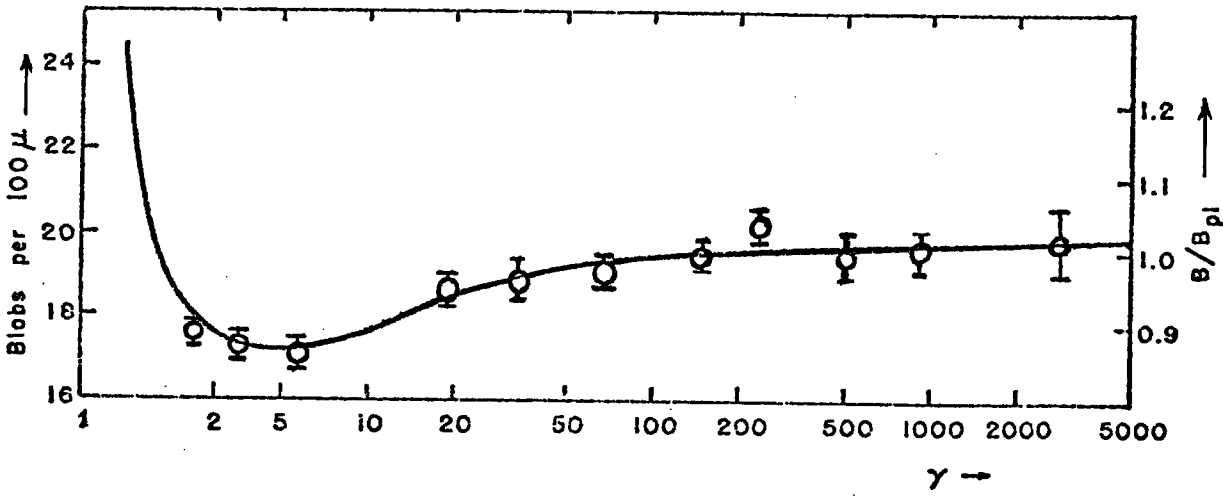

Figure 5-9. Relativistic rise of the rate of energy loss by ionization in emulsion. Blob density is plotted against the total energy of singly charged particles in rest-mass units. The scale at the right shows the normalisation of the blob count to the Fermi plateau (after Stiller and Shapiro, 1953).

and they concluded that the rate of ionization loss in AgBr saturated at $\gamma > 100$, and maintains the plateau value at least as far as γ of 3400. This particular investigation has the merit not only of obtaining data in the ultra - relativistic region but also in the region of the minimum ionization.

The one experiment which gave very different results was that of Zhdanov et al (1962) who claimed a new effect: that the energy loss begins to decrease again at a point soon after the plateau value has been reached (at $\gamma \simeq 100$), this experiment having been made with electrons in emulsions. The results of these workers were in agreement with the predictions of Tsytovich (1962 a,b,c) which have been described elsewhere.

Zhdanov et al, used two types of emulsions: NIKFIR. 10 type emulsions exposed to a proton beam of 8.7 GeV at Dubna and ILFORD G.5 emulsions exposed to proton beam at CERN. Their results are shown in figure 5.10. They determined the relative blob density along secondary electron tracks, the blob density along the tracks of primary protons crossing the same region of emulsion was measured and the electron energies were deduced from multiple scattering.

Later experiments by Buskirk et al (1964), Stiller (1963) and Hertz and Stiller (1964) however obtained results which agreed with conventional theory and did not support the measurements of Zhdanov et al. The results of Buskirk et al (1964) are shown in figure 5.11.

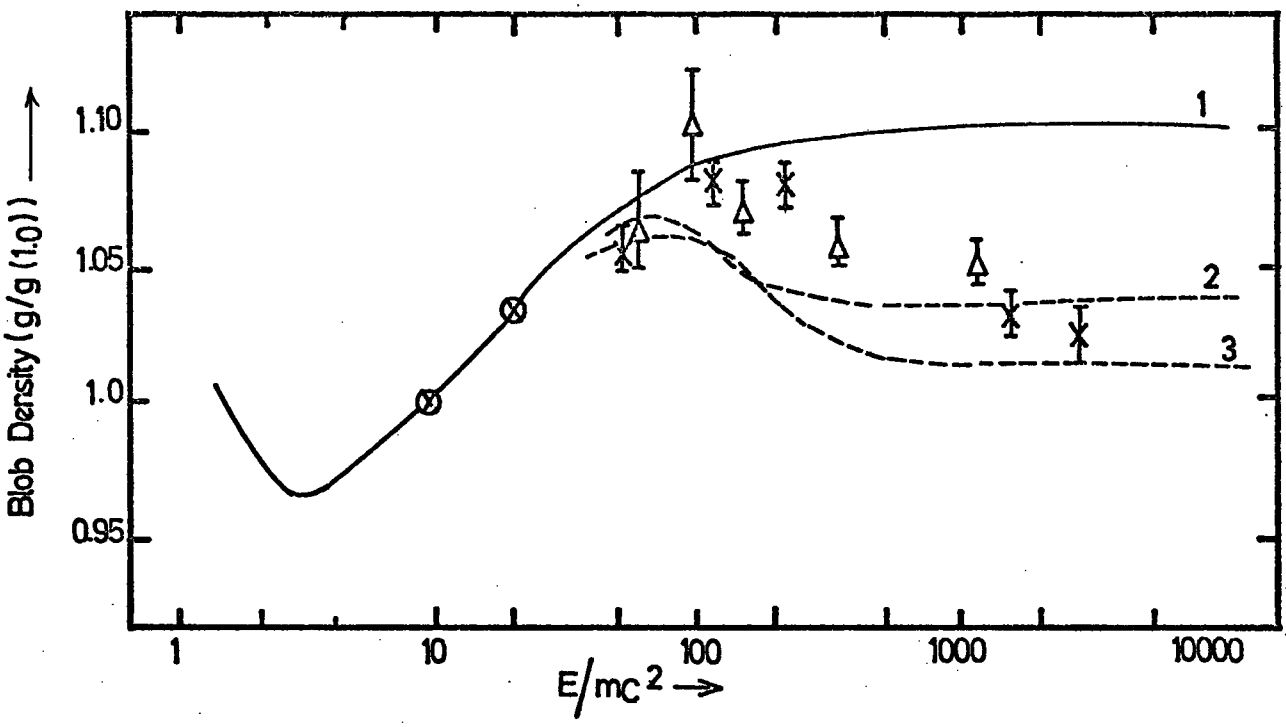

Figure 5-10. Results of Zhdanov et al. Using NIKFI(X) and ILFORD G.5.

(⊼) Showing blob density along the track plotted as a function of electron density.

Curve 1: the theoretical curve neglecting radiation corrections (Jongejans, 1960), Curves 2 and 3 are theoretical curves taking radiation corrections into account.

Experimental calibration points for each emulsion are encircled.

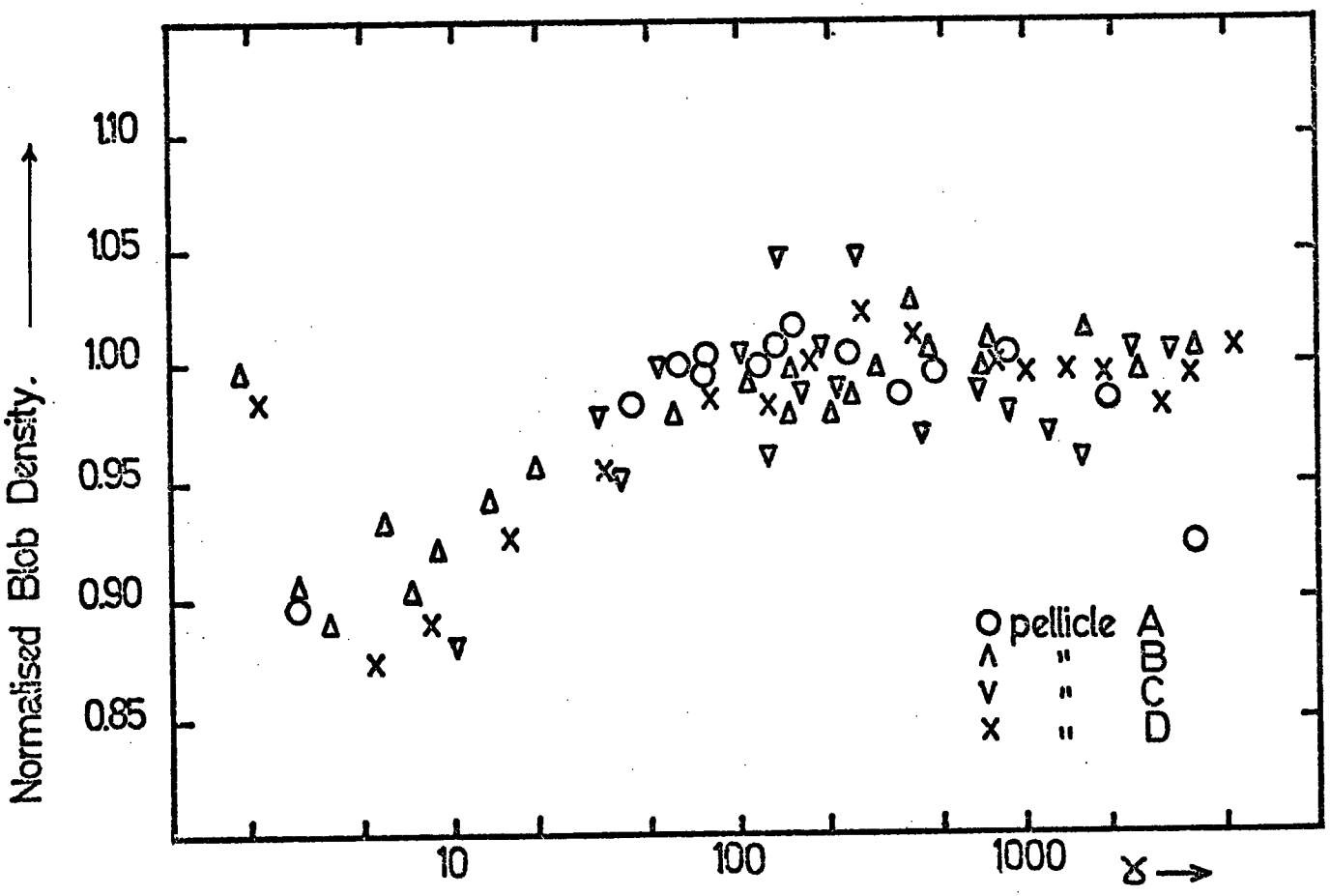

FIG.5.11 Normalised blob densities for electrons ($\gamma > 100$) and pions plotted as a function of γ. The data were gathered from four pellicles of 600 μ thick Ilford K.5 emulsion.

(After Buskirk et al (1964))

5.4 Discussion of previous Work:

The previous work on ionization loss shows that all experimental results demonstrate the logarithmic rise and subsequent plateau; we note that some workers have reported only a small value for the percentage rise, however; as ever, there is still a need for experiments of a high standard in technique which yield data of good statistical accuracy.

There is a need to quantitatively resolve the energy loss into its separate components of ionization, excitation and Čerenkov radiation, although the experimental means of accomplishing this is difficult. However, if such a resolution were successful, it would make possible a more direct comparison between the results and various theories.

CHAPTER SIX

The Experimental Results

6.1 Introduction:

The work described here has demonstrated the expected sensitivity of neon flash tubes to charge (and thus energy loss) of the traversing particles. The energy loss sensitivity of neon flash tubes has been shown using the flux of momentum - and charge - analysed nucleons and mesons available from the magnetic spectrograph. Similar work has been carried out previously by Diggory et al (1971); Ashton et al (1971) have shown that evidence already exists for the sensitivity to charge in their search for quarks.

6.2 The Experimental Procedure:

The equipment used for this experiment has been described in chapter 3. Measurement has been made of the number of flash tubes discharged in tray A1, A3, B3, B1 and Y of the equipment with a time delay before pulsing of 75 - 80 μs for both types of particle: Muons and NAP's, the particles having momenta in the range 0.1 - 10 GeV/c.

The distribution of numbers of flashed tubes for recorded muons are shown in figures 6.1 and 6.2. The mean layer efficiency (i.e. the number of flash tubes flashed along the length of the track divided by the number of layers) and the internal efficiency η derived from η_L by multiplying by the ratio R of the internal tube diameter to the separation of the tube centres, was determined for each event. This definition involves the reasonable assumption that only those particles traversing the gas of a tube can cause a flash in that tube.

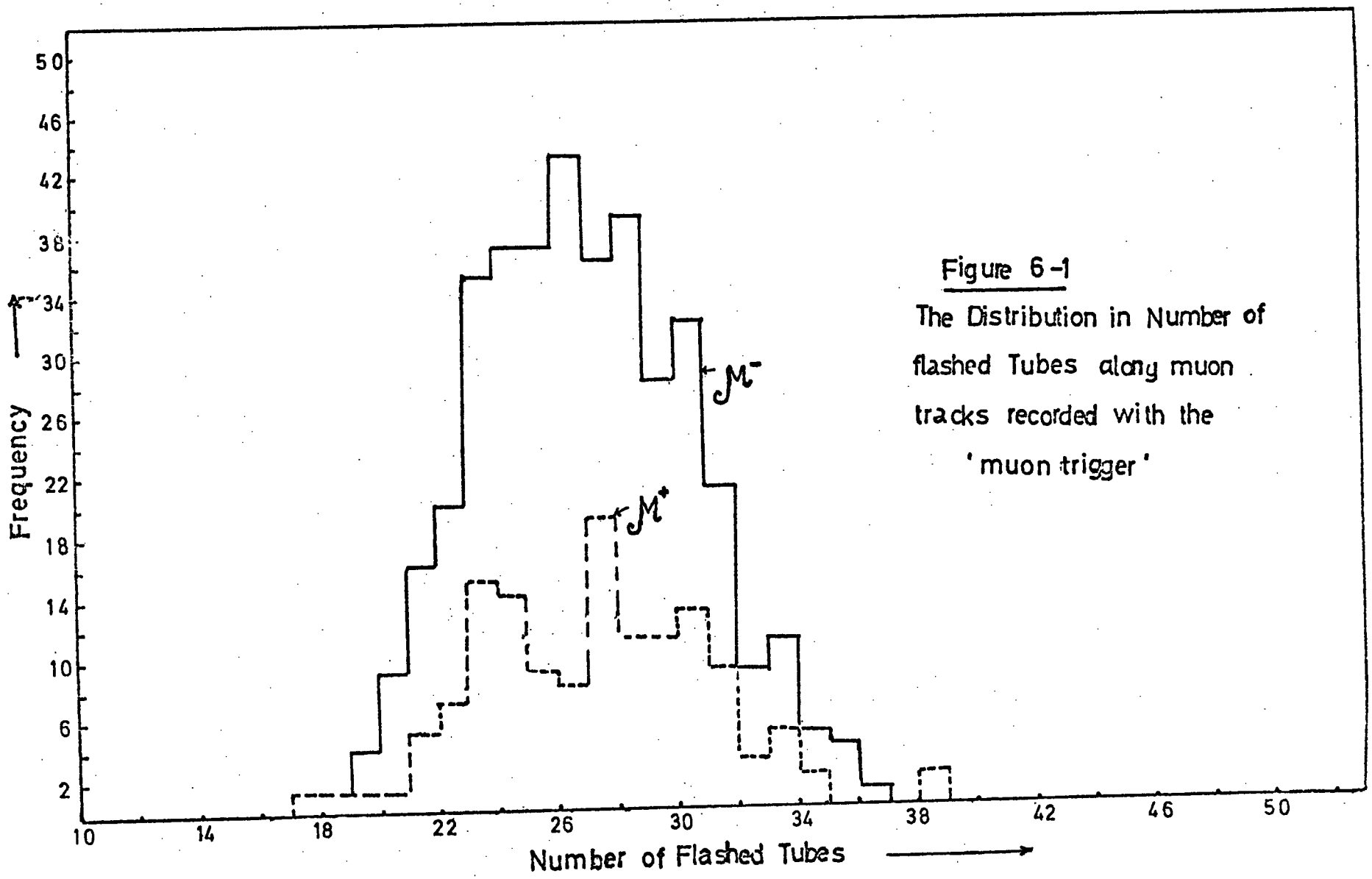

Figure 6-1

The Distribution in Number of flashed Tubes along muon tracks recorded with the 'muon trigger'

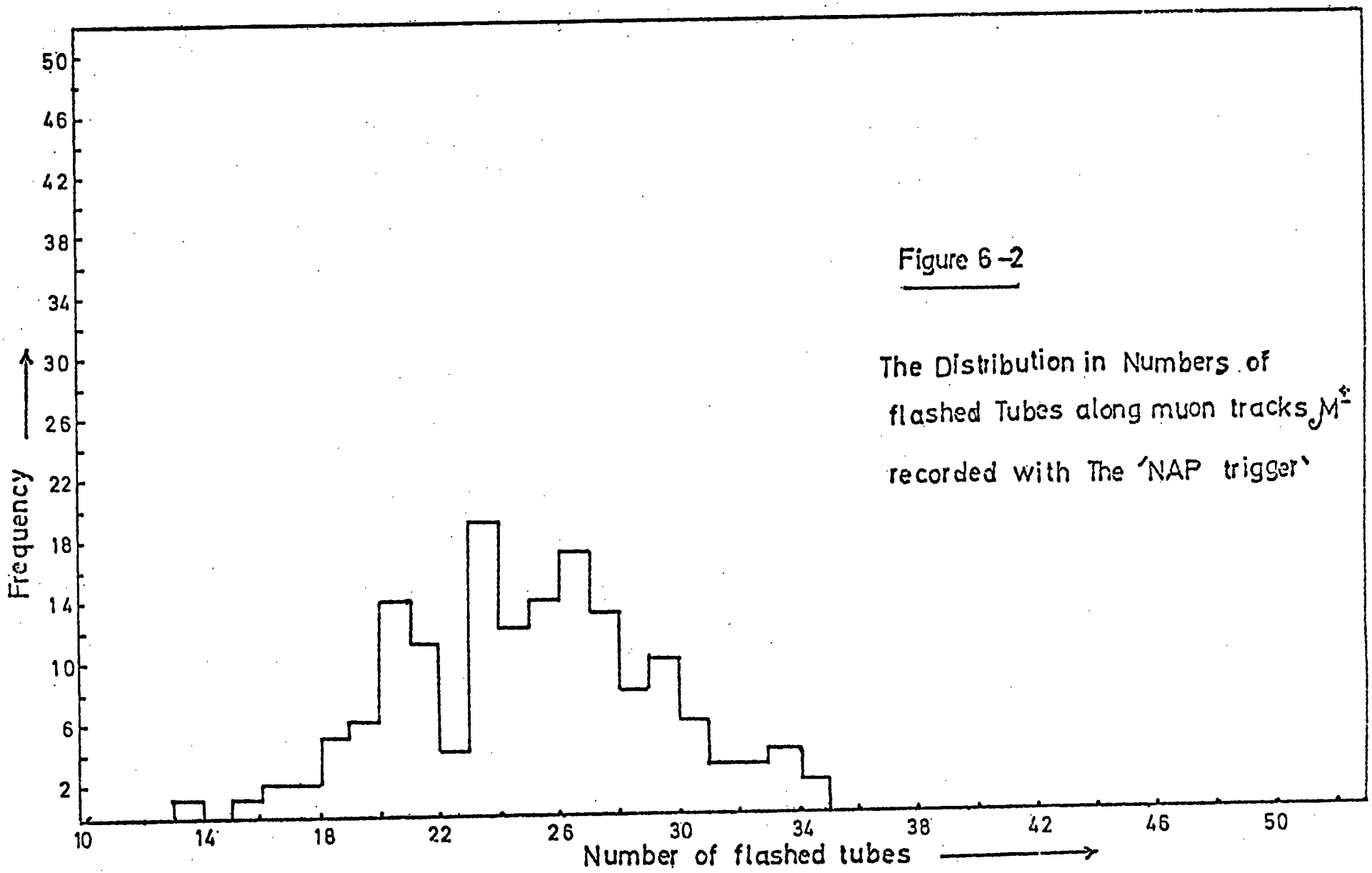

Figure 6-2

The Distribution in Numbers of flashed Tubes along muon tracks $M^{\pm}$ recorded with The 'NAP trigger'

The statistical uncertainty in η_L is derived from the experimental data using the following relation:

$$\sigma_L = \eta_L \ (1 - \eta_L)^{\frac{1}{2}}/n^{\frac{1}{2}}$$

Where n is the observed number of flashes, and the internal efficiency is thus:

$$\eta = R \left\{ \eta_L \pm \eta_L \ (1 - \eta_L)^{\frac{1}{2}}/n^{\frac{1}{2}} \right\}$$

In our experimental results we have derived the layer efficiency and from it the internal efficiency η.

The responses from the plastic scintillator detectors were recorded for mesons and protons as a measure of energy loss. The response from the threshold water Čerenkov detector was also recorded.

6.3 Detecting Muons in the cosmic ray beam and the relation between efficiency and delay in Pulsing:

Neon flash tubes like many other detectors, rely for their operation on the ionization left by charged particle. The sensitivity to ionization can be varied at will, for example by varying the time delay between the instant of the traversal of the particle and the application of the high voltage pulse. This decrease of efficiency with time delay arises from the diffusion of the initial electrons to the glass wall of the tube in the time interval between the passage of the particle and the application of the high voltage pulse. Also, a reduction in internal efficiency follows due to the failure on some occasions to have at least one electron available for initiating a cascade when the high voltage pulse is applied.

The relationship between the decrease in efficiency in detecting muons of the cosmic ray beam (typical momentum 1 GeV/c) with increasing delay in pulse application has been measured by Diggory et al(1971) and is shown in figure 6.3. The present work was undertaken under the same experimental conditions. According to the theory of flash tube operation (Lloyd, 1960), it seems that the fact that the shape of the efficiency - time delay curve is correct can be regarded as a measure of proof that the efficiency depends in a straight-forward way on the number of electrons left in the tube at the time the pulse is applied.

Lloyd gives universal curves for the expected variation of efficiency with time delay in terms of the parameter af_1Q where a is the tube radius, f_1 is the average probability that a single electron is capable of producing a flash when the high voltage pulse is applied, and Q is the average number of initial electrons produced per unit length in the neon gas.

Diggory et al (1971) have eliminated that for the tubes being used the probability of an electron initiating a discharge is 0.25. Hence we expect that such flash tubes operated at a delay of say, 80 μs would show a sensitivity to the energy lost by the traversing particle, this means that the number of electrons remaining inside the tube are proportional to the energy loss of the traversing particle (i.e. the larger the number of electrons inside the tube the higher the energy loss of the charged particles).

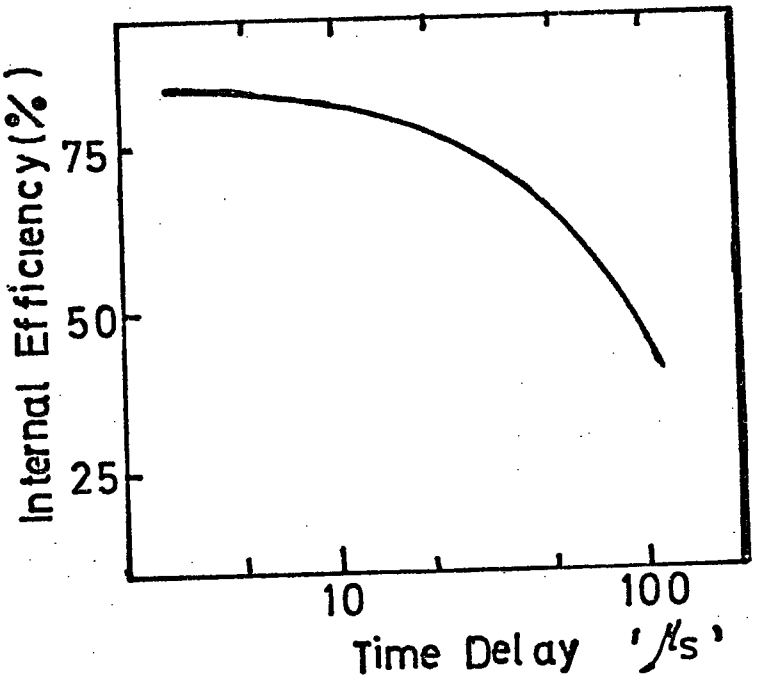

Figure 6-3. The time delay characteristics of the flash tubes (after Diggory et al 1971.)

6.4 The Efficiency of flash tube operation

6.4.1 Muons:

Figure 6.4 includes two relationships, firstly the number of flashed tubes versus muon momentum, and secondly the corresponding layer efficiency versus momentum. The results are also compared with a theoretical curve calculated from Sternheimer's theory (1956) and Lloyd's theory for flash tube operation (brief details of the calculation of this curve are outlined in the Appendix 1).

According to Sternheimer's theory, we would expect that the energy loss per unit path length would decrease as $1/\beta^2$ at very low momenta (where $\beta = v/c$, the velocity of the charged meson divided by c, the velocity of light). From the graph, it can be seen that the number of flash tubes does show this initial decrease. The data illustrates correctly that the minimum ionization takes place at a momentum of $\simeq$ 0.25 GeV/c. Above this momentum the number of flash tubes discharged begins to increase as $\log \beta\gamma$. The physical origin for this occurrence is that the relativistic lateral extension of the electric field of the moving muons in the neon gas, inside the tube allows the particle to ionize a larger number of neon atoms as it passes through the flash tubes. The data are seen to agree well.

6.4.2 Further data for the Energy Loss sensitivity of neon flash tubes:

The data of figure 6.5 represent the mean layer efficiencies (= Internal efficiency x 0.87) of neon flash tubes measured for mesons selected from muon films and mesons detected from films obtained using the NAP trigger.

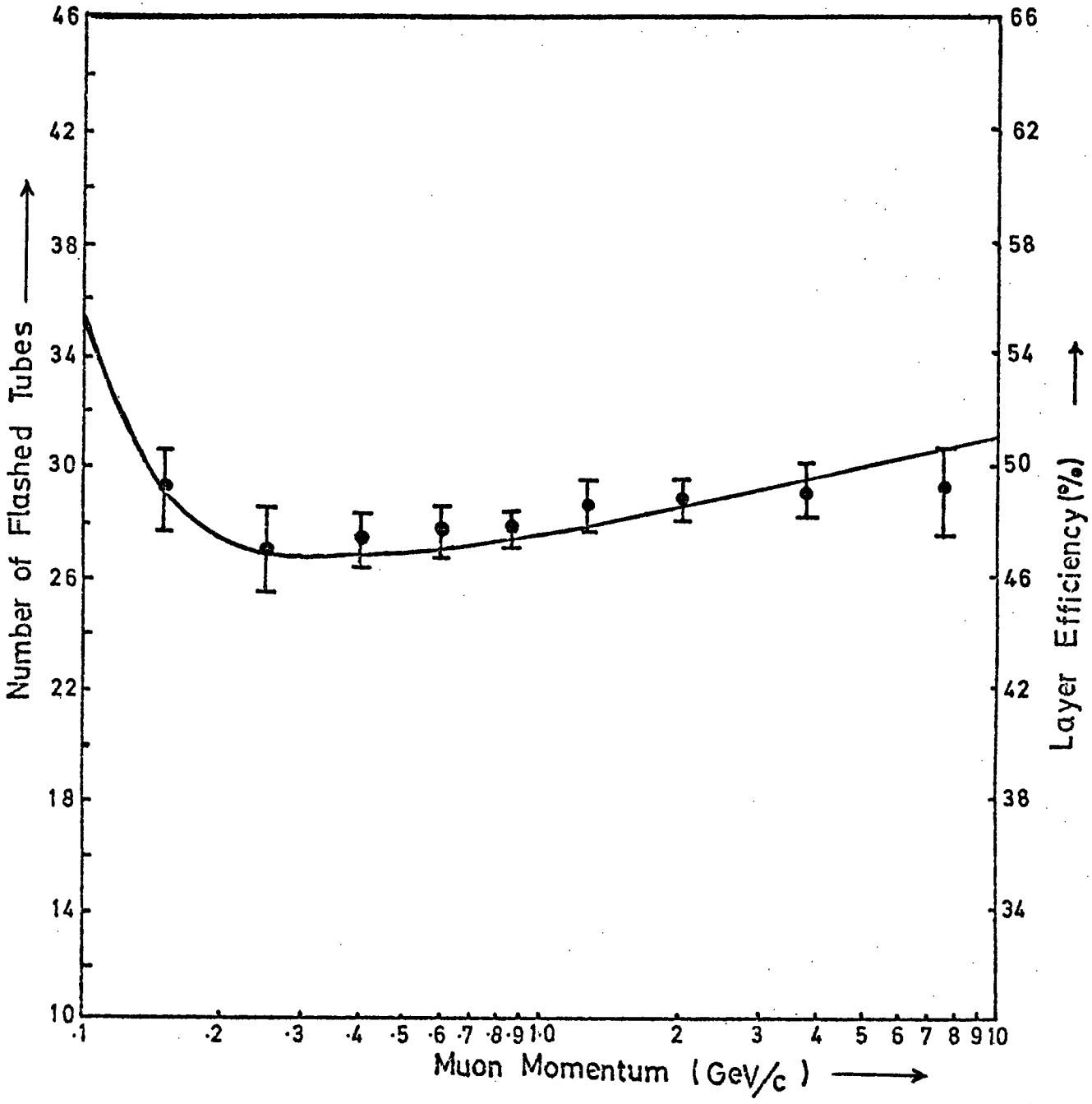

Figure 6-4:

The number of flashed tubes (left ordinate) and Layer efficiency (right hand ordinate) for muons of indicated momentum.

The solid line is based on the theory of energy loss forneon, Sternheimer (1956) and Lloyd's theory (1960) for flash tube operation.

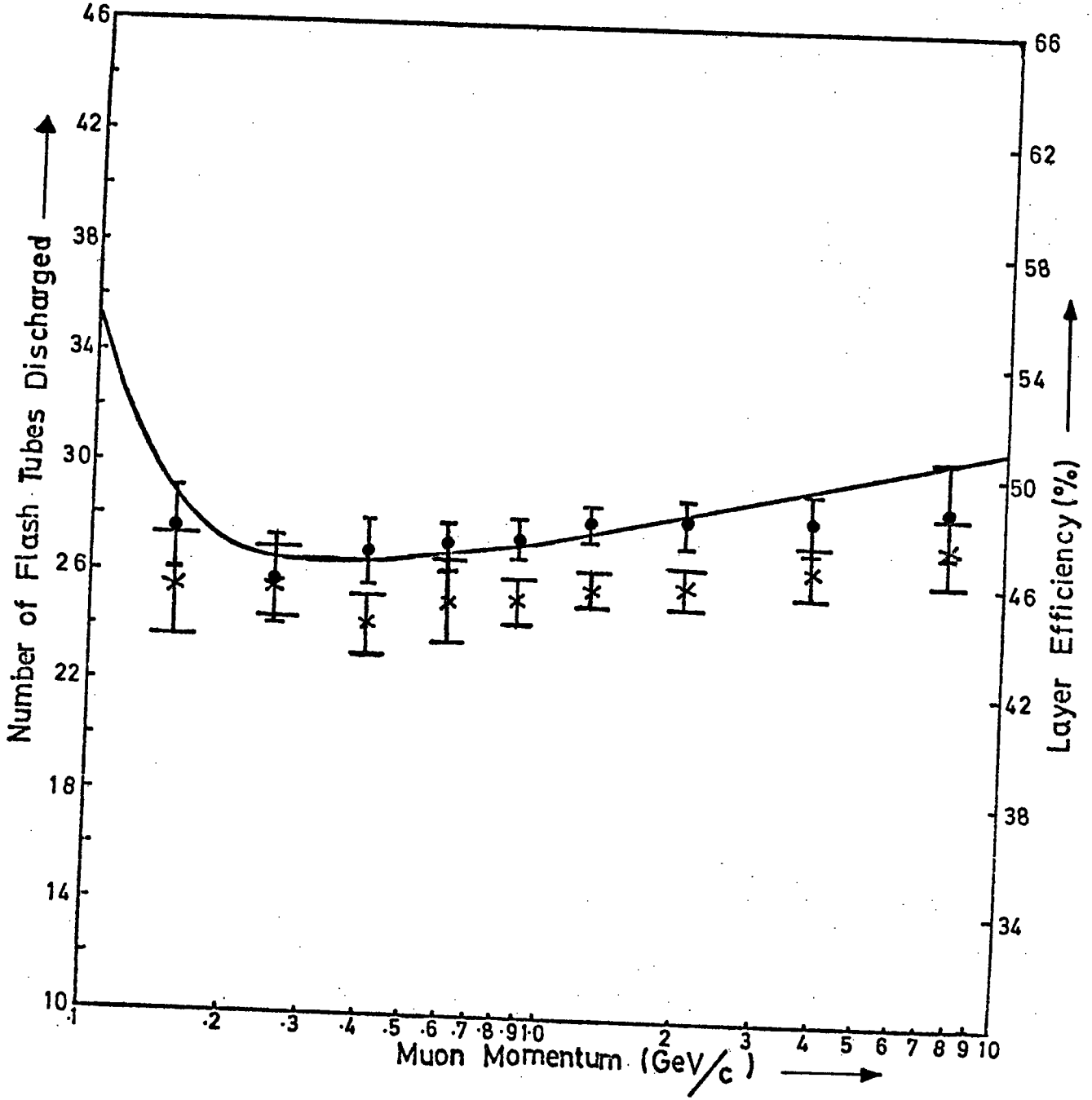

Figure 6-5 : As for Figure 6-4. The data shown (⊥•⊥) were obtained for specially selected muons ; The data shown (⊥✳⊥) were obtained for mesons recorded in the NAP trigger.

It is seen from the graph that the number of flash tubes discharged by mesons in the muon films is larger than the number of flash tubes by muons detected from NAP films. The reason for this is not understood (the event repitition rate in the muon films is larger than the rate for NAP under the triggering conditions and clearing field effects would be expected to be bigger, giving an efficiency difference opposite to that observed).

Despite the problem with absolute efficiencies the shape of the experimental efficiency versus muon momentum curve is in fair agreement with theory (the theory indicated in Appendix 1). Although there is a suggestion that the increase in efficiency with momentum is a little smaller than expected.

The main conclusion is that the muon data for the energy loss sensitivity of neon flash tubes are in fair agreement with expectation based on the energy loss curve for neon given by Sternheimer (1956) and the theory of flash tube operation given by Lloyd (1960). This will be discussed further later.

6.5 The Efficiency of flash tube operation for protons

6.5.1 Introduction:-

We have discussed in chapter three the classification of events recorded by the spectrograph. The events characterised by having a good impact in the N.M. and no X2 track are identified as nuclear active particles by the evaporation neutrons they produce in the neutron monitor. Class B^+ events are therefore assumed to be positive pions and protons, and class B^- events are negative pions in the absence of significant flux of anti-particles. The number of such particles selected from the NAP films during the experiment runs are shown in Table 6.1. The frequency distribution for the numbers of discharged flash tubes for B^+ and B^- events are shown in figure 6.6

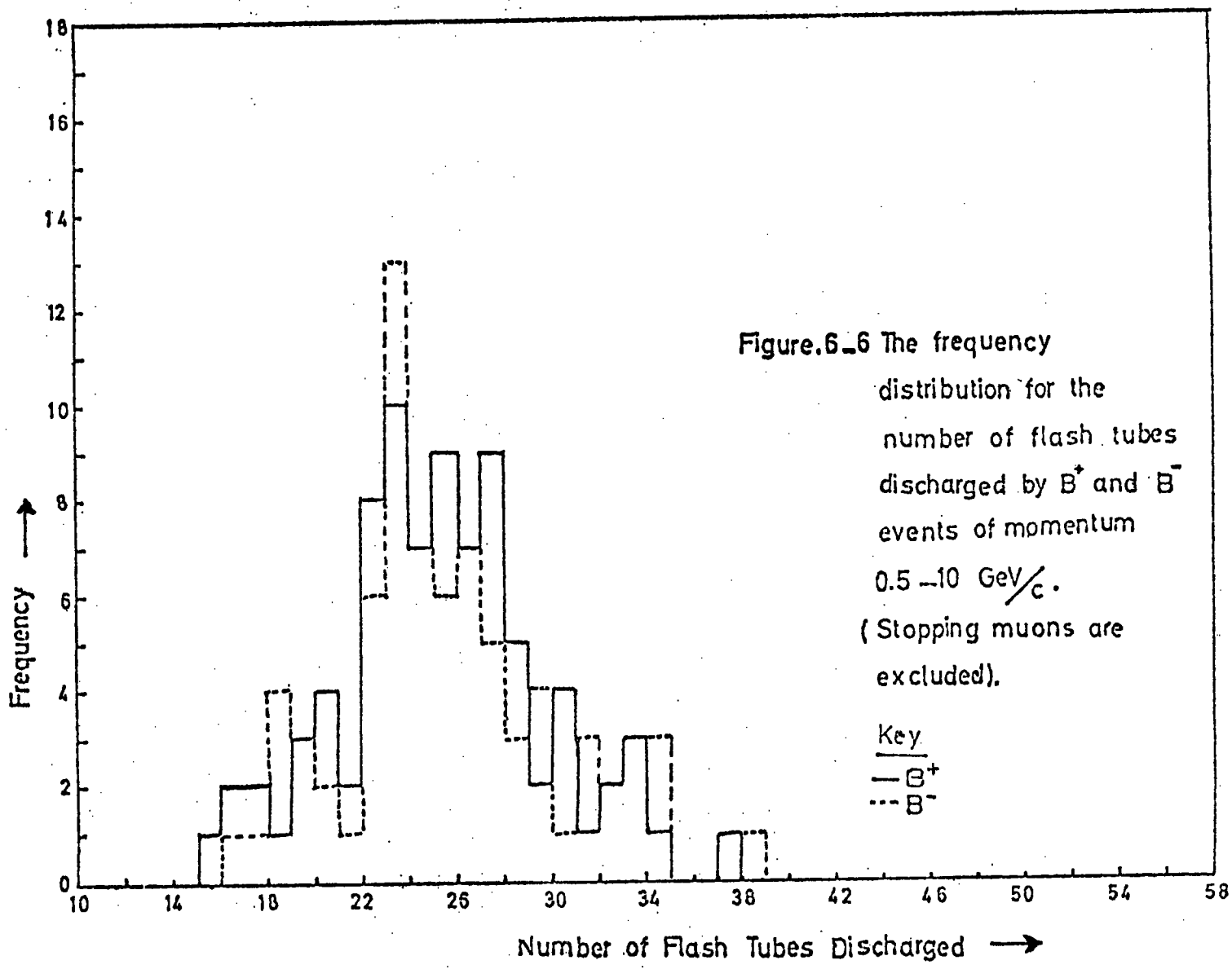

Figure.6_6 The frequency distribution for the number of flash tubes discharged by B^+ and B^- events of momentum 0.5 –10 GeV/c. (Stopping muons are excluded).

From the characteristics of those particles indicated in table 6.1, it may be concluded that the accuracy for protons is small. The main reason seems to be that only a small sample has been analysed during the experimental runs.

6.5.2 Basic data

Figure 6.7 includes the experimental results for class B^+ (π^+P), flash tube numbers versus momentum, for a time delay 75 - 80 μ secs. Seemingly here, the results show that neon flash tubes are satisfactory indicators of energy loss for mesons, and their performance is in substantial agreement with expectation.

The protons are identified by subtraction technique table 6.1. In this method the flash-tube distribution for class B^- (assumed to be π^-), in the absence of antiprotons in the cosmic ray beam at sea-level are subtracted from class B^+ (assumed to be protons and π^+). The result of subtraction gives the distribution for protons alone.

It has been assumed, that the number of antiprotons should be negligible, in fact none has been detected in the cosmic radiation at sea-level. (Hook and Turver, 1974). Thus the particles detected are exclusively protons and positive pions. It is assumed that the number of positive and negative pions are identical. With these assumptions it is possible to derive the number of protons from the data indicated in table 6.1.

The subtraction technique indicated above show that there is a difference in the B^+ and B^- events, although this difference is only significant statistically and is of limited value.

Table 6.1 A summary of data of class B^+ events. The events of momentum <0.5 GeV/c are dominated by stopping negative muons in the neutron monitor.

Number of momentum bin	1	2	3	4	5	6	7	8	9
Momentum Bins range GeV/c	0.1 <.2	.2 <.3	.3 <.5	.5 <.7	.7 <1.0	1.0 <1.5	1.5 <2.5	2.5 <5.0	5.0 <10.0
Mean momentum bins	0.15	0.25	0.4	0.6	0.85	1.25	2.0	3.75	7.5
Number of events of class B^+ (π^+P)	4	10	19	21	18	15	12	11	6
Mean flash tube number per event for class B^+	21.25	24.70	25	26.86	24.72	26.33	25.75	24.36	26.67
Standard error in the mean flash tube number	1.14	1.55	0.61	1.00	1.12	0.96	1.05	1.28	1.48
Number of events for class B^- (π^-)	12	15	27	16	18	13	11	7	8
Mean flash tube number per event for class B^- (π^-)	24.58	24.53	23.70	24.44	25.53	28.23	26.64	24.00	24.50
Standard error in the mean flash tube number for class B^- (π^-)	0.83	0.90	0.88	0.69	1.2	1.11	1.27	1.01	1.20
Number of proton events B^+ (π^+P) $-B^-$ (π^-)	$-8\pi^-$*	$-5\pi^-$*	$-8\pi^-$*	5P	0	2P	1P	4P	$-2\pi^-$
Mean flash tube number for proton events				34.6		14	16	24	

* Stopping negative muons.

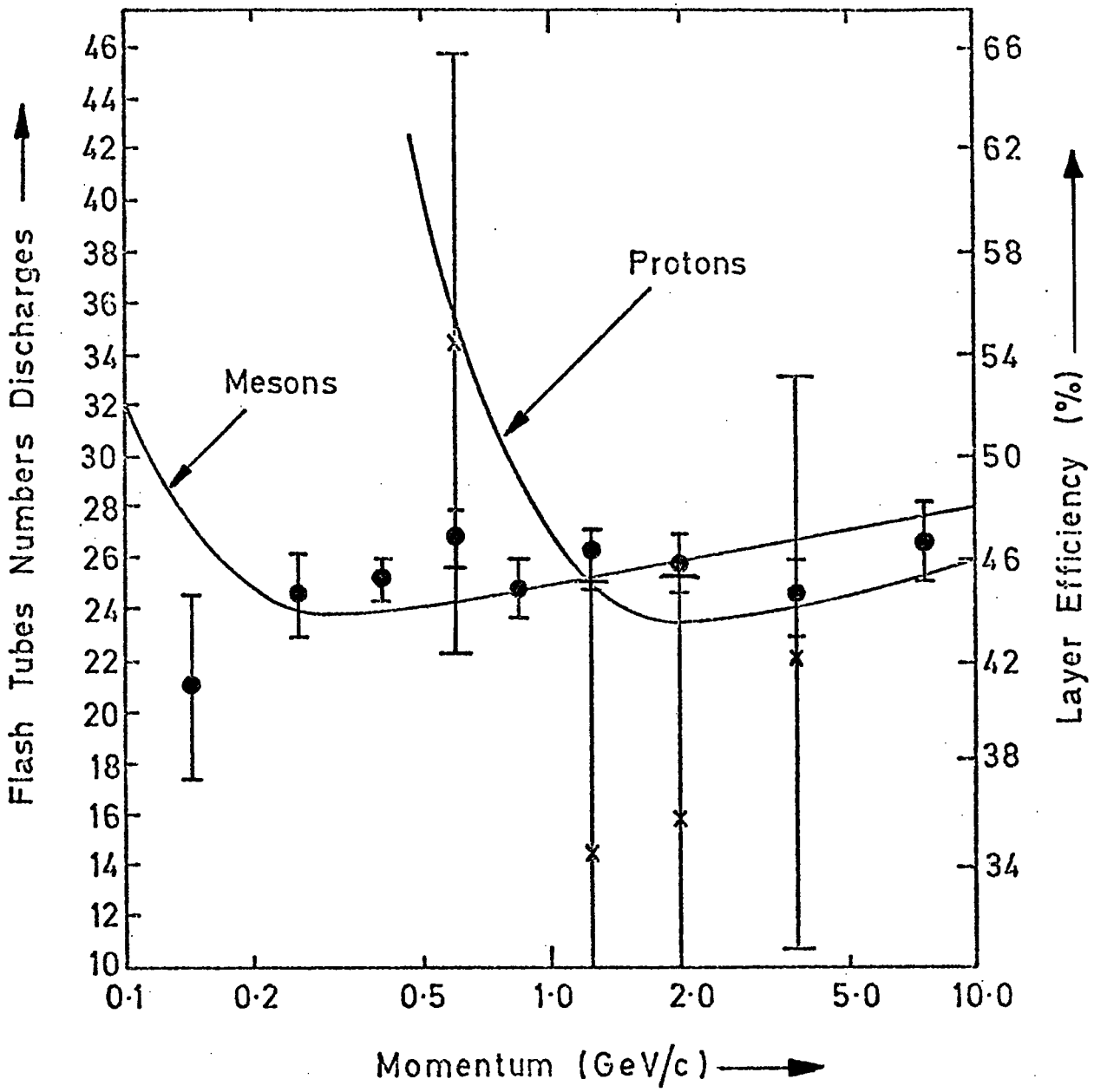

Figure 6-7. Flashed tubes (left hand ordinate); and Layer efficiency (right hand ordinate) for mesons and protons ; (Class B^+) of indicated momentum. The solid lines are based on the energy loss for neon Sternheimer (1956) , and Lloyd's theory for flash tube operation (1960).

results for protons derived from B^+ ($\pi^+ P$) -B^-(π^-).

It is seen from the graph (Fig. 6.7) that the results for protons give only poor agreement with theory, the main reason for this being, that a small sample is analysed in the recent work. The solid lines are based on Sternheimer's theory (1956) for the energy loss of mesons and protons and Lloyd's theory for flash tube operation.

On comparing our results with those of Diggory et al. (1971) using the same technique we observe that the former work gave excellent agreement with theory for the response of neon flash tubes to protons and mesons of known momentum in the range 0.1 - 10 GeV/c, this is because the high quantity of samples selected in the earlier work of Diggory et al. (1971), as shown in figure 6.8 was superior.

Ashton et al. (1971) have carried out similar work, their main aim being to examine the sensitivity of response of neon flash tubes to muons of varying ionization loss. Their results have shown that the logarithmic increase in ionization loss is reflected accurately in the variation of mean flash tube efficiency with muon momentum, as shown in figure 6.9.

6.6 Energy loss for mesons in plastic scintillation detectors

6.6.1 Introduction

Generally scintillator materials are divided into two categories: organic and inorganic. The phenomenon of the density effect in organic materials should be greater than that for the inorganic scintillators; therefore the relativistic increase should be practically eliminated. NE 102 A plastic phosphors have been used in many cosmic ray experiments. The energy loss in this material has been investigated here.

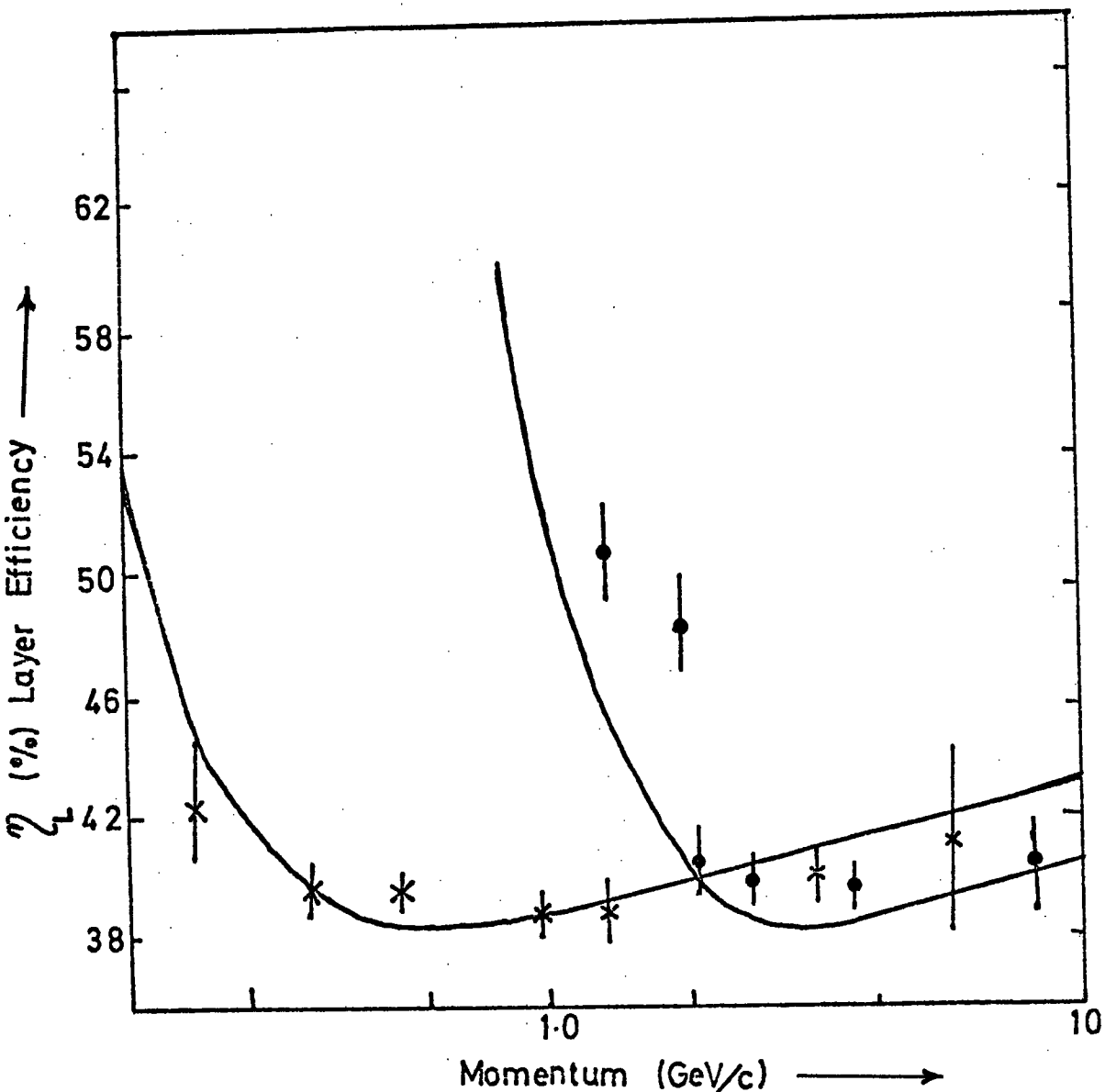

Figure 6-8:

The energy loss sensitivity of neon flash tubes operated with time delay of 80 μsecs.
The solid lines are based on the energy loss for neon, Sternheimer (1956). and Lloyd's theory of flash tube operation.
(After Diggory et al. (1971)).

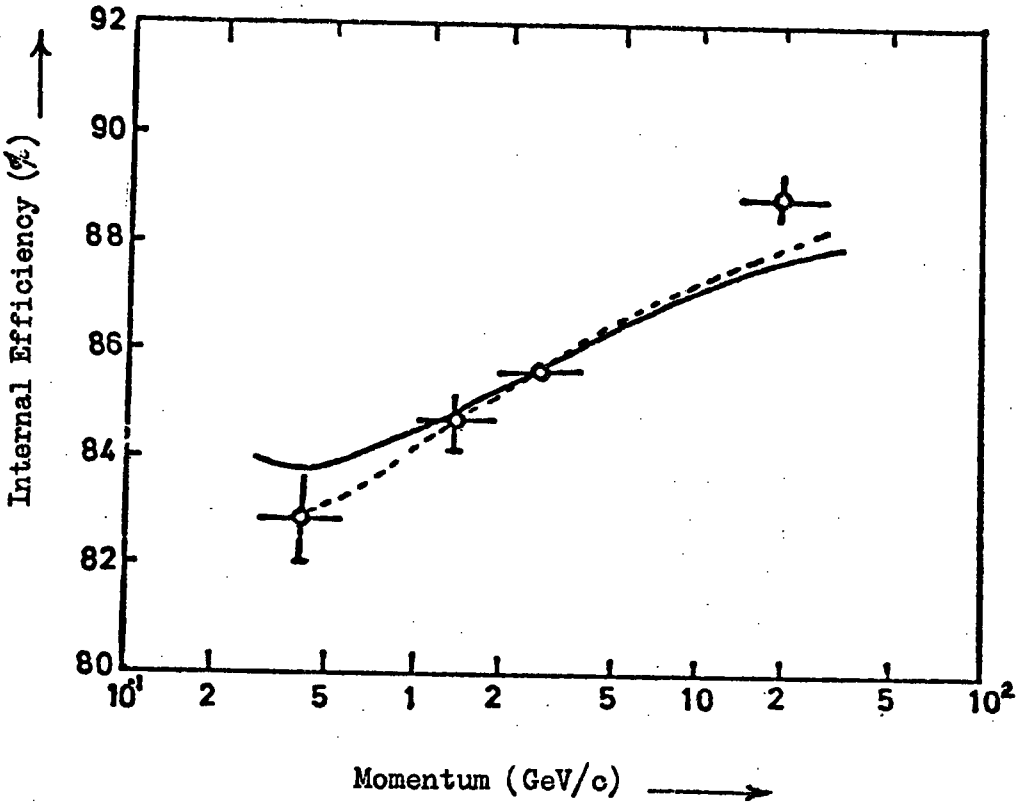

Figure 6-9. Variation of the mean internal efficiency with muon momentum. The full curve is derived from theory using the most probable ionization loss in neon as a function of momentum, and the broken curve includes a correction for unresolved knock-on electrons. Both are normalized to experiment at 2.1 GeV/c. (After Ashton et al. (1971)).

The results obtained in the present work using the mean pulse amplitude from the plastic scintillator detectors situated above Y tray in the equipment will be discussed in the following section.

6.6.2 Energy loss for positive and negative muons

The variation of the scintillator pulse amplitude with momentum for positive muons selected from muon films is shown in figure 6.10. The logarithmic rise is seen to be followed by the experimental points. The lowest momentum point is suspect of the undoubted presence of 'bad' events; its error has been increased accordingly.

Figure 6.11 represents the scintillator pulse amplitude versus momentum for negative muons selected from muon films and NAP's films together. The results here show also that the minimum ionization occurs at momentum 0.4 GeV/c, and the log rise is small. In both results, the expected responses for a plastic scintillator are good, and indicate the character of the system for calibration of energy loss detectors. The solid curve is based on Sternheimer theory of the energy loss for plastic scintillator. We used in our calculation ionization potential for plastic scintillator type NE 102 A $I = 13\ Z$ eV where $\bar{Z} = 3.65$ for this type of detector; and its atomic weight $\bar{A}$ is about 6.58.

6.7 Energy loss measurements for mesons and protons made using plastic scintillator detectors.

Figure 6.12 includes the mean pulse amplitude, measured in mV, versus momentum for mesons and protons class B^+ (π^+P) (a summary is given in table 6.2). There is good agreement with theory for mesons. But for protons there is again poor agreement for the same reason as indicated for flash tubes.

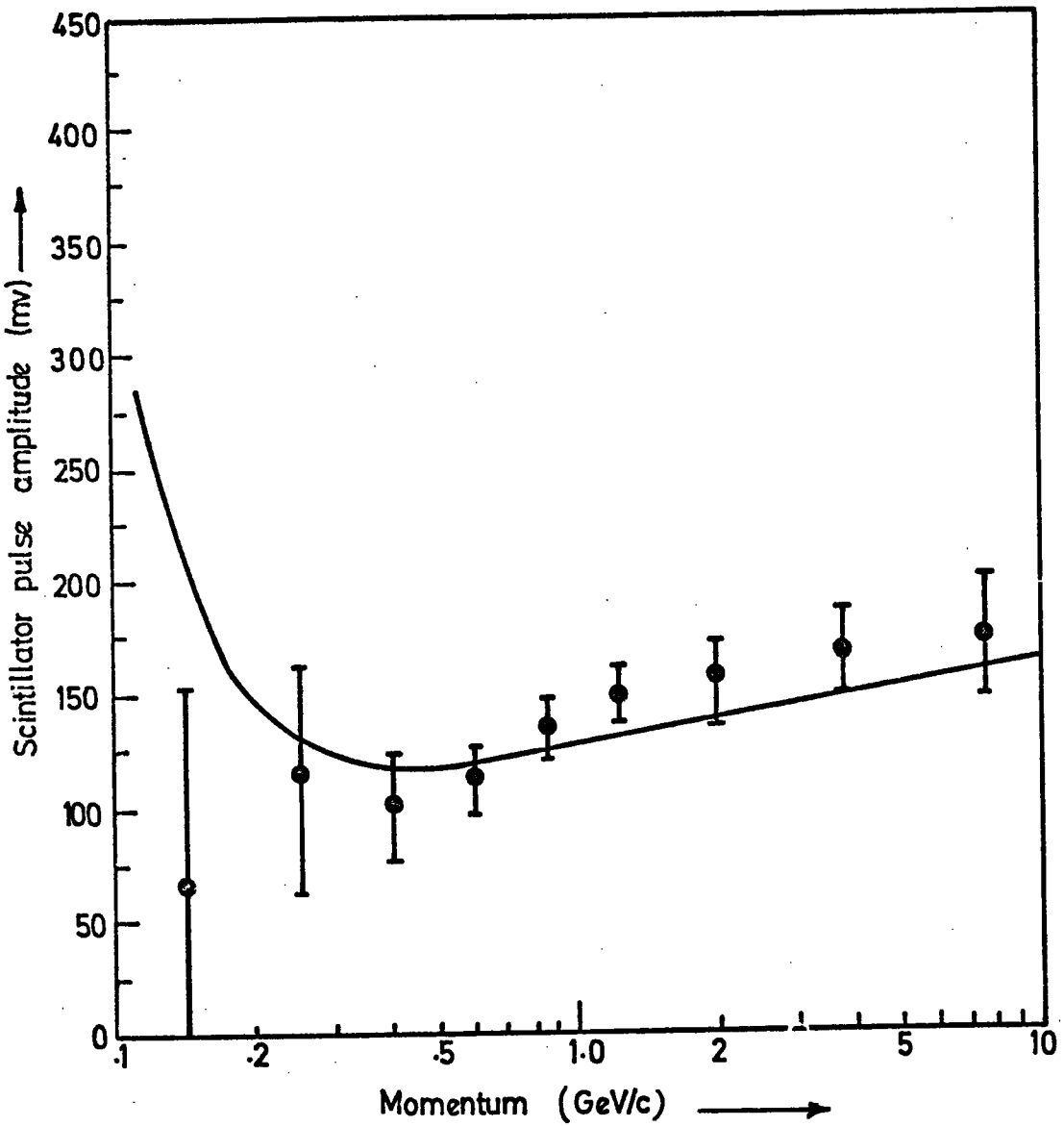

Figure 6-10.

The mean pulse amplitude (mV) versus momentum for positive mesons (from muon films.); The solid line is based on the energy loss for plastic scintillator with $\bar{Z} = 3.65$., $\bar{A} = 6.58$ Sternheimer (1956).

Comparison with the expected response for a plastic scintillator are good, and indicate the character of the system for calibration of energy loss detectors.

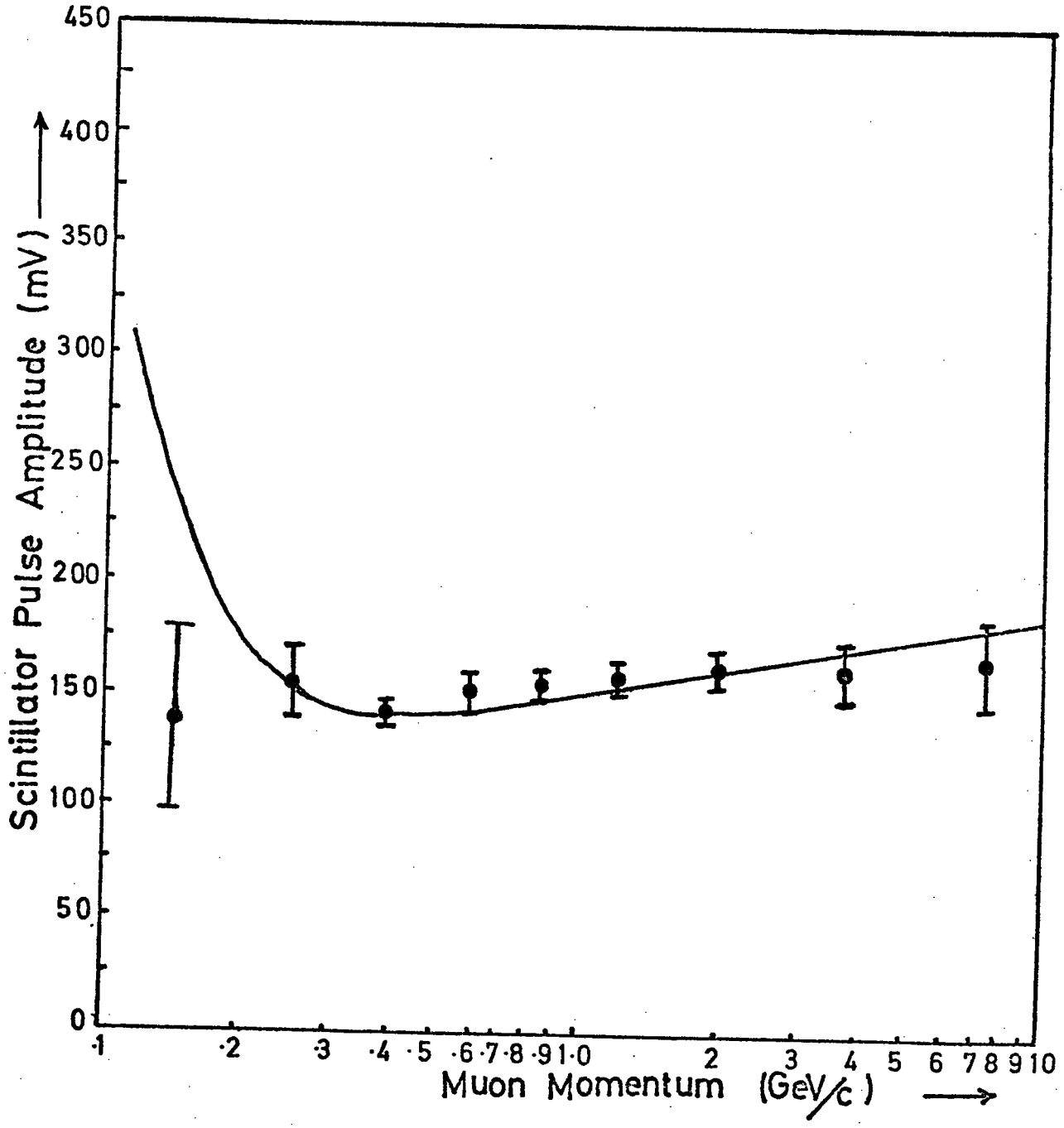

Figure 6-11. Scintillator pulse amplitude versus particle momentum for μ^--mesons , (muon films and NAP's) The solid line is based on the energy loss for plastic scintillator with $\bar{Z}$=3.65, $\bar{A}$=6.58 (Sternheimer 1956).

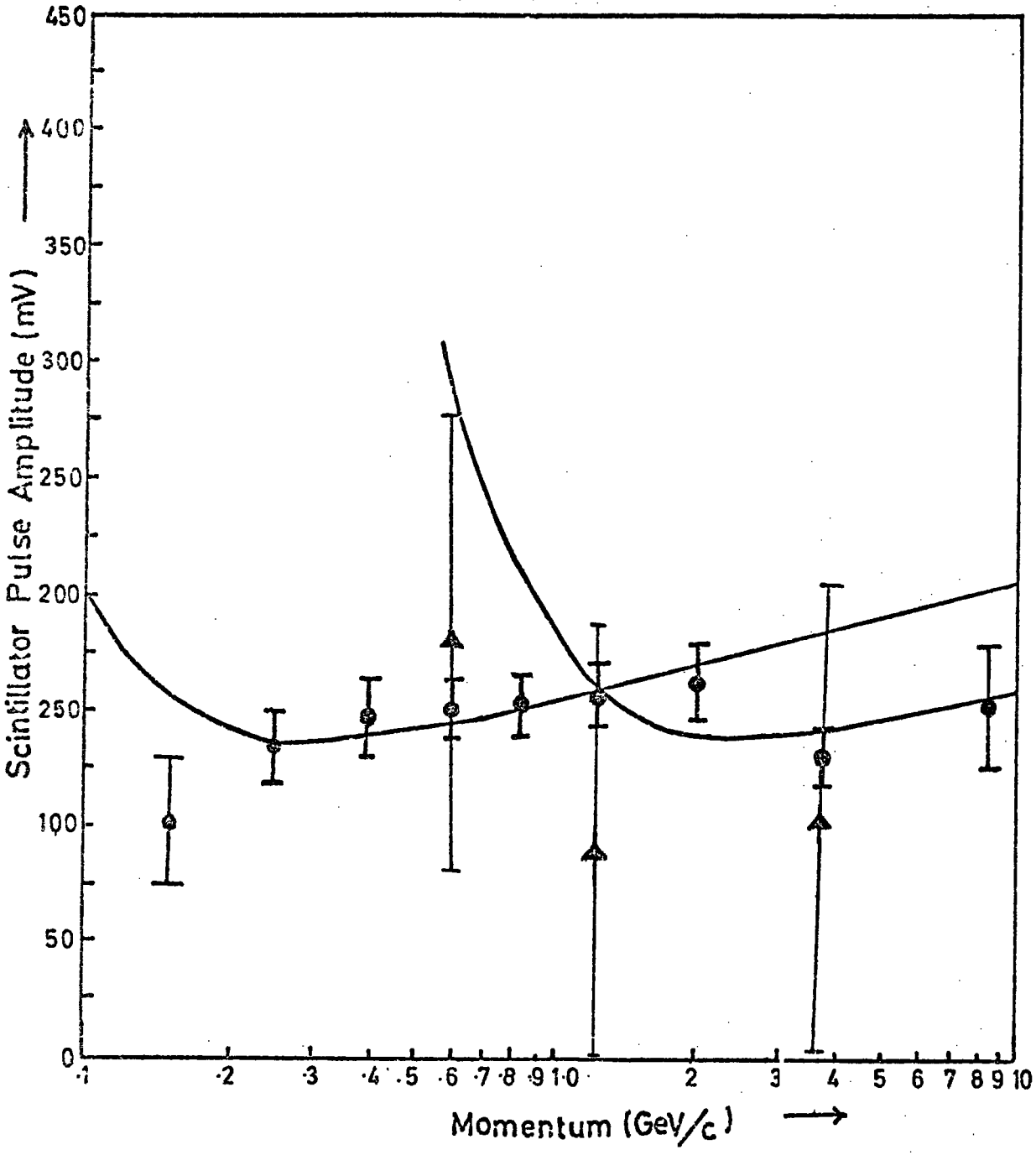

Figure 6-12:

Scintillator pulse amlitude versus particle momentum for mesons and protons of known momentum in the range 0.1-10 GeV/c.
The data shown (⊥●⊥) were obtained for mesons ; the data shown (⊥▲⊥) were obtained for protons as the result of $B^{+}(\pi^{+}P) - B^{-}(\pi^{-})$.

The former work of Diggory et al (1971), using the same technique of the present work shows good agreement for both mesons and protons, again this is because high quantity samples of particles were analyzed in the previous work. The results of the above authors can be seen in figure 6.13.

6.8 A Study of Čerenkov radiation phenomena, using the data obtained from the threshold water Čerenkov detector:

6.8.1 Introduction

Mallet (1926, 1928, 1929) was the first worker to study this phenomena, but his results did not indicate the main rule for this type of radiation to occur. Čerenkov (1934) bombarded a target comprising a solution of Uranyl salts with a gamma ray beam and during his experiment he discovered that a very weak radiation was visible in a cone about the direction of the gamma radiation. In 1937 Frank and Tamm pointed out the physical meaning of Č results, using a classical electromagnetic theory.The phenomenon came to be known as Čerenkov radiation.

Č radiation is electromagnetic radiation produced by particles when their velocity exceeds that of the propagation of an electromagnetic disturbance in the medium. In the present experiment the water tank is used to detect the radiation, by the way of 6 photo-multipliers.

Table 6.2 Scintillator pulse amplitude for class B^+ (π^+P) and B^- (π^-), (The mean scintillator pulse amplitude for proton events is derived from $(B^+ - B^-)$.

Number of momentum bins	1	2	3	4	5	6	7	8	9
Momentum range (GeV/c)	0.1 <0.2	0.2 <0.3	.3 <.5	.5 <.7	.7 <1.0	1 <1.5	1.5 <2.5	2.5 <5.0	5.0 <10.0
Mean Momentum Bins (GeV/c)	0.15	0.25	0.4	0.6	0.85	1.25	2.0	3.75	7.5
Number of events for class B^+ (π^+P)	4	10	19	21	18	15	12	11	6
Mean scintillator pulse amplitude for class B^+ (mV)	100	133	148	150	152	153	158	127	151
Standard error	7	16	19	12	12	15	15	13	26
Number of events for class B^- (π^-)	12	15	27	16	18	13	11	7	8
Mean Scintillator Pulse amplitude for class B^- (π^-) (mV)	151	122	140	141	127	155	127	127	101
Standard error	17	19	15	12	14	15	20	16	18
Difference B^+ (π^+P) - B^- (π^-)	$-8\pi^*$	$-5\pi^*$	$-8\pi^*$	$+5p$	0	$+2p$	$+1p$	$+4p$	$-2\pi^-$
Mean scintillator pulse amplitude for protons events (mV)	-	-	-	181.5	-	90	499	102	-

* Stopping negative muons

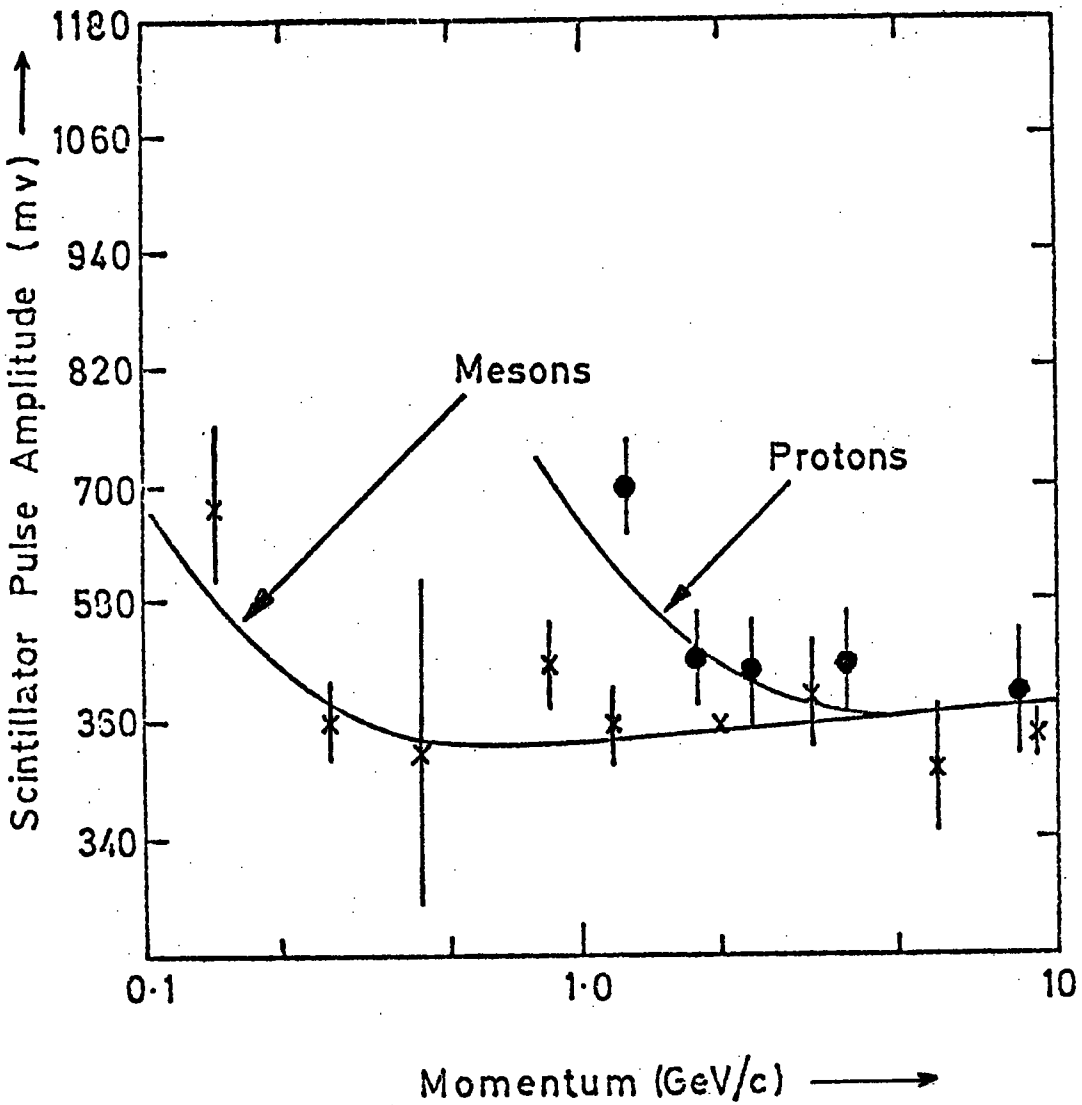

Figure 6-13:

The energy loss measurements made using plastic scintillator detectors. (After Diggory et al (1971)).

6.8.2 Principal concepts of Čerenkov radiation

The radiation is comparable to the bow wave produced by a ship, with reference to Huggens construction as shown in figure 6.14.

Straightforward theory shows that the coherent radiation is produced at angle θ where $\cos\theta = \frac{1}{\beta n}$.

From the above relation if $\beta n < 1$, it is clear that no radiation is emitted, thus the value $\beta = \frac{1}{n}$ gives a minimum energy, E_{min}, below which no radiation is produced. If $\beta n > 1$, i.e. if the velocity of the particle is greater than the phase velocity of light ($\frac{c}{n}$) in the medium, we have $\theta_{max} = \cos^{-1}(\frac{1}{n})$, this relation giving a value for E_{min} for μ - mesons in water of about 54 MeV, corresponding to a momentum of 119 MeV/c. Above E_{min} the intensity of the radiation is predicted to rise rapidly to a constant asymptotic value.

Many workers have studied this phenomenon after Čerenkov 1934, among them Tamm (1937) and Fermi (1940). A good account has been given by Jelley (1958), indicating various theories. The radiation is practically interesting for several reasons, as follows:

1. The radiation in EAS can give us a complete picture of the numbers of electrons as a function of height by measuring the light flux at different values of r (the distance from the core), and θ, the angle between the direction of the light and the direction of the shower axis.
2. Determination of the total amount of energy dissipated in the atmosphere, by calculation of the integrated light flux over all values r.

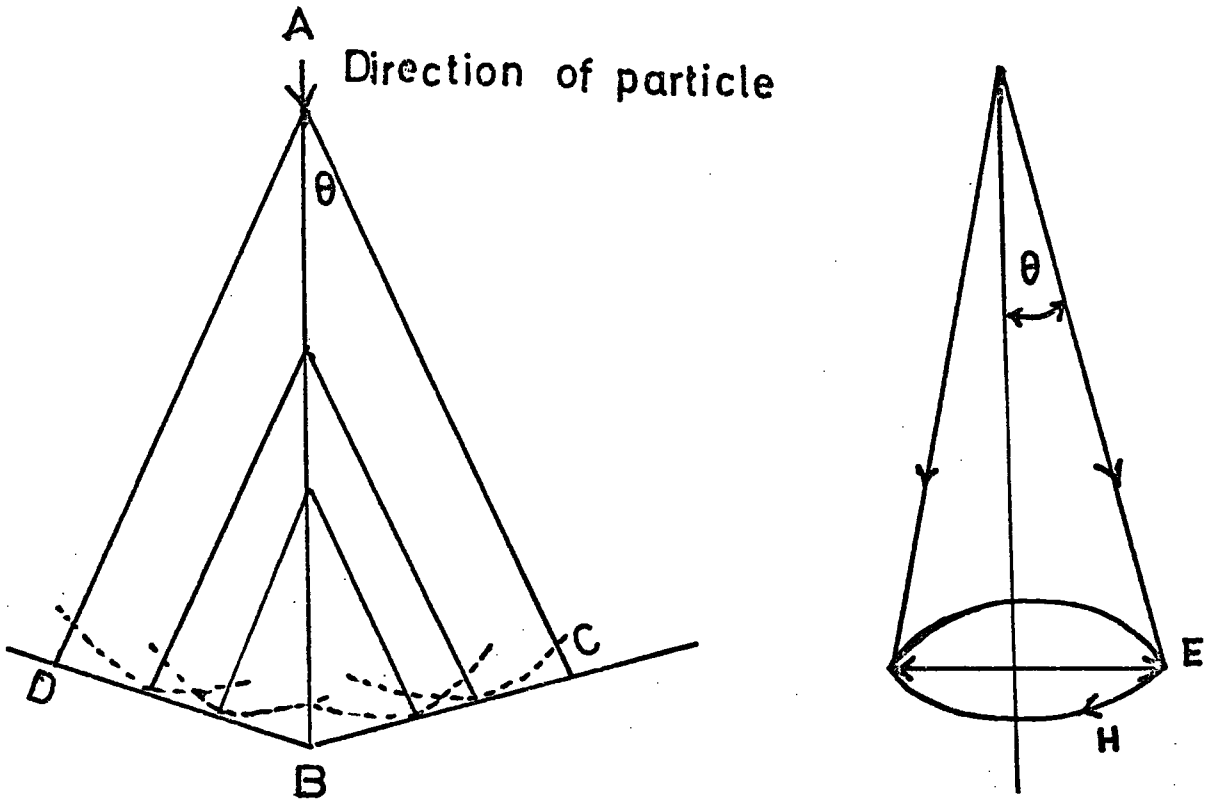

Figure 6-14 Illustrating The Emission of Čerenkov Radiation

6.9 Momentum threshold to give $\check{C}$ radiation in water $\check{C}$ detector for mesons and protons:

In the following some indication has been found for the momentum threshold for particles to produce Čerenkov radiation in the threshold water $\check{C}$ detector which is situated above the B1 tray in the equipment. The particles which penetrate the magnet are muons, pions, kaons, and protons. To determine the energy threshold for these particles, it is important to calculate the critical velocity β and $\gamma = \frac{1}{\sqrt{1-\beta^2}}$ as follows:

The critical velocity for producing $\check{C}$ radiation in water is given by:

$$\beta_c = \frac{1}{n} = \frac{1}{1.33} = 0.75$$

$$; \gamma = \frac{1}{\sqrt{1-\beta^2}} = 1.51$$

and the momentum of the particle is given by:

$P = m\gamma_c\beta_c$ the critical momenta for muons, pions, kaons and protons are shown in table 6.3. In the following a brief account of the experimental results is given.

Table 6.3

Momentum threshold for mesons and protons

Types of particles	Mass	Critical momentum for production Čerenkov radiation in water Č detector
Muons	105.6	119 MeV/c
Pions	139.6	158 MeV/c
Kaons	493.8	565 MeV/c
Protons	938.3	1062 MeV/c

Table 6.4

Characteristics of three events (muon films) giving pulse below momentum threshold in Č water detector

Film No.	Event No.	Momentum GeV/c	Flash tube No.	Č1	Č2	Č3	Č4
139	65985	0.09	20	95	22	89	220
136	65649	0.14	29	70	22	178	191
153	73018	0.14	24	189	22	89	605

6.10 Čerenkov pulse amplitude versus momentum for negative μ - mesons

Figure 6.15 represents the Čerenkov pulse amplitude measured in mV versus momentum for negative μ - mesons recorded by muon trigger. As we have mentioned the charged particle must lose about 143 MeV from its initial energy before penetrating the threshold water Č detector. But from the graph it is clear that in the first momentum bin there are some particles with low momentum which give a trigger (their characteristics are given in table 6.4). In fact it seems that the main reasons for these particles giving Č pulses below the momentum threshold are the following:

1. The momentum estimate is wrong.
2. Fluctuations in the number of electrons emitted by the photo-cathode.
3. Variations in the proportion of light collected from different regions of Č water detector.

Although the onset of Čerenkov radiation has not been defined the predicted constancy above the threshold has been demonstrated in this experiment.

6.11 General conclusions and Future Work

The aim of the work presented in this thesis was to re-examine the theoretical aspect of the energy loss of charged particle in matter and its relation to the experimental results.

The main conclusions which can be drawn from this investigation can be summarised as follows:

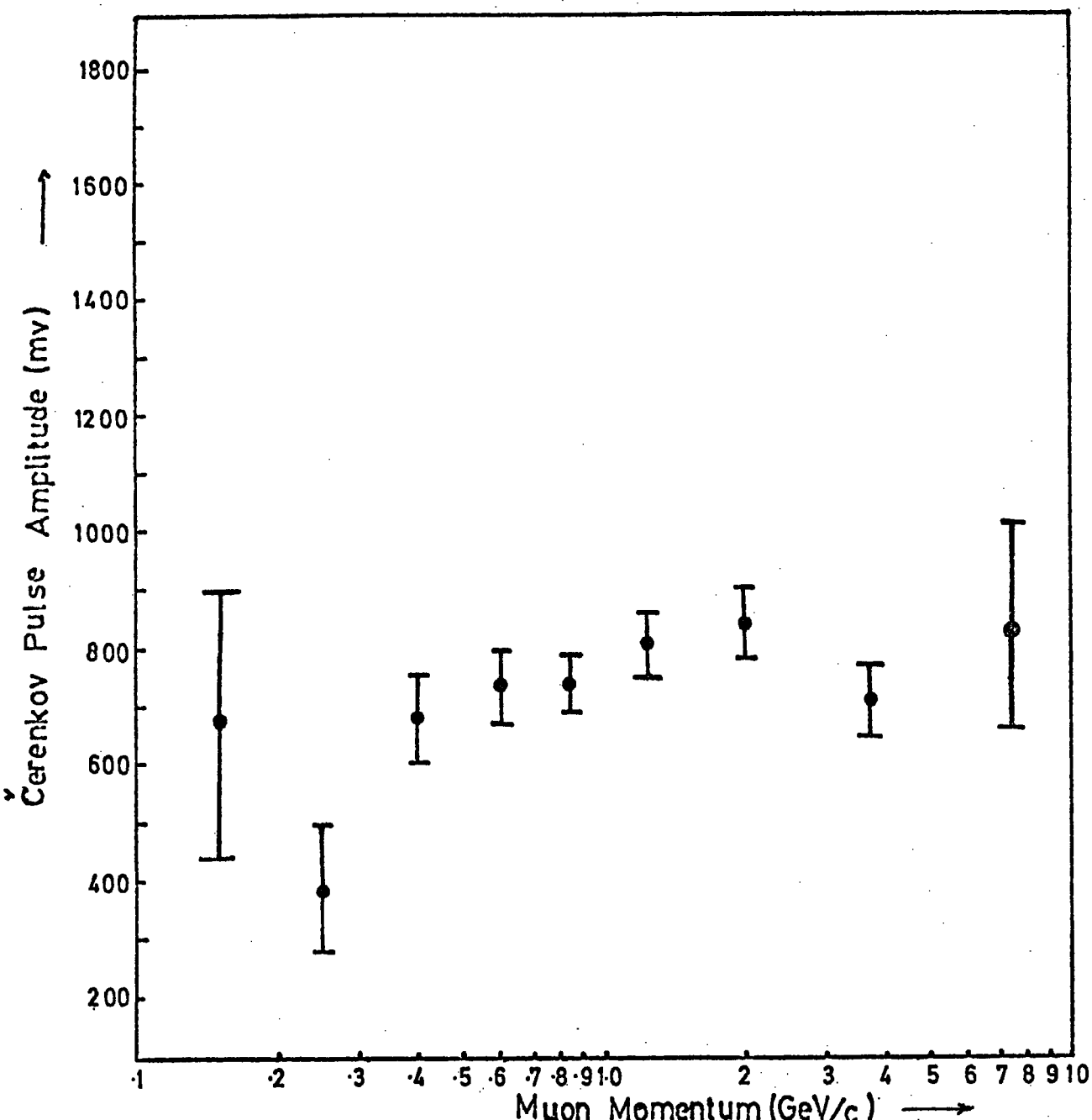

Figure 6-15:

Čerenkov pulse amplitude versus momentum ; The data shown (⊕) were obtained for negative muons specialy selected ; recorded in Muon trigger.

6.11.1 Neon flash tubes as energy loss measuring devices:

The response of neon flash tubes to protons and mesons of known momentum in the range 0.1 - 10 GeV has been measured and the results shown to be satisfactory as shown in figures 6.4 and 6.5. It is seen from the figures that the theoretical curve for mesons based on Sternheimer's theory (1956) for energy loss and Lloyd's theory for flash tube operation agrees with experiment, (the predicted absolute layer efficiencies are in fact about 1.5% higher than the experimental results, for example see figure 6.4, but this difference is not serious).

6.11.2 The reliability of the plastic scintillator as an energy loss detector.

As has been discussed in sections 6.6.1, 6.6.2 and 6.7 the mean pulse amplitude has been taken as a measure of energy loss for mesons and protons of various momentum. The results given in figure 6.10 and 6.11 indicate that the system is behaving normally, it means that comparisons with the expected response for a plastic scintillator are good and indicates the character of the system for the calibration of energy loss detectors.

The results for protons showed that there is poor agreement with theory as shown in figure 6.12, presumably due to the poor statistics in the present work. Diggory et al (1971) (figure 6.13) on the other hand indicated good evidence for the reliability of the system for the calibration of energy loss detectors for mesons and protons, the reason being that in their work a bigger sample has been analysed.

6.11.3 Momentum threshold for mesons to produce Čerenkov radiation in threshold water Č detector.

The momentum threshold for mesons has already been calculated theoretically in order to relate its value to the experimental results. It is seen from the results stated in figure 6.15 that the onset of Čerenkov radiation has not been defined precisely for reasons indicated in section 6.11. It is clear here from the graph representing the mean pulse amplitude versus muon momentum, that a better agreement for predicted constancy of Čerenkov pulse amplitude above threshold has been already observed.

6.12 Future Work

The experimental techniques used in the recent work may lead to the possibility of re-examining the momentum spectra of nuclear active particles in the cosmic radiation at sea-level, that is the additional information and momentum from flash-tube efficiencies may be used.

The present experimental system could form the basis of a feasible method of investigating the antiproton flux at sea-level. The main characteristics of candidates for identification as antiprotons would be:

1. Particle having momentum between 0.8 - 1.0 GeV/c.
2. A Negative charge.
3. A Neutron monitor response (within good impact), and
4. High energy loss signal from the plastic scintillators and neon flash-tubes, and zero Čerenkov pulse.

During our measurements some single events were in fact tentatively identified as antiprotons candidates, as follows:

Film Number	Event No.	F.T. No.	Charge	Momentum GeV/c.	-dE/dX	-dČ/dX
154	73488	35	Negative	1.16	128	Zero
192	83742	39	Negative	0.74	116	Zero
198	84688	35	Negative	1.44	346	Zero

It can be remarked that Antipov et al (1971) pointed out that the yield of antiprotons in p - p collisions at 70 GeV/c is 2% of that of negative pions. Albrow et al (1972) have pointed out that this yield increases with energy and so the flux of anti-protons may in fact be detectable in cosmic rays.

APPENDIX 1

A. Calculation of the theoretical energy loss curves for mesons and protons in neon based on Sternheimer theory (1956).

Sternheimer (1956) has calculated the energy loss for charged particles in several media based on the Bethe-Bloch formula, giving:

$$-\frac{1}{\rho}\frac{dE}{dX} = \frac{2\pi ne^4}{m\beta^2c^2\rho}\left[\ln\left(\frac{2m\beta^2c^2\,W_{max}}{I^2\,(1-\beta^2)}\right) - 2\beta^2 - \delta - U\right] \qquad (1)$$

We have used the above equation in our calculation for mesons and protons, ignoring the last two terms, these two terms refering to the density effect correction and shell correction.

The main causes for this are that the density starts to occur at momentum greater than our measurements, and also for gases the density effect at low energies is negligibly small.

Therefore equation (1) may be reduced to the following:

$$-\frac{1}{\rho}\frac{dE}{dX} = \frac{2\pi ne^4}{m\beta^2c^2\rho}\left[\ln\left(\frac{2m\beta^2c^2\,W_{max}}{I^2\,(1-\beta^2)}\right) - 2\beta^2\right] \qquad (2)$$

where W_{max} is the maximum energy transferred to an electron with mass m, by a particle of mass M. (i.e. meson 140 MeV/c^2 or proton 938 MeV/c^2).

$$W_{max} = \frac{E_o^2 - M^2c^4}{Mc^2\left\{\frac{M}{2m} + \frac{m}{2M} + \frac{T+Mc^2}{Mc^2}\right\}} \qquad (3)$$

$$\text{or} \quad = \frac{E_o^2 - M^2c^4}{Mc^2\left\{\frac{M}{2m} + \gamma\right\}} \qquad (4)$$

In equation (4), we ignore $\frac{m}{2M}$ due to its small value. γ represents the term $\frac{T+Mc^2}{Mc^2}$ for the particle, and $E_o = T + Mc^2$, where T is the kinetic energy of charged particle and Mc^2 its rest mass in units of MeV/c^2.

Equation (1) is based on the value of the average atomic ionization potential I = 13Z eV as calculated by Sternheimer 1956. The values for neon which applied in our calculations are:

Z = 10, A = 20.182 I = 130 eV.

Equation (2) has been applied in the calculations for the theoretical curves in plastic scintillators type NE 102 A for which $\bar{Z} = 3.65$ and $\bar{A} = 6.58$ and ionization potential I = 62.6 eV.

From equation (2), it is clear that the ionization potential should be proportional to Z. It is seen that equation (4) reduce to:

$$W_{max} \simeq m_e v^2/(1-\beta^2) \text{ for } E << (M^2/2m_e)c^2 \qquad (5)$$

In order to compute the ionization loss, it is useful to write equation 2 as follow :

$$-\frac{1}{\rho}\frac{dE}{dX} = \frac{A}{\beta^2}\left[B + 0.693 + 2\ln\left(\frac{P}{Mc}\right) + \ln W_{max} - 2\beta^2 \right] \qquad (6)$$

where A and B are constant and are defined by:

$$A = 2\pi ne^4/m_e c^2 \rho = 0.153\ (Z/A)\ MeV/g.cm^{-2}. \qquad (7)$$

and $$B = \ln\left[m_e c^2\ (10^6 eV)/I^2 \right] \qquad (8)$$

In the following it is more convenient to illustrate the meaning of the nomenclature used in equation (7) and (8)

m = mass of electron e = charge of electron

c = velocity of light

ρ = density of absorber n=number of electrons.cm^{-3} in absorber

I = mean excitation potential for absorber

Z = atomic number of absorber

A = atomic weight number of absorber

The value of the two constants A and B and the density of neon and plastic scintillator detectors type NE 102 A are given in the following table.

Material	(g/cm^3)	I(eV)	A MeV/ g cm^{-2}	B
Neon	0.8999×10^{-3}	130	0.076111	17.225
NE 102 A Plastic Scintill-ator	1.032	62.6	0.0833	18.69

In our calculation the incident energy for muons (with mass = 106 MeV/c^2) and proton (with mass = 938 MeV/c^2) is taken in the range 0.1 - 10 GeV.

It is remarked here that from the experimental points indicated in chapter 6, agree essentially with the curves especially the meson data in the region of $1/\beta^2$ and minimum ionization and also in the logrise region (in the case of neon flash tubes data). Although the best estimate showed that the theoretical curve is approximately a straight line beyond the log rise region, the discrepancy was due to experimental uncertainties as well as to uncertainties in the value of the mean excitation potential. It may also be noted that the original values of the energy loss theoretical curves are only approximate.

B. The connection between the energy loss curve based on Sternheimer's theory and flash tube efficiency based on Lloyd's theory.

It has been remarked already that Lloyd gives universal curves for the expected efficiency with time delay, as shown in figure A.1. These curves are given in terms of the parameter af_1Q where a is the tube radius, f_1 is the average probability that a single electron is capable of producing a flash when the high voltage pulse is applied, and Q is the average number of initial electrons produced per unit length in the neon gas.

The efficiency at a particular time delay is related to the probability that there are one or more electrons remaining in the tube when the pulse is applied. The internal efficiency can therefore be written as:

$$\eta_i = 1 - \exp(-Qf_1) \qquad (9)$$

It is assumed that f_1 is independent of the number of electrons present in the tube and since for muons Q varies somewhat with momentum, the efficiency will be momentum dependent. An estimate of the variation is given in figures 6.4 and 6.5. From a knowledge of the average rate of energy loss and mean energy per ion pair, Q can be found for each value of mean energy as follows:

$$Q = -(dE/dX) \;/\; \text{'the energy required to produce an electron ion pair in neon'} \qquad (10)$$

The magnitude of the mean energy per ion pair can be evaluated from the work of Jesse and Sadauskis (1955) as 36.7 eV.

Equation (2) in the Appendix 1(A) has been applied in order to evaluate the total energy loss for various momentum. Following equation (9), the internal efficiency (η_i) has been derived using the value of $f_1 = 0.25$ adopted by Diggory (1971).

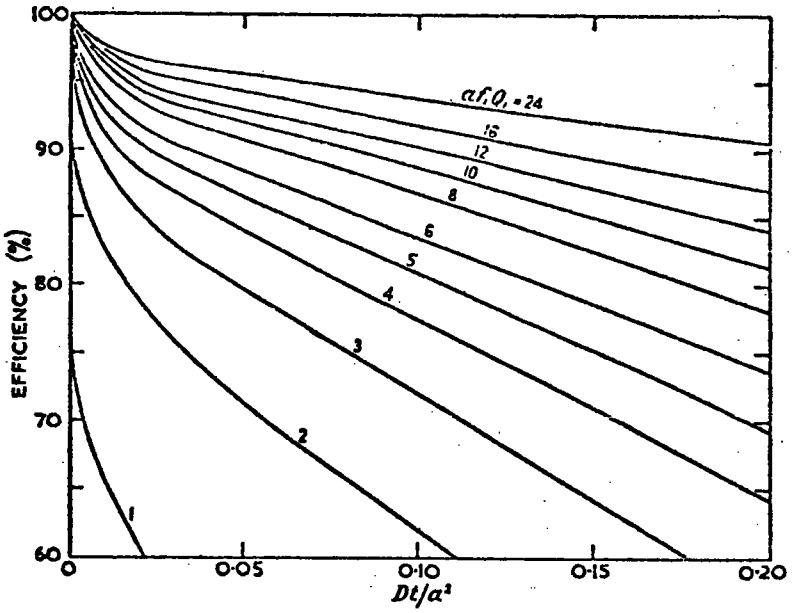

Figure A.1 Variation of computed efficiency with time delay, for small time delay, as a function of f_1, the 'electron efficiency'. D is the diffusion coefficient of thermal electrons in neon and a is the tube internal radius.

(After Lloyd (1960)).

The value for - (dE/dX), η_i and Q for each momentum are shown in table A.1. The data stated in this table are shown graphically in figures A.2, A.3 and A.4.

Figure A.2. shows the internal efficiency versus Q 'the average number of initial electrons produced in neon gas'. Figure A.3. shows the total energy loss per muon momentum (left ordinate), versus particle momentum and Q (right ordinate) versus particle momentum, and figure A.4 indicates the internal efficiency versus muon momentum.

The layer efficiency follows by multiplying by the area factor (0.87). It is seen in Figure 6.4 that the absolute layer efficiencies are about 1.5% higher than the experimental values, and downward reduction by this amount has been applied in that figure. The application of such a correction factor is considered reasonable; presumably the necessity comes from the factor that f_1 is not exactly 0.25.

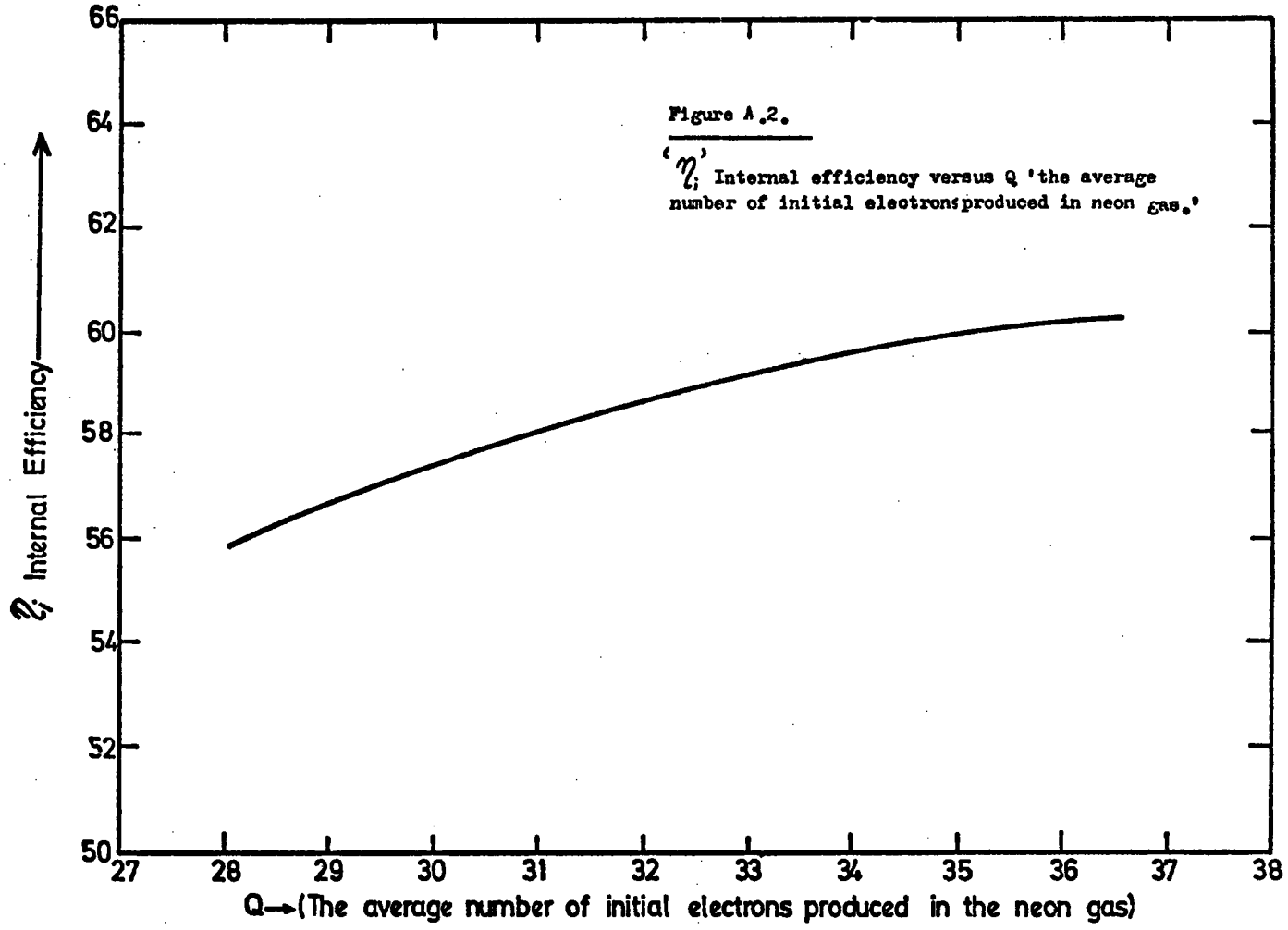

Figure A.2.

'η_i' Internal efficiency versus Q 'the average number of initial electrons produced in neon gas.'

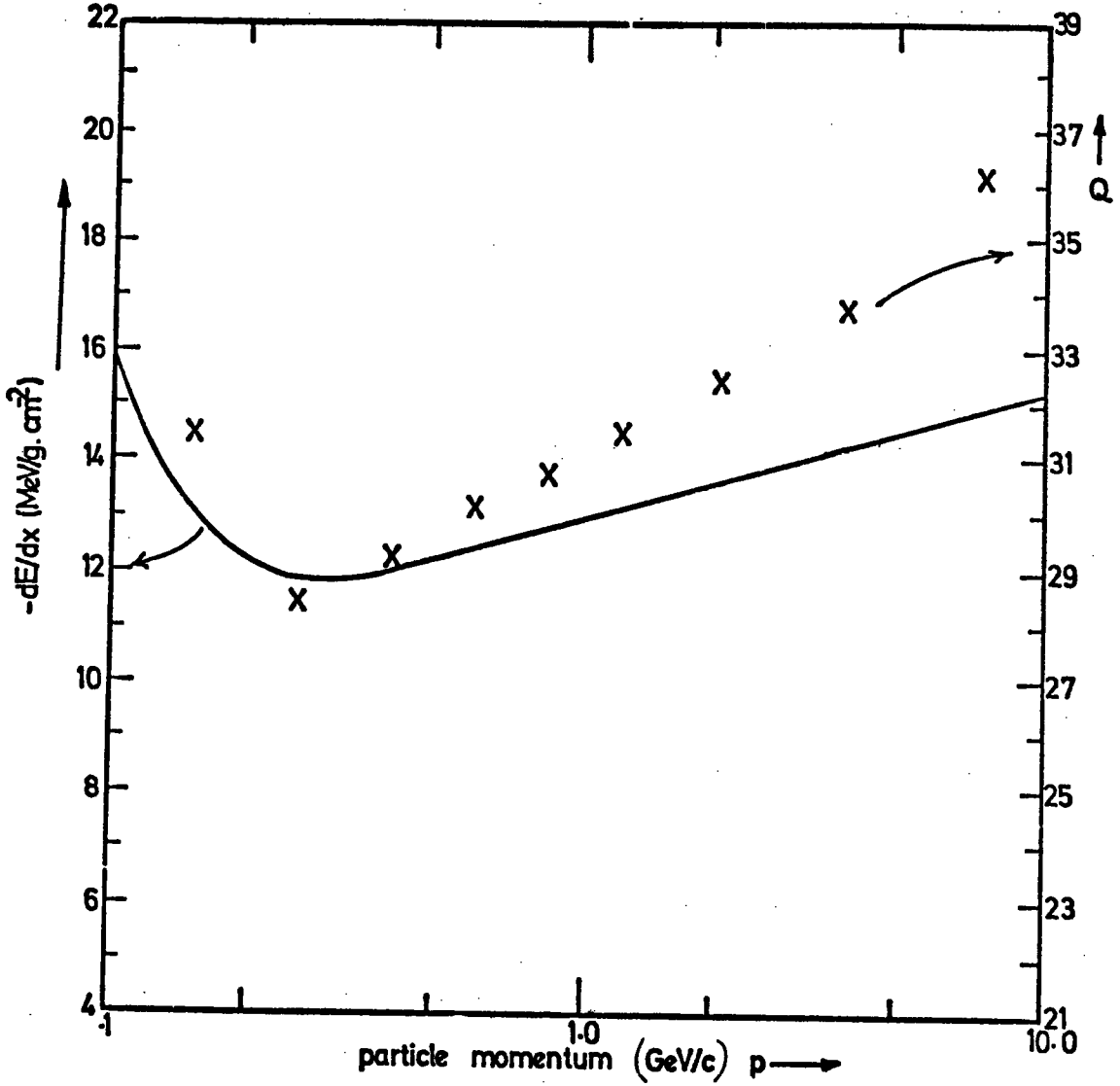

Figure A.3.

The theoretical energy loss curve is based on Sternheimer's theory. The data shown (×) and represent the average number of initial electrons produced per unit length in the neon gas.

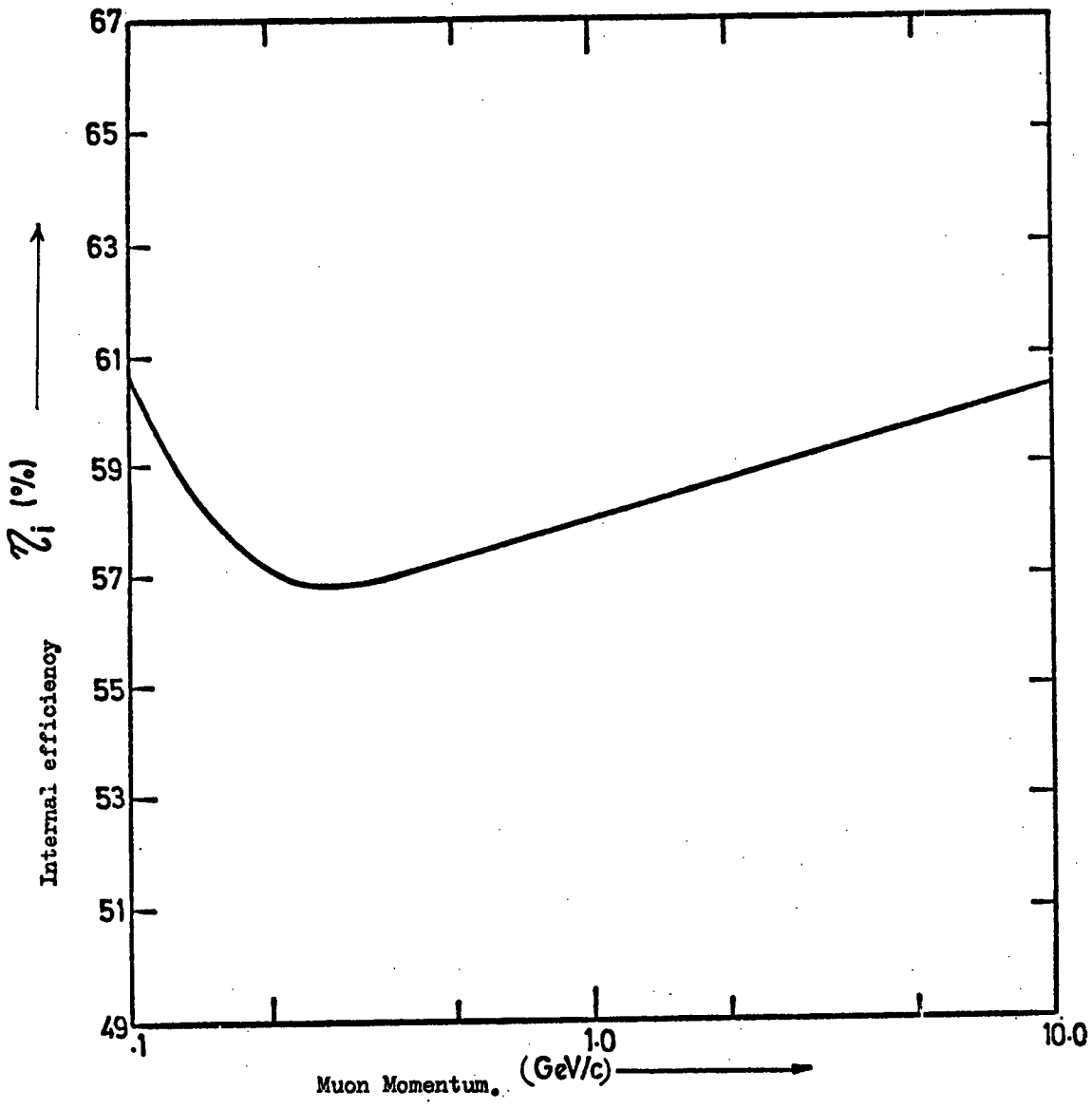

Figure A.4.

The internal efficiency versus muon momentum. The curve is based on Sternheimer's theory and Lloyd's theory for flash tube operation.

Table 1.A

Momentum Bin	Muon Momentum (GeV/c)	$-dE/dX$ MeV $g^{-1}cm^2$	Q ion pairs/cm	η_i (%) Internal efficiency
1	0.15	13	31.5	58
2	0.25	11.80	28.2	56.8
3	0.40	12.10	29.2	57.00
4	0.60	12.50	30.2	57.50
5	0.85	12.70	30.7	57.80
6	1.25	13.00	31.5	58.00
7	2.00	13.40	32.4	58.70
8	3.75	13.90	33.6	59.3
9	7.50	15.00	36.2	60.2

APPENDIX TWO

Table of the Elementary Particles

Family	Group	Particle — Anti-particle	Mass, electron masses	Charge	Mean life, sec	Decay modes
Photon	Photon	γ — γ	0	0	Stable	
Leptons	Neutrinos	ν_e — $\tilde{\nu}_e$	0	0	Stable	
		ν_μ — $\tilde{\nu}_\mu$	0	0	Stable	
			0	0	Stable	
			0	0	Stable	
	Electrons	e^- — e^+	1	−	Stable	
			1	+	Stable	
	μ mesons	μ^- — μ^+	206.8	−	2.212×10^{-6}	$e^- + \tilde{\nu}_e + \nu_\mu$
			206.8	+	2.212×10^{-6}	$e^+ + \nu_e + \tilde{\nu}_\mu$
Pi and K mesons	π mesons	π^0 — π^0	264	0	2×10^{-14}	$\gamma + \gamma$
		π^+ — π^-	273	+	2.55×10^{-8}	$\mu^+ + \nu_\mu$
			273	−	2.55×10^{-8}	$\mu^- + \tilde{\nu}_\mu$
	K mesons	K_1^0 — K_1^0	974	0	1×10^{-10}	$\pi^+ + \pi^-$
		K_2^0 — K_2^0	974	0	6×10^{-8}	$\pi^0 + \pi^0$
						$\mu^+ + \nu_\mu + \pi^-$
						$\mu^- + \tilde{\nu}_\mu + \pi^+$
						$e^+ + \nu_e + \pi^-$
						$e^- + \tilde{\nu}_e + \pi^+$
						$\pi^+ + \pi^- + \pi^0$
						$\pi^0 + \pi^0 + \pi^0$
		K^+ — K^-	966	+	1.22×10^{-8}	$\mu^+ + \nu_\mu$
						$\mu^+ + \nu_\mu + \pi^0$
						$e^+ + \nu_e + \pi^0$
						$\pi^+ + \pi^0$
						$\pi^+ + \pi^+ + \pi^-$
			966	−	1.22×10^{-8}	$\pi^+ + \pi^0 + \pi^0$
						$\mu^- + \tilde{\nu}_\mu$
						$\mu^- + \tilde{\nu}_\mu + \pi^0$
						$e^- + \tilde{\nu}_e + \pi^0$
						$\pi^- + \pi^0$
						$\pi^- + \pi^- + \pi^+$
						$\pi^- + \pi^0 + \pi^0$
	Nucleons	n — $\bar{n}$	1,839	0	10^3	$p + e^- + \tilde{\nu}_e$
			1,839	0	10^3	$\bar{p} + e^+ + \nu_e$
		p — $\bar{p}$	1,836	+	Stable	
			1,836	−	Stable	
	Hyperons	Λ — $\bar{\Lambda}$	2,183	0	2.2×10^{-10}	$p + \pi^-$
						$n + \pi^0$
						$p + e^- + \tilde{\nu}_e$
			2,183	0	2.2×10^{-10}	$\bar{p} + \pi^+$
						$\bar{n} + \pi^0$
						$\bar{p} + e^+ + \nu_e$
		Σ^0 — $\bar{\Sigma}^0$	2,332	0	$<10^{-11}$	$\Lambda + \gamma$
			2,332	0	$<10^{-11}$	$\bar{\Lambda} + \gamma$
		Σ^+ — $\bar{\Sigma}^+$	2,328	+	8×10^{-11}	$p + \pi^0$
						$n + \pi^+$
			2,328	−	8×10^{-11}	$\bar{p} + \pi^0$
						$\bar{n} + \pi^-$
		Σ^- — $\bar{\Sigma}^-$	2,341	−	1.6×10^{-10}	$n + \pi^-$
						$n + e^- + \tilde{\nu}_e$
			2,341	+	1.6×10^{-10}	$\bar{n} + \pi^+$
						$\bar{n} + e^+ + \nu_e$
		Ξ^0 — $\bar{\Xi}^0$	2,566	0	$\sim 10^{-14}$	$\Lambda + \pi^0$
			2,566	0	$\sim 10^{-14}$	$\bar{\Lambda} + \pi^0$
		Ξ^- — $\bar{\Xi}^-$	2,580	−	1.3×10^{-10}	$\Lambda + \pi^-$
			2,580	+	1.3×10^{-10}	$\bar{\Lambda} + \pi^+$

ACKNOWLEDGEMENTS

The author is greatly indebted to Professor A.W. Wolfendale for the privilege of working in his laboratories, he is also grateful to him for his guidance, encouragement, suggestions and sustained interest in this work, and also during the writing of this thesis.

The author is grateful to Professor G.D. Rochester, F.R.S., for his sincere encouragement and many other helpful discussions.

He also wishes to thank Dr. K.E. Turver for help, advice and for many valuable discussions in this work described.

In particular the author is grateful to the following:
Dr. J.V. Major for his kind help during this work.
Dr. F. Ashton for his support with many papers relative to the author's work. Dr. J.M. Breare for many useful discussions during his lectures this year 1974. He would like to thank all members of the Physics Department in the University of Durham for many useful discussions.

The author wishes to thank all his colleagues in the E.A.S. group, and offer special thanks to Mr. I.S. Diggory for untiring help in the running of the instrument.

He also wishes to express his sincere gratitude to his government 'Arab Republic of Egypt' for the award of a research studentship during the course of this work. The author wishes to thank Professor M.A. Koraitim, the director of Egyptian Education Bureau in London for his kind help, and also Mr. F.Abdelsaher for his guidance.

The author wishes to thank all staff members of the University of Assiut in Egypt, and offer a special thanks to Professor M.H. El-Nashaar the President of the University of Assiut for help and guidance since 1966.

Finally the author would like to thank his wife Mrs. Mostafa for her encouragement during this work, Mrs. J. Lincoln and Miss J. Watson are thanked for their patience and cooperation in typing this thesis.

References

1. Achar, V.C., Menon, M.G.K., Marasimham, V.S., Ramana Murthy, P.V., Sreekantan, B.V., Hinotani K., Miyake, S., Creed, D.R., Osborne, J.L., Pattison, J.B.M., and Wolfendale, A.W., 1955, Phys. Letters, 18, 196-199.

2. Aggson, T., and Fretter, W.B., 1962, Nuovo Cimento (Suppl.) 23, 75.

3. Albrow, M.G., et al., 1972, Nucl. Phys. B37 P.594.

4. Antipov Yum, et al, 1971, Phys. Lett. 34B, 164.

5. Ashton, F., and Simpson, D.A., 1965, Phys. Letters 16 78.

6. Ashton, F., et al., 1971 b J.Phys. A: Gen. Phys. 4, 895.

7. Ashton, F., et al., 1971a Nuovo Cim. Lett., 2, 707.

8. Ashton, F., and Simpson, D.A., 1963, Proc. Int. Conf. Cosmic Rays, Jaipur, India (IUPAR).

9. Ashton, F., and Wolfendale, A.W., 1963, Proc. Phys. Soc. 81, 593.

10. Aurela, A.M., and Wolfendale, A.W., 1967, Ann. Acad. Sci. Fenn., A6, 226.

11. Aurela, A.M., Mackeown, P.K., and Wolfendale, A.W., 1966, Proc. Phys. Soc., 89, 401.

12. Barber, W.C., 1955, Phy. Rev. 97, 1071.

13. Barber, W.C., 1956, Phys. Rev., 103, 1281.

14. Barnaby, C.F. 1961, Proc. Phys. Soc. (London) 77, 1149.

15. Baskin, R., and Winkler, J.R., 1953, Phys. Rev. 92, 464.

16. Bethe, H.A., 1930, Ann. Physik. 5, 325.

17. Bethe, H.A., 1933, Handbuch der Physik, Vol. 24, 515.

18. Bhabha, H.J., and Heitler, W., 1937, Proc. Roy. Soc., A159, 432 (1937).

19. Bhabha, H.J., and Chakrabarty, S.K., 1942, Proc. Ind. Acad. Sci., 15A, 464.

20. Bhabha, H.J., 1938, Proc. Roy. Soc., A164, 257.
1936, Proc. Roy. Soc., A154, 195.
1935, Proc. Roy. Soc., A152, 559.

21. Blandford, G.E., 1971, Proc. 12th Conf. on Cosmic Rays. (Hobart University of Tasmania) 1 269.

22. Bloch, F., 1933, Z. Physik 81, 363.

23. Bloch, F., 1933, Ann. Physik 16, 285.

24. Bohr, N., 1913, Phil. Mag., 25, 10.

25. Bohr, N., 1915, Phil. Mag. 30, 581.

26. Bowen, T., 1954, Phys. Rev. 96, 754.

27. Bradley, E.F., 1955, Proc. Phys. Soc. (London) A68, 549.

28. Breare, J.M., 1973, The Neon Flash Tube Technique, Cosmic Rays at ground level, edited by Wolfendale, A.W.

29. Brooke, G., et al., 1962, Proc. Phys. Soc., 80, 674.

30. Brooke, G. Hayman, P.J., Kamiya, Y., and Wolfendale, A.W., 1964, Proc. Phys. Soc., 83, 853.

31. Brooke, G., 1973, Protons and Pions,Cosmic Rays at ground level, edited by Wolfendale, A.W.

32. Budini, P., 1953, Nuovo Cimento 10, 236.

33. Bull, R.M., Coat, D.W., Nash, W.F., and Rastin, B.C., 1960, Nuovo Cim., (Suppl) 23, 39.

34. Bull, R.M., Nash, W.F. and Rastin, B.C., 1965, Nuovo Cim., 40A, 365.

35. Buskirk, F.R., Dyer, J.N., Hanson, H.D., Seng, R., and Weidman, R.H., 1964, Int. Conf. Nucl. Photography, CERN 2, IX - 9.

36. Carslaw, H.S., and Jaeger, J.C., 1947, Conduction of Heat in Solids (Oxford University Press), P313.

37. Čerenkov, P.A., 1934, Dokl. Akad. Nauk., SSSR, 2, 451.

38. Čerenkov, P.A., 1960, Sci, 131, 136.

39. Chou, C.N., 1952, Phys. Rev. 87, 903.

40. Conversi, M., and Gozzini, A., 1955, Nuovo Cim. 2, 189.

41. Conversi, M. et al., 1956, Nuovo Cim. Suppl. 4, 234.

42. Conversi, M., Gianoli, G., and Spillantini, P., 1972, Nuovo Cim. Lett. 3, 483.

43. Conversi, M., 1973, Recent developments in the Hodoscope Chamber Technique, LA, Rivista. Del Nuovo Cimento, Vol.3, No.3, 233-282.

44. Coxell, H., and Wolfendale, A.W., 1960, Proc. Phys. Soc., 75, 378.

45. Coxell, H., Mayer, M.A., Scull, P.S., and Wolfendale, A.W., 1961, Nuovo, Cim. Suppl. 21, 7.

46. Cranshaw, T.E., and de Beer, J.F., 1957, Nuovo Cim, 5, 1107.

47. Crispin, A., and Hayman, P.J., 1964, Proc. Phys. Soc. (London) 83, 1051.

48. Crispin, A., and Fowler, G.N. (1970), Rev. Mod. Phys. 42, 290.

49. Diggory, I.S., Hook, J.R., Jenkins, I.A., and Turver, K.E., 1974, J. Phys., A. Math., Nucl. Gen., Vol. 7, 741.

50. Diggory, I.S., Dixon,H.E., Earnshaw,J.C.,Hook,J.R., Jenkins, I.A., Maslin, G.C., O'Donnell, B.D., Orford, K.J., and Turver, K.E., 1971, Int. Conference on Cosmic Rays. Hobart.

51. Earnshaw, J.C., et al., 1967, Proc. Phys. Soc., 90, 91.

52. Eyeions, D.A., Owens, B.G., Price, B.T., and Wilson, J.G., 1955, Proc. Phys. Soc. (London) A68, 793.

53. Fermi, E., 1940, Phys. Rev. 57, 485.

54. Fowler, G.N. and Jones, G.M.D.B., 1953, Proc. Phys. Soc. A66, 597.

55. Fowler, G.N. and Hall, A.G., 1965, Proc. 9th Conf. on Cosmic Rays, London, P.976.

56. Fowler, P.H. et al., 1967, Proc. Roy. Soc. A301.

57. Fowler, P.H., et al., 1970, Proc. Roy. Soc. A318, P1-43.

58. Frank, I., and Tamm, I., 1937, Dokl. Akad. Nauk, SSSR, 14, 109.

59. Gardener, M., Kisdnasamy, S., Rossle, E., and Wolfendale, A.W. 1957, Proc. Phys. Soc., B70, 687.

60. Ghosh, S.K., Jones, G.M.D.B., and Wilson, J.G., 1952, Proc. Phys. Soc. (London) A65, 68.

61. Hall G., 1959, Can. J. Phys. 37, 189.

62. Halpern, O., and Hall, H., 1948, Phys. Rev. 73, 477.

63. Hazen, W.E., 1944, Phys. Rev. 65, 259.

64. Heitler, W., 1936, The Quantum theory of Radiation (Oxford University Press), P.218.

65. Hertz, A.J., and Stiller, B., 1964, Proc. Intern. Conf. Nucl. Photography, CERN 65/4, 1, 81-87.

66. Holmes, J.E.R., Owen, B.G., and Rodgers, A.L., 1961, Proc. Phys. Soc., 78, 505.

67. Hook, J.R., 1973, Ph.D. Thesis, University of Durham.

68. Hook, J.R., and Turver, K.E., 1974, J. Phys. A. Math., Nucl. Gen., Vol.7 No.5, 765.

69. Hyams, B.D., Mylroi, M.G., Owen, B.G., and Wilson, J.G., 1950, Proc. Phys. Soc., A63, 1053.

70. Jelley, J.V., 1953, Prog. Nucl. Phys. 3, 84.

71. Jelley, J.V., 1958, Čerenkov Radiation and its application (Pergamon Press London).

72. Jenkins, J.R., 1974, Ph.D. Thesis, University of Durham.

73. Jesse, W.P., and Sadauskis, J., 1955, Phys. Rev. 97, 1668.

74. Jesse, W.P., 1961, Phys. Rev. 122, 1195.

75. Jones, D.G., West, R.H., and Wolfendale, A.W., 1963, Proc. Phys. Soc. (London)81, 1137.

76. Jones, I.S. Pathak, K.M., and Thompson, M.G., 1968, J. Phys. A, (2) 1, 1-4.

77. Jongejans, B., 1960, Nuovo Cim. 16, 625.

78. Kepler, R.G., d'Andlau, C.A., Fretter, W.B., and Hansen, L.F., 1958, Nuovo Cimento 7, 71.

79. Landau, L., 1944, J. Phys. USSR., 8, 201.

80. Landau, R.E., and Kraybill, H.L., 1959, Phys. Rev. 133, 657.

81. Lloyd, J.L. 1960, Proc. Phys. Soc., 75, 387.

82. MacKeown, P.K., and Wolfendale, A.W., 1966, Proc. Phys. Soc., 89, 553.

83. Mallet, L., 1926, C.R. Acad. Sci. 183, 274.
1928, C.R. Acad. Sci, 187, 222.
1929, C.R. Acad. Sci, 188, 445.

84. Massey, H.S.W., and Burhop, E.H.S., 1952, Electronic and Ionic Impact Phenomena (Oxford: University Press), P.321.

85. Meek, J.M., and Craggs, J.D., 1953, Electrical Breakdown of Gases, Oxford.

86. Millar, C.H., Hincks, E.P., and Hanna, G.C., 1958, Can. J. Phys. 36, 54.

87. Parry, J.K., Rathgeber, H.D., and Rouse, J.L., 1953, Proc. Phys. Soc. (London) A66, 544-548.

88. Rossi, B., 1940, Phys. Rev. 57, 660.

89. Rossi, B., 1952, High Energy particles, New York.

90. Rossi, Hilberry, and Hoag, 1939, Phys. Rev., 56, 837.

91. Sengupta, R.L., 1940, Nature, London, 146, 65.

92. Shapiro, M.M., 1958, Handbuch der physik, Vol. 45, 342.

93. Shapiro, M.M., and Silberberg, R., 1970, Ann. Rev. Nucl. Sci., 20, 323-392.

94. Shapiro, et al., 1971, Proc. 12th Conf. on cosmic rays (Hobart University of Tasmania). 1221-1227.

95. Smith, A.M. and Stewart, D.T., 1966, Phys. Letters 22, 633.

96. Sternheimer, R.M., 1952, Phys. Rev. 88, 851.
1953, Phys. Rev. 89, 1148.
1953b Phys. Rev. 91, 256.
1954, Phys. Rev. 93, 735.
1954, Phys. Rev. 93, 1434.
1956, Phys. Rev. 103, 511.
1959, Phys. Rev. 115, 137.
1966, Phys. Rev. 145, 247.
1967, Phys. Rev. 164, 349.
1973, Phys. Rev. Vol.3, No.11, 3682.

97. Stiller, B., and Shapiro, M.M., 1953, Phys. Rev. 92, 735.
Stiller, B.,1963, Karpuskularphotographic IV,Munchen, 542-555

98. Swann, W.F.G., 1938, J. Franklin Inst. 226, 598.

99. Tamm, I., 1939, J. Phys. (U.S.S.R.), 1, 439.

100. Thompson, M.G., 1973, Energetic muons, Cosmic Rays at ground level, edited by Wolfendale, A.W.

101. Tsytovitch, V.N., 1962a, Sov. Phys. Doklady 7, 411.

102. Tsytovitch, V.N., 1962b, Sov. Phys. JETP, 15, 320.

103. Tsytovitch, V.N., 1962c, Sov. Phys. JETP, 16, 1260

104. Turner, J.E., 1964, NAS - NRC Publ. No. 1133, 99.

105. Waddington, P. Progress in Nuclear Physics, Frisch, Pergamon, Press 1960.

106. Weiss, J., and Bernstein, W., 1956, Phys. Rev. 103, 1253.

107. Wick, G.C., 1943, Nuovo Cimento (9), 1, 302.

108. Williams, E.J., 1929, Proc. Roy. Soc. (London) A125, 420.

109. Williams, E.J., 1932, Proc. Roy. Soc. A135, 108.

110. Williams, E.J., 1937, Proc. Cambridge Phil. Soc. 33, 179.

111. Wolfendale, A.W., 1967, Proc. Int. Conf. Cosmic Rays, Calgary, Canada, Pt.A., 558.

112. Wolfendale, A.W., 1962, Cosmic Rays, "George Newnes Press".

113. Wolfendale, A.W., Cosmic Rays at ground level, 1973, The Institute of Physics, London and Bristol.

114. Wolfendale, A.W. (i) Introductory Cosmic Rays Lectures, 1972/73 and 1973/74. (ii) Private Communication, 1973/74.

115. Zhdanov, G.B., Tret'yakova, M.I., Tsytovich, V.N., and Shecherbakova, M.N., 1962, Sov. Phys. JETP 43, 342.

116. Zhdanov, G.B., Tret'yakova, M.I. and Shecherbakova, M.N., 1964, Int. Conf. Nuclear Photography, CERN 2, IX - 41.